Journal
of
The Franklin Institute
Devoted to Science and the Mechanic Arts

Vol. 216 OCTOBER, 1933 No. 4

SURFACE CONDITIONS AND STABILITY OF CHARACTERISTICS IN SCREENED-GRID TUBES.

BY

PAUL L. COPELAND,

Massachusetts Institute of Technology.

ABSTRACT.

The characteristics of screened-grid tubes are discussed and the influence of secondary emission is emphasized. The marked change in secondary emission with surface contamination causes instability of characteristics. Experiments with carefully evacuated '24 tubes indicate that the evaporation of active material from the cathode considerably increases the secondary emission from the plate and that the liberation of "getter" in a completed tube limits the stability attainable.

Schottky [1] introduced multiple-grid tubes and discussed their action. Hull and Williams [2, 3] experimented further with such devices and pointed out uses destined to find wide application in amplifier work. Previously Hull [4] had developed the dynatron, a tube utilizing the secondary electrons from the anode of a valve. The influence of secondary emission was quite apparent in the characteristics of the screened-grid tube discussed by Hull.[3] A widely used device involving these principles is the type '24 tube.

[1] W. Schottky, *Archiv f. Elektrot.*, **8**, 1–31; 299–328 (1919).

[2] Hull and Williams, *Phys. Rev.*, **27**, 432–438 (1926).

[3] Hull, *Phys. Rev.*, **27**, 439–454 (1926).

[4] Hull, *Phys. Rev.*, **7**, 141 (1916).

(Note.—The Franklin Institute is not responsible for the statements and opinions advanced by contributors to the JOURNAL.)

The source of electrons in a '24 tube is a cylindrical cathode coated with oxides of the rare earths to make it emit electrons at low temperatures. The cathode is surrounded by a spiral wire serving as a control grid. Close to this first grid, and coaxial with it and the cathode, is a second spiral used to screen the control grid from the fields of the plate and called therefore the "screen grid" or simply the "screen." The anode or plate is a nickel cylinder, the diameter of which is considerably greater than that of either grid. Outside of the plate there is a cylinder of fine nickel mesh which is connected electrically within the tube to form part of the screen. The advantages of this arrangement are well known. The shielding of the control grid from the influence of the plate facilitates the amplification of high frequency currents. The almost complete shielding of the cathode from the influence of the plate makes possible an extremely high plate resistance and a correspondingly high voltage amplification. In the present paper a brief report is made of some experiments to show how conditioning of the anode surface influences tube characteristics.

The electrical circuit used in these experiments contained nothing unusual. Desired potentials were supplied to the electrodes of the tube from potential dividers. The potential of any element relative to the cathode was measured with a suitable voltmeter connected at the divider. The electron current collected by any electrode was measured by a suitable milliammeter connected between the socket terminal and the slide of the divider establishing the potential of the electrode.

The graphs of Fig. 1 were obtained using a '24 tube of a well known manufacturer. The cathode heater current was fixed at its normal value (about 1.75 amperes). The control grid was maintained 4 volts negative and the screen grid 90 volts positive with respect to the cathode. Under these conditions the electron current from the cathode and the electron currents to the screen grid and plate were measured as a function of the plate potential relative to the cathode. Since under these conditions the potential gradient at the cathode is almost independent of the plate potential, the emission of the cathode, as shown by the dashed line of Fig. 1, is almost independent of the plate voltage. The manner in which this

FIG. 1.

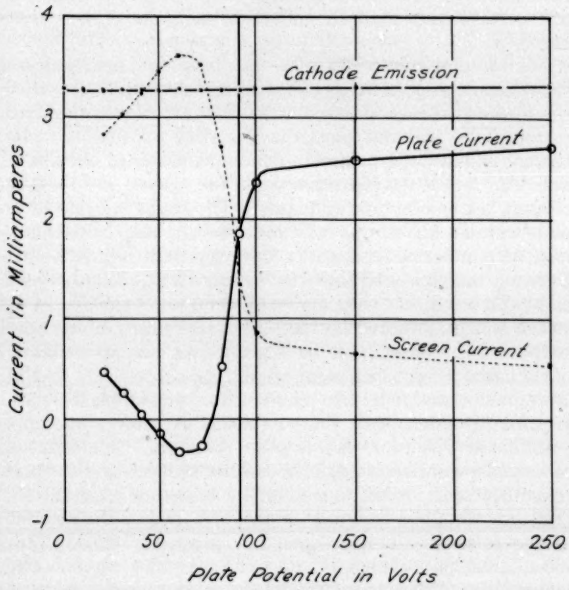

current divides between the screen and the plate, however, varies rapidly as a function of the plate potential. If the plate is but a few volts positive with respect to the cathode (as shown at the extreme left of the graph by the solid line), a small electron current is collected by the plate and indicated on the milliammeter; the remainder of the current supplied by the cathode goes to the screen (as shown by the dotted curve of Fig. 1). As the plate potential is increased, however, the plate current diminishes and even reverses in sign. This is due to the increased energy of the electrons impinging on the plate surface. The electron current to the plate becomes negative when the average incident electron causes the emission of more than one secondary which is collected by the screen. Since in this case both the cathode and the anode

act as sources of electrons, the screen grid current is the sum of the two rather than the difference as in other parts of the curve.

As the potential of the plate becomes more nearly that of the screen, the percentage of secondary electrons collected by the screen grid is diminished. As shown in Fig. 1, the screen current falls and the plate current rises. When the plate becomes a few volts positive to the screen, few of the secondaries emitted at the plate can reach the screen, and the plate current becomes almost constant. The slight increase in the plate current above 150 volts must be due largely to the decreased number of secondaries from the plate which are able to reach the screen against the increased retarding potential and to an increase in the number of secondaries emitted by the screen which are drawn to the plate. A comparatively small portion of the change can be explained as increased emission of the cathode [5] or as leakage between the electrodes. Secondary emission and reflection phenomena, with which this paper is primarily concerned, thus dominate the determination of plate current as a function of plate potential. The influence of secondary emission might be further reduced and the plate resistance still further increased by inserting an additional grid near the plate and maintaining this grid at the potential of the cathode. This is done in "pentode" tubes. Since secondaries then experience a strong retarding force as they move away either from the plate or the screen grid, the emission of secondaries which might change the plate current is suppressed, and the grid nearest the plate in a "pentode" tube is therefore called a "suppressor grid."

While in tubes of the kind used here it is not possible to measure the ratio of the secondary emission to the primary current accurately,[6] it is possible to make an estimate of its value. For this purpose the difference between the electron current emitted by the cathode and that collected by the plate divided by the current emitted by the cathode may be used. If all the electrons emitted by the cathode reached the plate

[5] In ordinary triodes the change in plate current is dominated by the increased emission of the cathode.

[6] This task requires the use of special apparatus, one form of which has been described by the writer. (JOUR. FRANK. INST., 215, 593 (1933).)

and if all the secondaries emitted by the plate reached the screen grid, this computation would give accurately the desired ratio. The screen intercepts some of the primaries and fails to collect all of the secondaries; so that the ratio is somewhat in error. It will, however, be quite permissible to compare values obtained by this procedure with others obtained in the same way. This is done here.

A point of interest is that the curves of plate current against plate voltage are not exactly reproducible. This has been recognized by tube manufacturers, and certain parts of their graphs showing characteristics are marked with: "values unstable." Not only do such characteristics vary from tube to tube, but in a single tube they depend on the previous operation. Figures 2 and 3 (obtained in the same way as the solid curve of Fig. 1) indicate variations in the plate currents during the operation of two tubes of different make. The arrows indicate the direction in which the readings were taken.

While the plates in the '24 tubes are nickel, it is obvious that some form of contamination dominates the surface characteristics. The secondary emission obtained here (which reaches a value of more than one secondary per primary at energies for the primaries below 100 volts) is much higher than that obtained from clean nickel (for which the ratio becomes greater than unity only at primary energies considerably above 100 volts).[7] This influence of a foreign substance in increasing the secondary emission from a plate was early recognized by Hull [3, 4] and used by him in the construction of his tubes. The variation of the secondary current from tube to tube may be explained as accidental variations in the amount of contamination. If the substances within the tube can be removed from electrodes as they heat in normal operation, the variation of the plate current while the tube is being used may be explained. Several experiments were performed to determine what might move about in this way.

Several '24 tubes assembled from standard vacuum tube parts were evacuated by the writer. All of these special tubes were exhausted by a two stage mercury condensation pump backed by an oil pump. Liquid nitrogen was main-

[7] Petry, *Phys. Rev.*, **26**, 346 (1925).

FIG. 2.

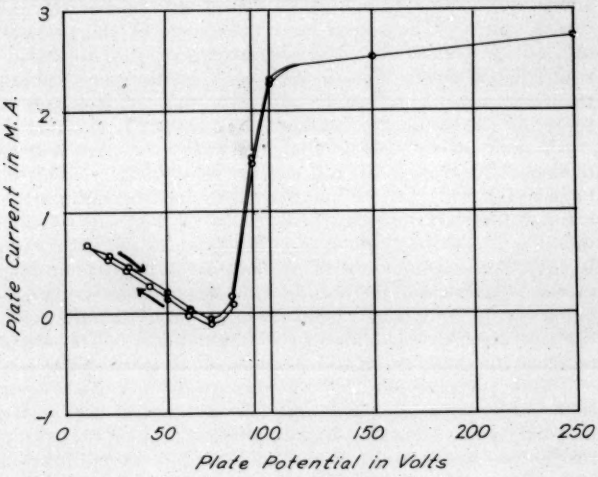
Plate Current in M.A.
3
2
1
0
-1
0
50
100
150
200
250
Plate Potential in Volts

FIG. 3.

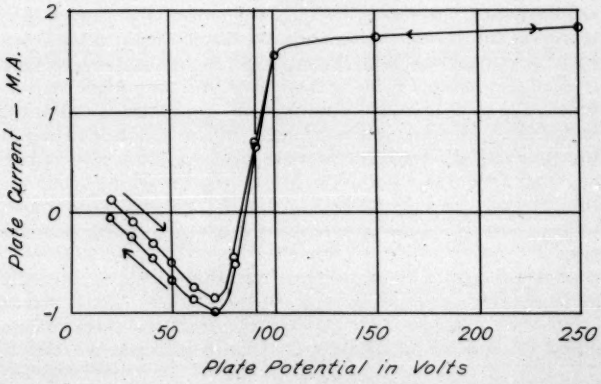
Plate Current — M.A.
2
1
0
-1
0
50
100
150
200
250
Plate Potential in Volts

tained on a cold trap throughout the pumping and baking schedule. The tubes were first baked in an electric oven at 350 to 400° C. for two or three hours. The metal parts were then raised to red heat in an induction furnace. After this the tubes were baked in the electric oven for another hour. At the end of the baking schedule, the cathodes were activated by running the direct heaters (which normally operate on 2.5 volts) on potentials as high as 5 volts for at least thirty seconds. This treatment causes a breaking down of the carbonates in the cathode coating with the liberation of CO_2 and it renders the surface active. Cathodes were aged by running tubes at normal voltage on the pumps for 10 or 15 minutes. As a final step in the treatment, the metal parts were again raised to a bright red heat by induction. Immediately following this treatment a given tube was sealed from the pumps. Although getter was included within the tube, it was not liberated by heating the cup.

Tubes obtained by this procedure had characteristics which differed from those in common use. When the tubes were first placed in operation at abnormally low cathode temperatures, the screen grid was maintained at 140 and the plate at 100 volts positive to the cathode. Readings were taken of the electron current supplied by the cathode and the currents collected by plate and screen. From these readings the ratio of the secondary current to the primary current was estimated by the procedure described above. The results, as shown in Fig. 4, indicate a secondary emission at the start of the run which is not much in excess of that expected from clean nickel. As the cathode was heated to normal operating temperatures (heating current about 1.75 amperes), the ratio of the current leaving the target to that incident on it increased. The rate of increase in the secondary emission became more marked as the temperature of the cathode was raised above recommended operating temperature.[8] When the temperature of the cathode was reduced, the secondary emission did not return to its initial value. Figure 4 thus gives unmistakable

[8] This effect is masked somewhat through the reduction of secondary emission by space charge which took place at the higher current densities. Some of the apparent increase of the secondary emission as the heating current is reduced is due to the reduction of space charge.

FIG. 4.

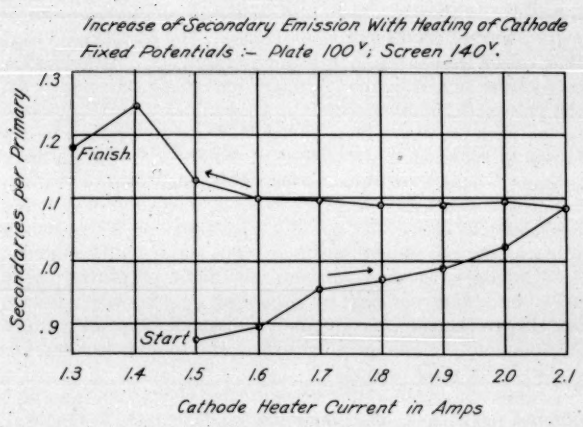

evidence of some change in the condition of the anode during the operation of the tube.

After several hours of operation, the tube was allowed to stand idle for several days. When placed in operation again, the secondary emission from the plate was high as it had been when taken out of use. The tube was then placed in an induction furnace and the plate was raised to a bright red heat. When the tube was placed in operation after this treatment, the secondary emission was again almost as low as it had been at the start of Fig. 4, and it increased as the tube was operated in substantially the same way. All this experimental work indicates that the active material of the cathode evaporates at normal operating temperatures and covers the plate.

After several hours of operation for such a tube, the secondary emission became stable. It was then possible to obtain reproducible curves of plate current as a function of plate potential like curve 1 of Fig. 5.

After such results, the getter cup was heated by induction until the magnesium getter was evaporated onto the glass walls. The tube was operated several hours. In the absence

of liberated getter, this should have resulted in rather stable conditions. The results actually obtained, however, showed variations in the plate current during the operation of the tube (indicated in curves 2 and 3 of Fig. 5) which were fully as large as the changes observed with commercial tubes.

FIG. 5.

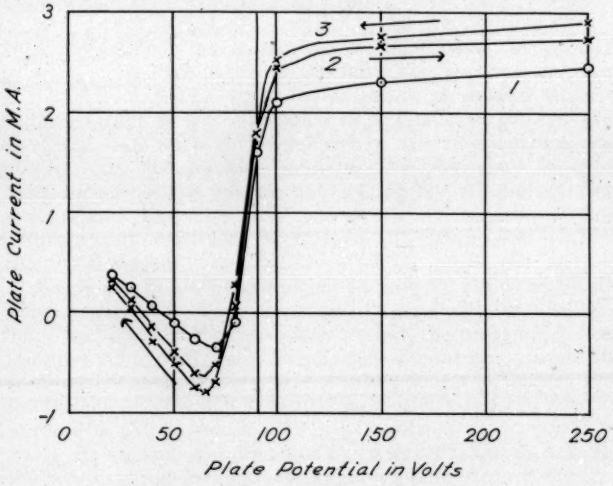

SUMMARY AND DISCUSSION OF RESULTS.

The plates in the carefully evacuated experimental tubes described here could be cleaned by heating until the initial secondary emission obtained from them was but little higher than that obtained from clean nickel. The evaporation of material from the cathode soon contaminated the plate and increased the secondary emission. After considerable operation of tubes without free getter, reproducible results were obtained, indicating presumably that after a certain stage, the evaporation of further material onto the plate failed to change the secondary emission.

The liberation of getter in the tube reduced the stability of the results attainable. This indicates that the surface conditions at the plate change as the tube is operated. The interpretation may be that getter is removed from the plate by the normal heating of the plate during the operation of the tube.

THE POSSIBILITY OF THE EMISSION OF POSITIVE ELECTRONS FROM THE NUCLEUS BY γ RAYS.

BY

ARTHUR BRAMLEY, Ph.D.,

Assistant to the Director.

BARTOL RESEARCH FOUNDATION

Communication No. 76.

Various speculations have been made concerning the structure of the nucleus. The early investigators of nuclear physics supposed that it was composed of α particles, protons and electrons; but with the discovery of the new entities, the neutron and the positive electron, the physicist's ideas of the structure of the nucleus have changed. A number of investigators [1] have recently advanced the suggestion that neutrons and positive electrons form the entities out of which the nuclei are built.

Curie and Joliot [2] have obtained positive electrons by the bombardment of aluminium and boron with α particles. This fact has led them to suppose that the proton is a combination of a positive electron and a neutron. From the reaction $B^{10} + \alpha \rightarrow C^{13} + n + \epsilon^+$ they found an upper limit for the binding energy between the neutron and the positive electron in the proton of 5×10^6 el. volts.

If the nucleus contains entities of small mass, such as the positive electron, we should expect a photo-electric emission of these particles when the nucleus is radiated with sufficiently hard γ rays. The photo-electric effect for a frequency ν of the photon is determined primarily by two factors, the mass of the entity and the binding energy E_{n0}. From an application of wave mechanics, we find for the effective cross section σ the expression

$$\sigma = \frac{8\pi}{3} N \frac{e^4}{m^2c^4} \left\{ \frac{(h\nu)^2}{(E_{n0})^2 - (h\nu)^2} \right\}^2, \qquad (1)$$

[1] Sexl, *Nature*, **132**, 174, July 1933. Mandel, *Phys. Zeits. der Sowjetunion*, **3**, 551, 1933. Grinberg, *Comptes Rendus*, **197**, 318, 1933. Anderson, *Phys. Rev.*, **43**, 491, 1933. Elsasser, *Nature*, **131**, 764, 1933.

[2] Curie and Joliot, *Comptes Rendus*, **197**, 237, 1933.

where **N**, **e** and **m** are the number, charge and mass respectively of the entities in the nucleus. From this formula we see that the mass of the particle is of primary importance in determining the efficiency of the process.

In their experiments on the bombardment of boron with α particles, Curie and Joliot have obtained positive electrons. The theory of the creation of pairs applicable when the primary entity is a photon or high energy particle does not seem able to account for the presence of positive electrons in these experiments, so that they may be taken as evidence of the correctness of the supposition advanced by various investigators that positive electrons exist in the nucleus.

The formula for the efficiency of the photo-electric effect of positive electrons within the nucleus combined with a knowledge of an upper limit of 5×10^6 el. volts for E_{n0} shows that the photo-electric effect of positive electrons should be realizable with γ rays attainable from radioactive sources. If the nucleus, however, were composed of heavy particles, for example protons, the efficiency of the photo-electric emission of the protons under the action of γ rays would be negligible.

The application of formula (1) to a limited region like the nucleus involves assumptions which are extremely problematical. However, an examination of the application of the wave mechanics reveals that the parts played by **m** and by the relationship of E_{n0} to $h\nu$ are such as to transcend such modifications of the fundamental equation as would be necessary to justify its application to the nucleus.

THE ELECTRICAL BREAKDOWN OF LIQUID DIELECTRICS.

BY

F. M. CLARK,

General Electric Company, Pittsfield, Mass.

ABSTRACT.

Throughout this paper data have been presented showing that the apparent inconsistency of the reported dielectric strength behavior of insulating liquids can be satisfactorily correlated if proper consideration be given to the state of the "purity" of the liquid itself. As a result it is suggested that insulating liquids should be classified as (*a*) "pure," indicating those liquids free from dissolved gases as primary "impurities"; and (*b*) "impure," including those liquids which contain dissolved gas. The breakdown mechanism depends on the distinctive behavior of these two general classes. "Pure" liquid breakdown is a function of charged particle formation. In part, this may be caused by the assumption of a charge by molecular aggregates, colloidal-like in nature. In part, the charge may arise from molecular ionization by collision. The latter occurs chiefly in the voltage range immediately preceding electrical rupture and is the chief cause of "pure" liquid insulation failure. The presence of the first type of charge—that is, the existence of a difference of potential between molecular aggregates and the liquid—is chiefly responsible for the variation in the time factor to breakdown.

The breakdown of "impure" liquids is a function of dissolved gas elimination. This dissolved gas is eliminated as a result of changing solubility produced (*a*) by electro-striction effects, or (*b*) by changing pressure or temperature. The presence of secondary impurities such as dust particles and fibers, acts chiefly through the effect on increasing gassing tendencies.

It is suggested further that the localization of dielectric breakdown in liquids, irrespective of the type or degree of "purity," is chiefly in the "neutral membrane" located near the electrodes and formed by the discharge of particles. Such a "neutral membrane" results in a space charge effect giving marked drop in potential and as a result promoting ionization by collision effects in "pure" liquids and electro-striction effects in "impure" liquids.

The dielectric strength of insulating liquids has been the subject of careful investigation. A vast amount of data has been accumulated forming the basis of numerous explanations of the phenomena involved. Unfortunately, in many instances the subject has received theoretical analysis without proper attention to the physical and chemical condition of the liquids investigated.

Mineral oil, as representative of liquid insulation, has received special attention. The nature of oil conductivity

has been intensively investigated. Such work has thrown little, if any, light on those factors which determine the ultimate dielectric strength of the material. No relation between electrical conductivity and dielectric strength has been established or seems likely to be established. Specially purified oils with conductivity decreased to an abnormally low value show no consistently higher dielectric strength than the more conducting types. Liquids, normally characterized by relatively high dielectric losses even when pure, show as good if not better resistance to dielectric breakdown as do the best refined mineral oils. Oxidation of oil, although increasing the conductivity, shows no effect on the dielectric strength. It is obvious that liquids of different chemical type should show conductivities of a different nature; that the type of conductivity in an oil should depend on the degree of oxidation, factors which can be expected to have little effect on the dielectric strength.

Perhaps the most widely accepted theory of liquid breakdown is that suggested by Gunther-Schulze (1). In accordance with this suggestion, the liquid itself is vaporized as a result of the kinetic motion of charged particles. Such vaporization results in ionization under voltage, leading ultimately to dielectric breakdown. The dielectric strength of a liquid, therefore, depends on a variety of factors—ion size, liquid viscosity, heat of vaporization of the liquid, its density and the ionization potential of its vapor. To separate and clearly evaluate the various factors of importance in determining the dielectric strength of the liquid, in accordance with the Gunther-Schulze suggestion, is difficult. Accumulated data, however, appear to indicate that liquids of the same chemical type (for example, the hydrocarbons) have high dielectric strength values, independent of those factors which should be of controlling importance under the Gunther-Schulze hypothesis.

It is the object of the present paper to offer an explanation of those factors which determine the dielectric strength of insulating liquids.

CLASSIFICATION OF INSULATING LIQUIDS.

In considering the dielectric strength characteristics of insulating liquids, classification must be made in two groups.

These groups, unlike the usual classification of insulating materials, are not based on fundamental physical and chemical distinctions but on the state of "purity." In the first group are classed those liquids designated as "pure." The distinction is not based on chemical purity of the usual type but rather on the presence or absence of dissolved gases. A "pure" liquid in this sense is a totally degassed product. It may consist of a mixture of two or more liquids of essentially similar physical and electrical characteristics as, for example, a mineral oil or a mixture of isomers such as those present in technically pure xylene or the chlorinated benzenes. The essential feature is the absence of dissolved air or other soluble gases.

An "impure" liquid, on the other hand, is a material completely or partially saturated with dissolved gas. The dissolved gas is considered as the major impurity. Secondary impurities which act only in their effect on the dissolved gas characteristics are dust particles, fibers and other insoluble or partially soluble foreign materials.

Such a classification of insulating liquids is recognized as a difficult distinction in the region approaching a totally degassed state. The importance of dissolved gases in determining the dielectric strength characteristics of insulating liquids, however, compels this classification.

THE CONTRASTING BEHAVIOR OF "PURE" AND "IMPURE" LIQUIDS.

The published literature of insulating liquids is filled with apparent inconsistencies. The effect of temperature has been shown to lead to decreased as well as increased dielectric strength. The effect of pressure has been stated to be both of negligible and of marked importance. No agreement has been reached describing the relation of gap distance to breakdown. Even the presence of water has no well-recognized result. Such inconsistencies disappear, however, if proper consideration be given to the "purity" of the liquid tested.

THE TRANSITION OF A "PURE" TO AN "IMPURE" INSULATING LIQUID.

Since the fundamental classification of insulating liquids is based on the degree of gassification, it is of importance to trace the dielectric strength of an insulating liquid as it passes

from the "pure" to the "impure" state. Such a transition is shown in Fig. 1. Here an almost completely degassed ("pure") liquid is allowed to absorb air. With air absorption, the dielectric strength falls to a minimum, further gas absorption leading to increased dielectric strength as the gas saturated value is approached. The initial drop in dielectric strength constituting as it does a 28% change demands investigation and immediately challenges explanation of the phenomena involved.

FIG. 1.

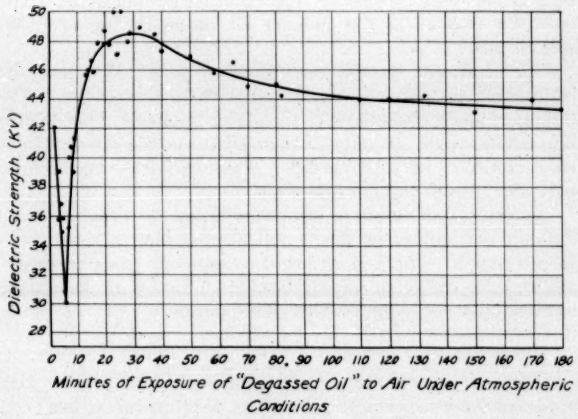

The dielectric strength of transformer-oil as a function of its dissolved air content (2). (*Note:* The oil is degassed at 700 microns pressure before test. It is then exposed to air and tested for breakdown as illustrated.)

THE ELECTRICAL CONDITION OF INSULATING LIQUIDS.

Insulating liquids contain charged particles. Conductivity, even in the most chemically pure, non-polar liquids, although low is always present. Compton and Foulke (3) have shown that in air the formation of corona leading to spark-over is greatly affected by radioactive radiation from the earth. A similar effect is obtained on insulating liquids (4). Radiation with ultra-violet light gives ion formation, probably caused by molecular disintegration. A similar effect pro-

duced under the milder action of daylight has been demonstrated by Schrader (5). With the higher testing voltages needed for dielectric breakdown, charged molecules or molecular aggregates, colloidal in character, may be the fundamental current-carrying particle. Irrespective of the means of formation, the presence of these charged bodies must not be ignored.

The presence of charged particles in mineral oil has been demonstrated by Oelschlager (6). Under A.C. or D.C. voltage, a mass movement of mineral oil can be observed. With uni-directional voltages, the movement in the narrowest part of the field is from cathode to anode. At greater gap distance, it is the reverse. With changed polarity, the movement is altered accordingly. Under A.C. potential, the movement, although clearly evident, is somewhat less vigorous. These and related observations (7) (8) demonstrate the presence of charged particles in oil.

The dielectric strength of liquids, irrespective of "purity," is a direct function of the presence of charged particles. The presence of these charged particles, however, is manifested in a manner dependent not only on the condition of the test, but also on the "purity" of the liquid as well. Under exactly the same conditions, the dielectric strength may respond in an entirely different manner depending on the degree of "purity" of the liquid tested.

MANIFESTATION OF CHARGED PARTICLES.

In the usual dielectric strength test, the liquid is tested with its normal amount of dissolved gas (generally air). Such liquids are designated by the classification suggested as "impure." The explanation of the behavior of "impure" liquid under varying physical conditions is based on the elimination of the dissolved gas and its subsequent ionization under voltage stress. No need exists to localize the initial ionization although it occurs in all probability in the region of greatest potential difference. It remains, however, to determine the cause of the elimination of dissolved gas by the liquid. It is definitely not due to liquid vaporization since there appears no relation between the thermal and dielectric properties of the liquid in the "impure" state.

There are two probable causes of gas elimination in "impure" liquids, both of which may be involved and both of which would allow gas elimination in the region of greatest stress concentration. These causes are (*a*) hollow space formation resulting from the kinetic motion of charged particles, and (*b*) electro-striction effects.

Hollow space formation occurs in the wake of spheres moving rapidly through water. This has been demonstrated by Schmieden (9) and Ramsauer and Dobke (10). The formation of such hollow space in "impure" liquids, being a function of speed of motion, would give the most pronounced gas elimination in the region of greatest stress. A necessary corollary, however, would demand that for the same chemical type increased molecular weight would give decreased gassing and therefore increased dielectric strength, a phenomenon which in some cases at least is true as is shown by the increased dielectric strength of the more dense insulating oils as compared to the lighter transformer oils. Such effects, however, involve a variety of factors—usually increased viscosity and changing gas solubilities—so that a clear illustration of the effect is not easily possible. At the present time, it can only be concluded that the motion of charged particles may, and probably does, contribute to increased dissolved gas elimination with resulting disastrous effects on the dielectric strength of "impure" dielectric liquids.

A second explanation of the gassing of "impure" liquids involves the phenomenon of electro-striction (11) (12) (13). Changing liquid volume under electric stress gives reduced gas solubility. Electro-striction involves ionic and molecular forces. Electrically neutral, di-polar molecules have an effect of the same order of magnitude as ions. Electro-striction decreases as the applied pressure increases. This phenomenon appears to be of major importance in determining the dielectric strength of "impure" insulating liquids.

Although the explanation of "impure" liquid breakdown is, like that suggested by Gunther-Schulze, an ionization effect, the two explanations are fundamentally different. As already stated, Gunther-Schulze suggests liquid vaporization as the fundamental factor. The explanation suggested in this paper definitely eliminates the liquid as being of major

importance. The gas pocket formed owes its source to the presence of dissolved gases in the liquid. Thus breakdown of this type becomes a distinct function of the nature and solubility characteristics of the dissolved gases present and independent of those liquid properties directly involved in the Gunther-Schulze theory.

With totally degassed liquids, classified as "pure," gas formation is not directly involved. Instead, the charged particles move to the electrode (anode in the case of mineral oil under D.C. voltage). There they are discharged and establish a film of neutral molecules resembling a semi-permeable membrane of colloidal-like characteristics, across which a difference in potential of high value is established. It is the rupture of this film which results in ionization and general dielectric failure.

Breakdown in pure liquids is determined by those factors which affect molecular ionization of the liquid itself. Following the research results obtained by Nikuradse (14), it seems evident that breakdown in "pure" liquids results from ionization by collision, subject to the same characteristics as observed in gases by Townsend (15) and others, modified as is necessary from the well-recognized characteristics of liquids under varying conditions of pressure and temperature as contrasted to similar behavior of gases.

Since gas elimination from "impure" liquids is a time-consuming factor, the shorter the time interval of voltage application, the more important becomes the semi-permeable membrane or film-forming action until with impulse breakdown, the classification of "impure" and "pure" liquids on the basis of the dissolved gas content disappears entirely. All breakdown then follows the necessary dictates of the "pure" liquid theory. The dielectric strength under such conditions reaches its maximum value.

STRESS DISTRIBUTION IN LIQUID DIELECTRICS.

In strong electrical fields, dielectric liquids become conductive. Investigation of the distribution of the electrical field in liquid dielectrics has shown that with polar materials at relatively low voltage there occurs a sharp rise in the field strength from the anode to the cathode. The field appears

to depend not only on the distance from the electrode surface, but also on the degree of purity of the liquid. Field distortion increases with the amount of moisture present (16) (17).

Working with transformer oil, Whitehead and Marvin (25) have demonstrated the presence of a space charge, the time of formation of which, together with the resulting non-uniform distribution of voltage, has been measured. Referring to the earlier work of Mie (26), these authors state, "he (Mie) finds and accounts for a steeper potential gradient near the electrodes, this gradient becoming less as saturation is approached."

At higher potentials with pure, non-polar dielectric liquids the current increases proportionally to the voltage applied (14), reaches a saturation stage in which increase in potential has little effect, and finally enters a third stage where the current again increases with increased voltage. Such behavior bears close resemblance to air and other gases and suggests ionization of neutral molecules as a result of the voltage applied. In the last stage of current increase with voltage, it becomes apparent that the charged molecules or molecular aggregates should closely parallel the behavior of polar molecules, the presence of which gives unequal field stress distribution between the electrodes, resulting in a steep potential drop in the region adjacent to the electrode surface. This steep potential drop promotes still further the formation of new ions or charged molecular residues or aggregates, thus introducing increased conduction and leading to insulation breakdown.

Schiller (18) from a study of experimental data and careful consideration of possible explanations of liquid insulation conductivity under high potential, has reached similar conclusions.

This marked drop in potential in the region of the electrode surface has already been referred to as an insulating semi-permeable membrane or film of neutral molecules resulting from the discharge of ions or molecular aggregates at the electrode. It is in this region of high potential stress that (*a*) electro-striction becomes pronounced, (*b*) kinetic motion of charged particles becomes accelerated, and (*c*) ionization by collision of liquid molecules reaches its maximum importance.

"PURE" INSULATING LIQUIDS.

The Effect of Pressure.

With "pure" insulating liquids, breakdown is a direct function of what has been called the "semi-permeable membrane" or "neutral film" formation resulting in localized high potential areas near the electrodes. The condition may be compared to a space charge phenomenon similar to that recognized in gaseous dielectrics. Because of the non-compressibility of liquids, the formation and rupture of this membrane is independent of pressure effects. The breakdown of "pure" liquids, therefore, should be unaffected by applied pressure. This is true. In Fig. 2 "pure" (degassed) xylol is

FIG. 2.

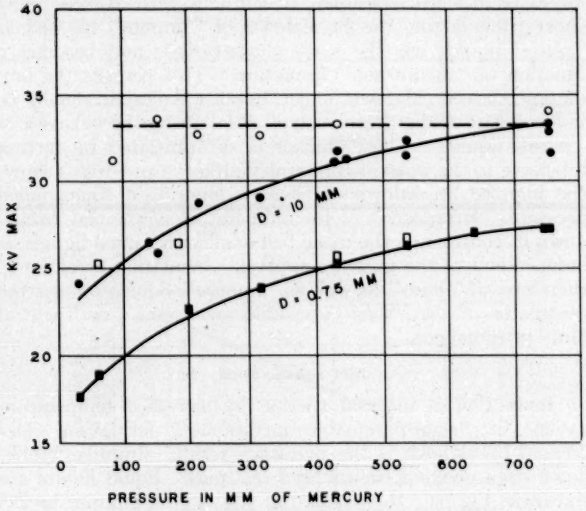

The relation between electrical breakdown and pressure for xylol under D.C. voltage at 20° C. (19).

■—Not degassed xylol .75 mm. gap.
□—Degassed xylol .75 mm. gap.
●—Not degassed xylol 1.0 mm. gap.
○—Degassed xylol 1.0 mm. gap.

studied at 20° C. under a uni-directional voltage. The data are those of the researches of Inge and Walther (19). With a gap distance of either 1.0 or .75 mms. degassed xylol shows a breakdown value independent of the pressure applied. The marked effect of pressure on "impure" xylol is given for comparison.

The Effect of Time.

The formation of the insulating membrane in "pure" liquids is, within limits, a time-consuming factor. The time value, however, is of short duration as compared to the time factor involved in the breakdown of "impure" liquids, which is described in subsequent paragraphs. Thus with decreasing time of voltage application, even gassed liquids should show increased dielectric strength. Eventually with an exceedingly short time factor, the breakdown of "impure" as well as "pure" liquids has the same characteristic and becomes a function of "membrane" formation. This permits the prediction that breakdown under impulse voltages should be independent of the pressure applied following the behavior of "pure" liquids. This behavior is substantiated by further reference to the work of Inge and Walther (19). Fig. 3 shows the impulse breakdown of oil as a function of the applied pressure. Irrespective of the temperature of the test, breakdown in contrast to the usual behavior with gassed liquids, is independent of the pressure applied. Insulation breakdown, therefore, of "pure" as well as "impure" liquids follows the postulates of the "semi-permeable membrane" or "neutral film" phenomenon.

The Temperature Factor.

Reduction of internal friction by increased temperature assists in "semi-permeable membrane" formation. Decreased breakdown is the necessary result. Impulse breakdown data obeying the dictates of "pure" liquid failure are shown in Fig. 3. Reproduced in Fig. 4, the impulse breakdown is shown to fall in a linear relation to the increase in temperature. Such behavior, as is illustrated in later discussion, is in direct contrast to the effect of temperature on the breakdown of "impure" liquids under 60 cycle test voltages.

FIG. 3.

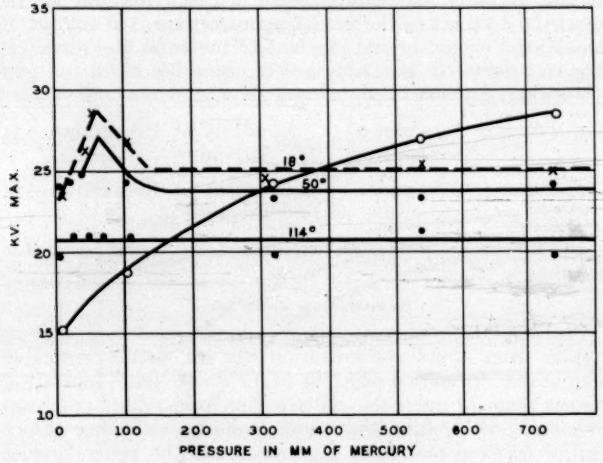

The relation between breakdown and pressure for mineral oil (19).

○—D.C. Voltage breakdown at 20° C.—.75 mm. gap.
●×—Impulse breakdown at temperature indicated—.30 mm. gap.

FIG. 4.

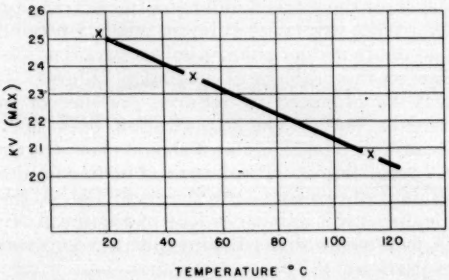

The relation between impulse breakdown and temperature for mineral oil.

(*Note:* These data are based on the experimental results of Fig. 3.)

The Gap Distance.

Since "pure" liquid breakdown is a function only of the potential drop across the insulating membrane, the voltage at breakdown should be independent of the total gap distance. Figure 2 shows the breakdown of degassed liquids at two gap distances. Summarized, the data show:

Gap Distance—.75 mm.	Gradient at Breakdown—34 kv./mm.
Gap Distance—1.0 mm.	Gradient at Breakdown—34 kv./mm.

This behavior meets the demands of the "semi-permeable membrane" theory.

The Behavior at the Boiling Point.

In the breakdown of "pure" liquid insulation, failure results from stress concentration due to "semi-permeable membrane" formation adjacent to the electrodes. Ionization results from (*a*) molecular collision due to increased potential difference, or (*b*) from the assumption of a difference in potential between molecular aggregates and the neutral molecules in the liquid. Both causes of ionization are internal phenomena. The transition from the "pure" to the "impure" type of liquid breakdown already given in previous paragraphs demonstrates the changing behavior of a liquid as it passes from the first to the second state. A further illustration will show the marked difference in electrical properties manifested by the two types of liquid insulation failure.

A liquid at its boiling point involves vaporization by factors foreign to the problem of insulation failure. Thus the boiling may be produced by reduced pressure or increased temperature or both. The vaporization does not involve electrical causes. The breakdown should show the characteristics of a "pure" liquid. Breakdown of boiling liquids should be independent of pressure. As shown in Fig. 5, the breakdown of boiling xylol is independent of the means by which the liquid is brought to its boiling point (temperature and pressure variation).

At the boiling point, liquid vaporization eliminates dissolved gases and "pure" liquid behavior results. As the

pressure falls, the temperature remaining constant, the boiling of the liquid ceases, the liquid absorbs air or other gas in proportion to the pressure applied, and enters the classification of "impure" liquids. The breakdown at once becomes a function of the dissolved gas content, depends on pressure and temperature and other testing factors. The importance of

FIG. 5.

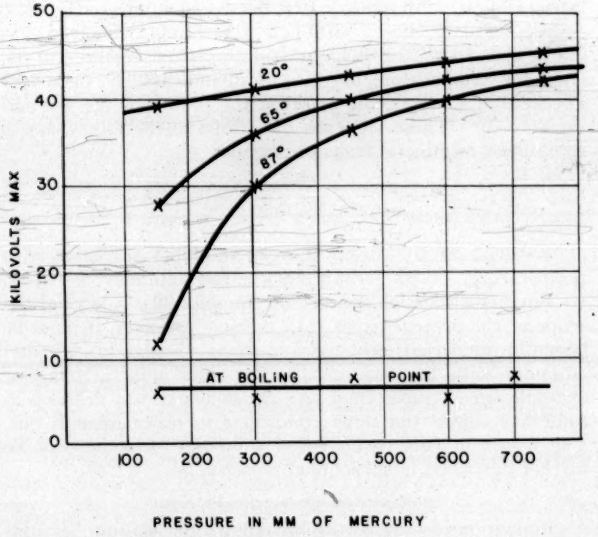

The relation between breakdown and temperature of xylol tested under A.C. voltages with a .75 mm. gap.

(*Note:* These data are based on the tests shown in Fig. 15.)

pressure on the two classes of insulating liquids is illustrated in Fig. 5. At the boiling point under the "pure" liquid conditions necessarily resulting, the breakdown is independent of both pressure and temperature. With reduced pressure, boiling is eliminated, dissolved gases are involved and breakdown becomes a distinct function of pressure and temperature.

"IMPURE" INSULATING LIQUIDS.

In considering the behavior of "impure" liquids, the focal point is the presence of dissolved gases, the effect of which may be modified by changing solubility in the liquid. This as once compels attention to those factors which affect gas solubility.

In a previous paper, the author has discussed the role of dissolved gases in determining the behavior of mineral insulating oils (2). All gases do not dissolve in liquids to the same degree. Furthermore, although the liquid dissolved gas obeys the postulates of Henry's Law as to pressure effects, changing temperature may result in increased or decreased gas solubility, depending both on the nature of the gas and the solvent. These facts are illustrated in the following gas solubilities in mineral transformer oils:

Air	10.8% at 25° C.	12.7% at 100° C.
Hydrogen	5.0% " "	7.0% " "
Carbon Dioxide	99.0% " "	50.0% " "

With air or hydrogen, the gas solubility increases with temperature. With carbon dioxide, gas solubility decreases.

Further discussion concerning gas solubility is beyond the scope of the present paper. In passing, however, it must be borne in mind that although a gas may dissolve in increased amounts with temperature rise for some mineral oils (for example, air in transformer oil), the same gas may decrease in solubility under the same conditions in other mineral oils. The result of this peculiar gas solubility behavior will be further described in subsequent paragraphs.

The Cause of Ionization in "Impure" Liquids.

Ionization leading to the breakdown of "impure" liquids under varying physical conditions results from the elimination of dissolved gases from the liquid under voltage stress. The initial gas elimination should occur at the point of greatest stress concentration. This under the suggested behavior outlined in previous paragraphs will occur adjacent to the electrodes in what has been called a "semi-permeable membrane" of neutral molecules. It has already been pointed out that stress concentration produces gas elimination from the liquid as a result of electrostriction effects. Breakdown then becomes a function of gaseous ionization.

Relation of "Impure" Liqiud Breakdown to Gaseous Breakdown.

Since "impure" liquid breakdown depends on the generation of a dissolved gas pocket, the breakdown of such insulating liquids should be a function of the electrical characteristics of the gases, modified as is necessary by the physical and chemical characteristics of the liquid itself. This is true. In subsequent paragraphs, this relation will be repeatedly observed.

The Type of Dissolved Gas Affects the Breakdown of "Impure" Liquids.

The dielectric strength of "impure" mineral oil tested under atmospheric pressure at 25° C. may be altered by the nature of the dissolved gas. The effect is related to the minimum sparking potential of the gas. This is illustrated in Table I (2).

TABLE I.

The Dielectric Strength of Transformer Oil as a Function of Its Gas Content at Atmospheric Pressure (25° C.).

Gas Used to Saturate the Oil.	Minimum Sparking Potential of Gas.	Average 60 Cycle Dielectric Strength of Oil Gas-Saturated at Atmospheric Pressure (Rapidly Applied Tests).
Hydrogen	302 volts	31.8 kv.
Air	341 "	34.8 "
Carbon Dioxide	419 "	36.1 "

For Small Gaps, the Breakdown of Air Increases.

Increased breakdown of air in small gaps results from "striking distance" phenomena. With gaps sufficiently small to bring into play the striking distance of gas generated pockets in oil, a similar effect should be observed.

The increase in dielectric strength of oil with decreased gap distance has been demonstrated by Dräger (21) and by Sorge (20). Figure 6 is taken from Sorge's published data. The increase in dielectric strength with decreased gap distance is clearly shown for xylol, hexane, benzine and oil.

With Larger Gaps, the Gradient of Air is Independent of the Distance.

For larger gap distance, the dielectric strength of oil becomes a function of the test set-up as a result of gas evolution and collection on the electrode surface. Under conditions which prevent gas accumulation effects on the electrode surface, the gradient at breakdown approaches a condition independent of the gap distance. Figure 7 reproduced from a previous article shows the relationship (2).

FIG. 6.

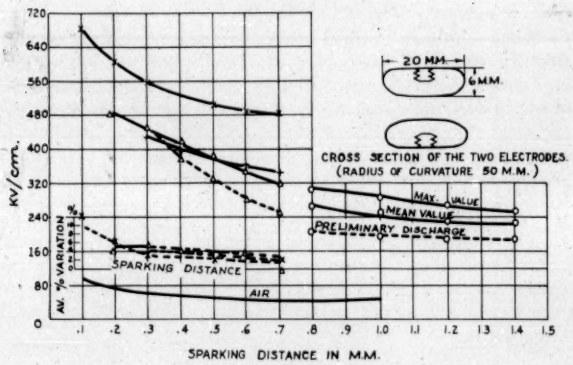

The effect of gap distance on the breakdown of liquid dielectrics (20).

X—Xylol.
+—Hexane.
△—Benzine.
O—Oil.

FIG. 7.

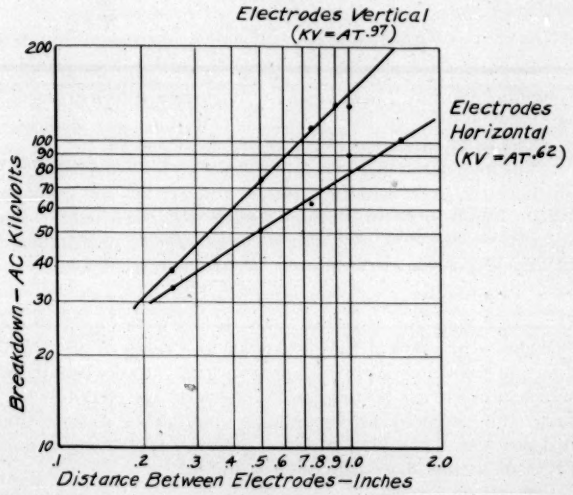

The relation between dielectric strength and gap distance for transformer oil tested at 60 cycles, 25° C. (2).

Dielectric Strength as a Function of Suspended Impurities.

The effect of dissolved gases in oil is stated to change the dielectric strength characteristic of the liquid through their elimination as a gas pocket. Secondary impurities present tending to assist gas elimination further serve to change the dielectric strength. The increased ease of gas evolution in such a manner is recognized in the well-known nucleus effect, the suspended particle acting as a nucleus of the formation of the initial gas bubble. Figure 8 reproduced from the researches of F. Schroeter (7) shows the increased strength obtained by the elimination of secondary impurities through filtration. With a gap setting of 1 mm., the dielectric strength is increased more than sixfold through the reduction of gassing tendencies produced by the removal of secondary impurities.

FIG. 8.

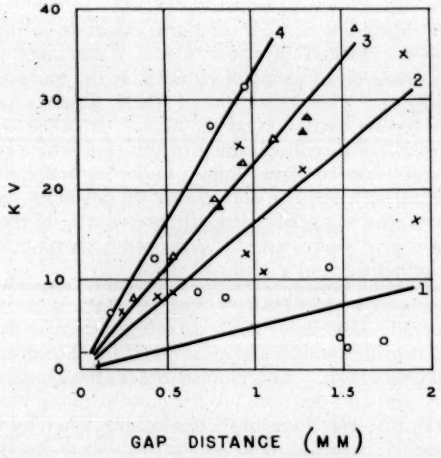

The dielectric strength of mineral oil as a function of dissolved liquid or solid impurities (7).

1.—Impure oil.
2.—Oil filtered through ordinary filter.
3.—One filtration through hard filter.
4.—Two filtrations through hard filter.

Microscopic Observations of the Behavior of Impurities in Oil Under Voltage.

Schroeter (7), Oëlschläger (6) and MacLaughlin (8) have each examined pure and impure mineral oil in the electrical field. In addition to the mass movement of oil already referred to, small bubbles and particles move irregularly with an intensity dependent upon the value of the field. They gradually approach the narrowest part, following the lines of force. Above all the irregular movements observed is a steady flow from cathode to anode.

Under alternating voltages, the action of microscopic fibers depends on the voltage applied. From a quiet condition, the fibers dance about, gradually accumulating in bundles. Materials of high dielectric constant or high conductivity are sucked into the field. Water and gaseous products are evolved as small bubbles on the surface of the fibers present. The ionization of these gaseous products results in corona formation on the fibers. It is the evolution and ionization of gaseous products of this type which are cited as the basic cause of liquid failure under normal conditions. The ease of such gassing determines the ultimate dielectric strength of the material. Impurities present in the liquid under test give decreased dielectric strength only in their effect in promoting gas evolution.

The Effect of Ease of Gas Formation and Escape.

As already described, the ease of gap escape from the electrical field determines the relation of the gap distance to electrical breakdown. This emphasizes the importance of the electrode type and position. With parallel, plain electrodes faced vertically (gap horizontal), gas bubbles when formed are easily ejected from the field as the combined result of oil circulation under voltage and the dielectric constant of the gas itself. With horizontally faced electrodes (gap vertical), the ease of gas ejection is reduced with resultant lowering of the dielectric strength of the liquid and a marked effect on the gap distance and electrical breakdown relationship. Such effects are illustrated in Fig. 7.

Agents tending to increase the gassing tendencies of the liquid under stress will lower the dielectric strength but have no effect on the dielectric strength—gap distance relation. This follows necessarily from the fact that the gap distance

relation to breakdown is affected only as the ease of gas pocket formation is altered. The data obtained by Schroeter (Fig. 8) illustrate the point. Irrespective of the degree of filtration, the ease of gas pocket formation remaining unchanged, the oil breakdown is always a linear function of the gap distance.

The Dielectric Strength of Air Decreases with Decreased Density to a Minimum Point Beyond Which Further Density Decrease Leads to Increased Dielectric Strength.

The breakdown of "pure" liquids is independent of applied pressure. With "impure" liquids, however, change in pressure reflects the relation of this type of liquid to its dissolved gas content. Just as the dielectric strength of air falls with reduced pressure, so the dielectric strength of "impure" oil

FIG. 9.

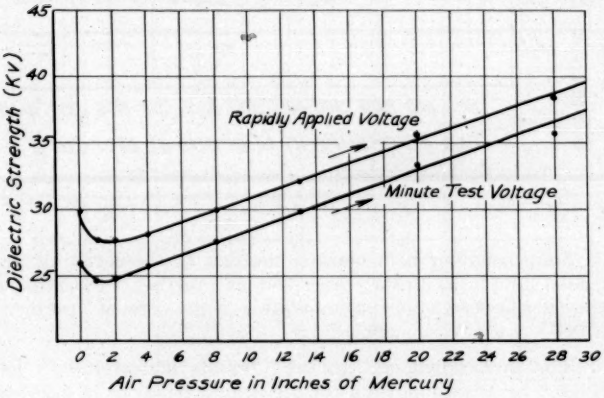

The A.C. dielectric strength of "impure" oil as a function of applied gas pressure (2).

falls. This is shown in Fig. 9. Whether tested by the so-called rapidly applied or minute (step-up) test, the dielectric strength falls to a minimum value beyond which further decrease in pressure leads to increased strength. That the change in dielectric strength with changing pressure is a function of the dissolved gas content is demonstrated by

Figure 10. Here the oil is evacuated at the pressure selected, thus controlling the amount of gas dissolved in the liquid. The liquid is then sealed to prevent gas re-absorption and is brought to hydrostatically applied atmospheric pressure. The dielectric strength is still a function of the dissolved gas content despite the fact that the liquid itself is under atmospheric conditions.

FIG. 10.

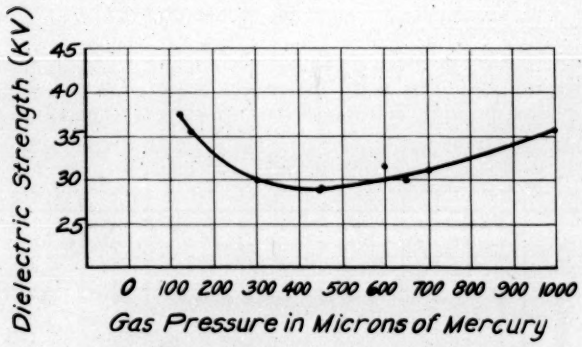

The dielectric strength of mineral oil as a function of dissolved gas content (2).

(*Note:* In this figure the dielectric strength of oil is determined under hydrostatically applied atmospheric pressure, the oil having been previously degassed at the gas pressure shown in the figure.)

Such behavior is in marked contrast to the action of degassed liquids, as already described, and further demonstrates the classification of insulating liquids on the basis of "purity."

The Effect of High Pressure Application.

The breakdown of "impure" liquids increases with increased pressure following the recognized behavior of gaseous breakdown. Since the dielectric strength of the latter does not increase indefinitely with pressure, it might be expected that oil would behave likewise. This is true. A second factor, however, must be considered. Electro-striction, so important in gas elimination from liquids, depends on the pressure, decreasing with increased pressure. Such an effect would also lend to the experimental results obtained by Kock who found that liquid materials increase in dielectric strength

with pressure but eventually reach a maximum value characteristic for each material (22). That all materials do not reach the maximum dielectric strength at the same high

FIG. 11.

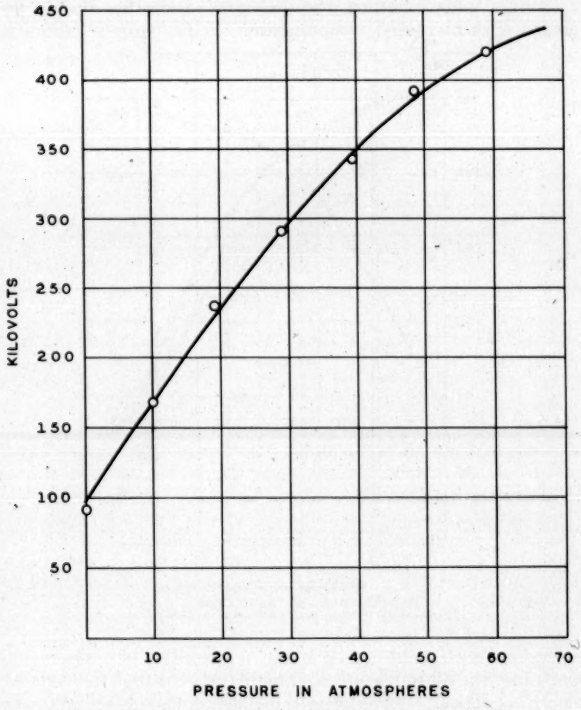

The effect of pressure on the dielectric strength of transformer oil (22).

pressure would be expected from the electro-striction-pressure relation varying from liquid to liquid.

Figures 11, 12 and 13 show the increase in dielectric strength of transformer oil, benzol and petroleum for high

pressure application. That the discontinuity in the pressure-dielectric strength relation at pressures between 20 and 50 atmospheres depends on the material itself is clearly illustrated.

The Dielectric Strength-Temperature Relation.

With "pure" liquids, the dielectric strength can only decrease with increased temperature. With "impure" liquids,

FIG. 12.

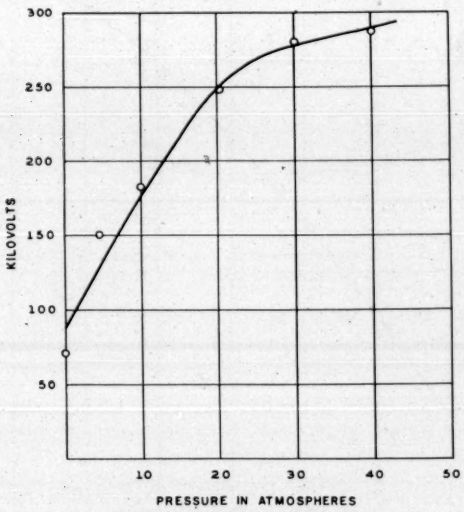

The dielectric strength-pressure relation for benzol (22).

no general statement can be made. The effect of temperature can affect the dielectric strength indirectly through its effect on electro-striction. Even then the effect of the major influence is modified by the changing solubility of the dissolved gas with changing temperature. For those gases whose liquid solubility increases with temperature, increased dielectric strength results. Where decreased solubility is obtained, decreased dielectric strength results. The effect is further complicated

by the fact that the same gas may increase in solubility with temperature in one liquid and decrease in another, thus giving increased dielectric strength with temperature for the first, and decreased dielectric strength with temperature rise for the second liquid. Figure 14 illustrates the behavior. Here

FIG. 13.

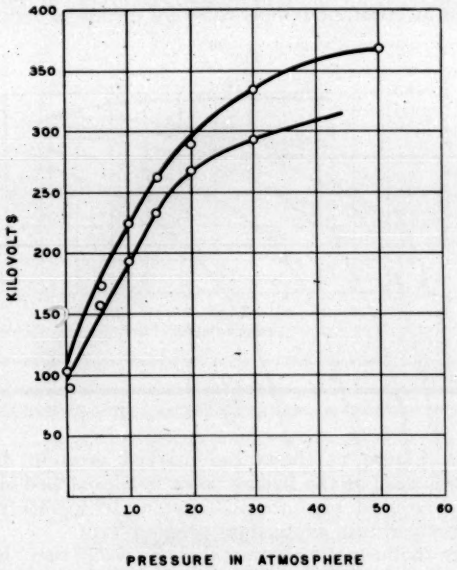

The dielectric strength-pressure relation for petroleum (22).

three liquids, oil, hexane and xylol, are illustrated (20). With oil, an increase in dielectric strength from 10 to 90° C. is obtained. With xylol the dielectric strength falls slowly over the same range of temperature. The more volatile hexane shows a more rapid drop in breakdown with temperature, the drop being more pronounced as the boiling point is approached. The drop in dielectric strength of hexane with

temperatures approaching the boiling point is characteristic of all insulating liquids. The effect is that of reduced gas pressure application. The increased vaporization of the liquid under test results in a changing pressure equilibrium between the gas above and the gas dissolved in the liquid, thereby increasing the gassing tendencies of the dissolved gas and giving decreased electrical breakdown. A similar effect is produced at constant temperature by means of reduced gas

FIG. 14.

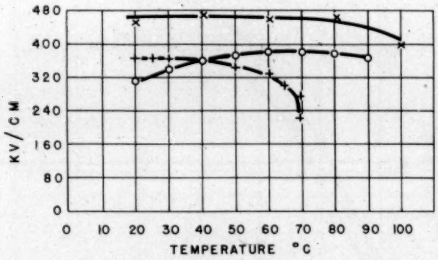

The dependence of disruptive field strength on the temperature—(Reference—Spath.)

X—Xylol.
+—Hexane.
O—Oil.

pressure. Figure 15 shows the marked drop in dielectric strength of xylol as the boiling point is approached either by means of reduced pressure at constant temperature or increased temperature at constant pressure (19).

Figure 16 illustrates contrasting behavior of two "impure" mineral oils tested in the author's laboratory. Both oils are from the same source. Oil *A* is of low viscosity and of the transformer type. Oil *B* is a more viscous cylinder oil. The dielectric strength of the former increases with temperature while that of the latter decreases. The explanation is found in the contrasting air solubility.

	% Air Solubility.	
	25° C.	100° C.
Oil A	10%	11.5%
Oil B	6%	4.8%

Decreased gas (air) solubility with increased temperature promotes gas pocket formation and results in the decrease in dielectric strength of Oil *B*.

The decreased dielectric strength with temperature above 100° C. for Oil *A* results from oil volatilization. This effect has already been discussed in previous paragraphs touching on the drop in dielectric strength of liquid dielectrics which is

FIG. 15.

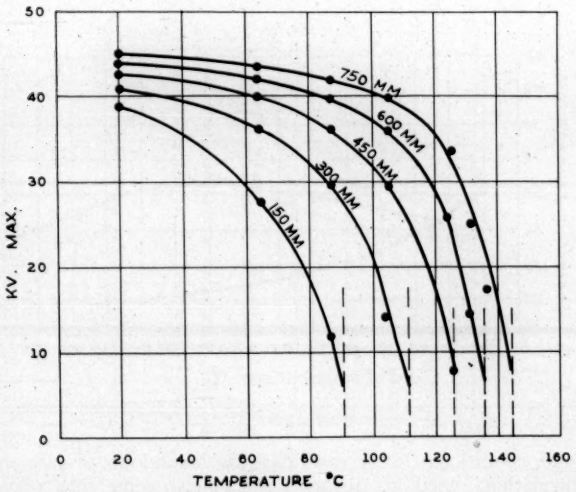

The dependence of breakdown on temperature for xylol at different pressures under A.C. voltage with a gap distance of .75 mm., using spherical electrodes (19).

met as the boiling point of the liquid is approached. With increased liquid volatilization, decreased gas solubility is obtained in accordance with the well-recognized partial pressure effects.

The Time Factor.

Gaseous breakdown involves a time factor of exceedingly short duration. Since breakdown of "impure" liquids involves secondary factors affecting gas elimination in addition

to gaseous ionization, the time to breakdown should be of longer duration. This is true. The shorter the time interval the more nearly the breakdown approaches that characteristic of the same liquid under impulse voltage, and, as has been shown also, the less the difference between the "pure" and "impure" classification.

With the breakdown of non-volatile liquids, involving electrostriction effects, the quantity of gases evolved is distinctly a time-consuming function. The breakdown under

FIG. 16.

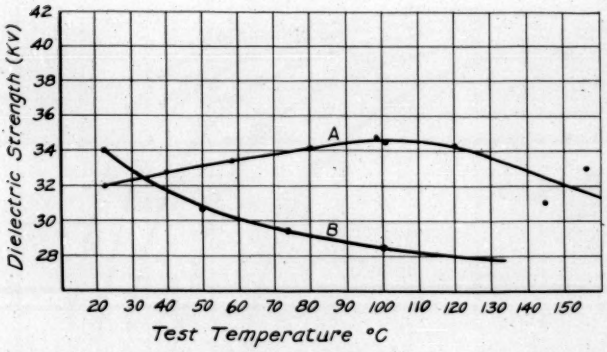

The dielectric strength-temperature relation for mineral oils tested at atmospheric pressure, 60 cycles.

such conditions closely resembles the breakdown of gaseous insulation. Striking distance phenomena come into play. As a result the breakdown falls continuously with increased time to a stable but lower level characteristic of the liquid being tested. This behavior is illustrated for oil in Fig. 17. With decreased time, the impulse breakdown is gradually approached and the gassing type of electrical failure merges into the impulse or molecular ionization type.

A study of the time effect on breakdown of different insulating liquids allows an insight into the normal electrical condition of the liquid. Peek has already shown (23) that for gases, breakdown occurs when ionic saturation is reached

along a given path. Previous ionization has an effect only on the time necessary for failure, the actual breakdown value (30 kvs./cm. for air) being unaffected. With "pure" liquids or with liquids tested under conditions approaching the impulse type of failure, electrical rupture involves charged particle formation in accordance with the ionization by collision mechanism. It can therefore be expected to resemble gaseous breakdown in its general characteristics. A comparison of pure xylol and mineral oil illustrates the issue.

FIG. 17.

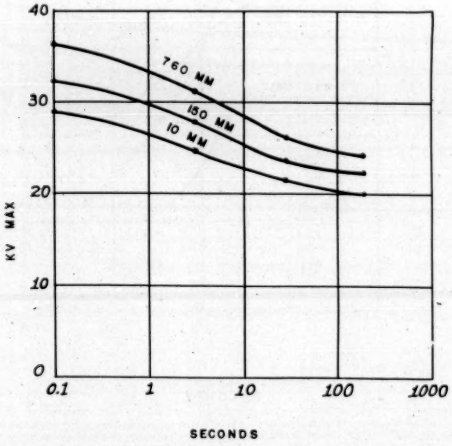

The relation between breakdown voltage and time for mineral oil tested under A.C. voltages with a .75 mm. gap at 20° C. (19).

In Fig. 17, the dielectric strength of oil increases continually as the time is decreased, the increased voltage to breakdown being applied as rapidly as 12,000 volts per second (19). Charged colloidal-like or ionic particles must necessarily exist in the oil in its normal condition. With xylol chemically purified, the reverse is expected and demonstrated. In Fig. 18, a definite time factor is observed. With voltage increased at a rate between 12,000 and 400 volts per second, no

effect on breakdown is observed. As expected, therefore, xylol is essentially an electrically neutral liquid, the charged particles being formed during the application of voltage.

FIG. 18.

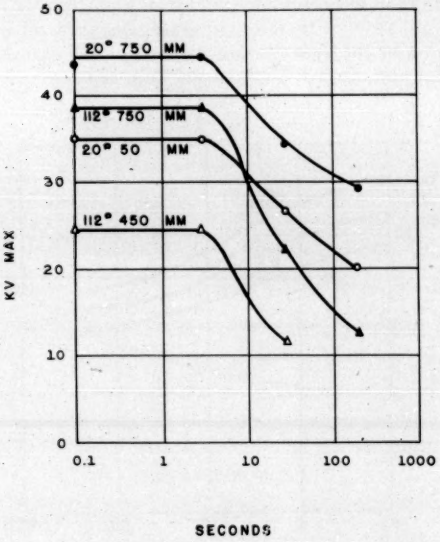

The dependence of breakdown on time for xylol at different temperatures and pressures when tested under A.C. voltage with a .75 mm. gap using spherical electrodes (19).

Figure 16 and Figure 17 are of further interest. Even with voltages applied as fast as 12,000 volts per second, the breakdown is still characteristic of the "impure" gaseous liquid. This is demonstrated by the marked effect of pressure wholly absent in the breakdown of degassed insulating liquids.

The Effect of Electrode Shape.

The radius of electrode curvature affects the breakdown of impure liquids only in the range of relatively short radii. In this respect, "impure" oils bear close resemblance to the

behavior of air. The dielectric strength of both air and the various liquids illustrated in Fig. 19 shows an increase with decreased radius of electrode curvature. The data are based on tests taken with disc facing disc, sphere facing sphere and point facing point, having a radius of curvature 5.0, 3.5 and .5 mm. respectively (20).

FIG. 19.

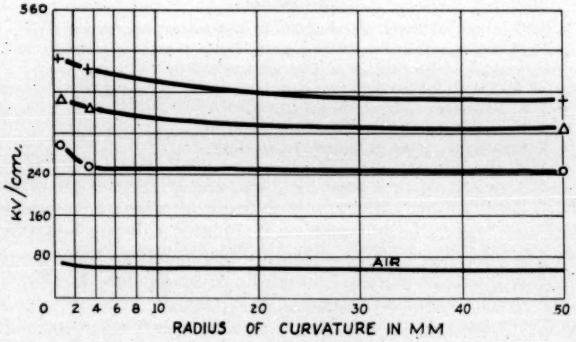

The relation of breakdown to radius of electrode curvature (20).

X—Xylol.
+—Hexane.
O—Oil.

The Effect of Frequency.

Space charge effects in gases decrease with increased frequency. A similar condition holds with reference to "semi-permeable membrane" or "neutral layer" formation for liquids. Since electro-striction and gassing effects become less pronounced with decreased stress concentration, an increase in dielectric strength with increased frequency is to be expected. This is true. Sorge (20), for example, reports the following data for tests made on hexane with copper discs using a gap of .5 mm.:

Frequency.	Dielectric Strength in Kvs. (Maximum) per Cm.
Direct Current	305
50 Cycles	335
500 "	456

As a result, the D.C.-A.C. (maximum) ratio decreases with increasing frequency.

Such relation must not necessarily be expected to hold true indefinitely. With extremely high frequency, gases may be eliminated from the liquid with resulting change in the relation of frequency to dielectric strength. The work of Richards and Loomis clearly anticipates such an effect (24).

BIBLIOGRAPHY.

1. A. GUNTHER-SCHULZE. *Jahrb. Radioakt Electronik*, **19**, 92 (1922).
2. F. M. CLARK. J. FRANK. INST., **215**, 39 (1933).
3. COMPTON AND FOULKE. *G. E. Rev.*, **26**, 755 (1923).
4. W. H. ELLER. *J.O.S.A.*, **20**, 71 (1930).
5. J. E. SCHRODER. *Elec. J.* **16**, 334 (1919).
6. E. OELSCHLÄGER. *Siemens Zeitschrift*, **1**, 29 (1925).
7. F. SCHROETER. *Arch. f. Electrot.*, **12**, 67 (1923).
8. T. A. MACLAUGHLIN. *Elec.*, **86**, 325 (1921).
9. C. SCHMIEDEN. *Ann. d. Physik.*, **2**, 3, 359 (1929).
10. C. RAMSAUER AND G. DOBKE. *Ann. d. Physik.*, **84**, 6, 697 (1927).
11. G. BRUHAT AND M. PAUTHENIER. *J. de Physique et le Radium*, **6**, 1 (1925).
12. GEHARDT JURG. *Z. Physik. Chem.*, Abt. B, **3**, 204 (1928).
13. A. L. TH. MOESVELD AND H. J. HARDON. *Zeit. Physik. Chem.*, A, **155**, 238 (1931).
14. A. NIKURADSE. *Naturwissenschaften*, **19**, 233 (1931).
15. J. S. TOWNSEND. *Trans. Int. Elec. Congress*, St. Louis, I, 106 (1904).
16. J. DANTSCHER. *Ann. Physik.*, **9**, 179 (1931).
17. G. YA DILLON. *Z. Physik.*, **61**, 386 (1930).
18. H. SCHILLER. *Zeits. Techn. Physik.*, **6**, 11, 588 (1925).
19. INGE AND WALTHER. *Archiv f. Elektrot.*, **23**, 279 (1930).
20. J. SORGE. *Archiv f. Elektrot.*, **13**, 189 (1924).
21. K. DRÄGER. *Archiv f. Electrot.*, **13**, 189 (1924).
22. F. KOCK. *Electrot. Zeits.*, **8**, 85 (1915); *Electrot. Zeits.*, **9**, 99 (1915).
23. F. W. PEEK. *A. I. E. E.*, 1695, (1915).
24. W. T. RICHARDS AND A. L. LOOMIS. *J. A. C.*, **49**, 3086 (1927).
25. J. B. WHITEHEAD AND R. H. MARVIN. *Trans. A. I. E. E.*, **49**, 647 (1930).
26. G. MIE. *Ann. d. Physik.*, **26**, 597 (1908).

THE AMPLITUDES OF NON-HARMONIC VIBRATIONS.

BY

J. P. DEN HARTOG.*

ABSTRACT.

Two new approximate graphical solutions are given for the problem of forced vibration of an undamped single degree of freedom vibrating system with a non-linear spring, whose characteristic is given in the form of a curve. One of these solutions gives much more accurate results than the approximation known so far.

INTRODUCTION.

In the usual theory of the vibration of an undamped single mass system, the spring is assumed to have a linear characteristic, i.e. the force-deflection diagram is represented by a straight line through the origin. It is known that the free as well as the forced vibrations of such a system can be completely calculated in all detail. This is entirely different when the spring characteristic ceases to be linear. Then only the *free* vibrations of the system can be determined for a given starting condition by a process of graphical or numerical calculation.[1] Though this is rather complicated and generally requires a considerable amount of work, at least the solution can be obtained with any desired degree of accuracy, according to the simple rule: "the more work, the greater accuracy."

The results thus found are by no means as general as those for the case of linear springs, because the natural frequency comes out to be dependent on the amplitude. Moreover, the principle of superposition ceases to be valid, so that each particular case has to be solved by itself.

When steady state *forced* vibrations are considered the situation becomes even worse. Here not only is there no superposition, but even the golden rule of "the more work, the greater accuracy" is no longer true. An approximate solution exists, originated by Martienssen [2] on the analogous

* Assistant Professor of Applied Mechanics, Harvard University.

[1] Timoshenko, "Vibration Problems in Engineering," pp. 72–81.

[2] O. Martienssen, *Elektrotechnische Zeitschrift*, 1910, p. 204.

electrical problem of the alternating current in a circuit containing a condenser and an iron cored inductance in series.

This solution was later applied to mechanical problems by Duffing [3] and by Rüdenberg.[4]

For the special cases of spring characteristics represented by an ordinary or by a cubic parabola, Duffing in his book gave a method whereby this result can be improved by successive approximations.

An exact solution was obtained by S. J. Mikina and the author for spring characteristics made up of three sections of straight lines.[5]

For that case (the only one for which an exact solution exists so far) a comparison was made with the approximation of Martienssen, showing that this approximation may be 75 per cent. off or more.

It is the object of this paper to propose two other approximate methods applicable to *any* kind of spring characteristic and to compare their results with those of the exact solution for the case quoted before.[5]

THE SOLUTION OF MARTIENSSEN.

The problem consists of finding a periodic solution to the equation:

$$m\frac{d^2x}{dt^2} + f(x) = P \sin \omega t, \qquad (1)$$

where $m\frac{d^2x}{dt^2}$ is the inertia force of the mass, $f(x)$ is the spring force and $P \sin \omega t$ the externally applied force. The spring force for a conventional or linear spring is written as kx, where k is the spring constant (expressed in lbs. per inch deflection). For a non-linear spring however it is necessary to give the characteristic in the form of a curve like Fig. 1. The ordinate of this curve is the spring force, while the abscissa is the deflection of the spring.

We want to find a periodic solution of equation (1) with the frequency ω. It is evident that this solution cannot be a

[3] G. Duffing, "Erzwungene Schwingungen bei veränderlicher Eigenfrequenz." Braunschweig, 1918.

[4] R. Rüdenberg, *Zt. f. angew. Math. u. Mech.*, 1923, p. 454.

[5] *Trans. A. S. M. E.*, 1932, Paper APM54, 15.

simple sine wave of the form $x_{max} \sin \omega t$. If such an assumption were made it is seen that the first term, the inertia force $m\frac{d^2x}{dt^2}$, is proportional to sin ωt. The right hand member of (1) is also proportional to sin ωt, but the spring force $f(x)$ is of an entirely different character. Therefore no sine wave can

FIG. 1.

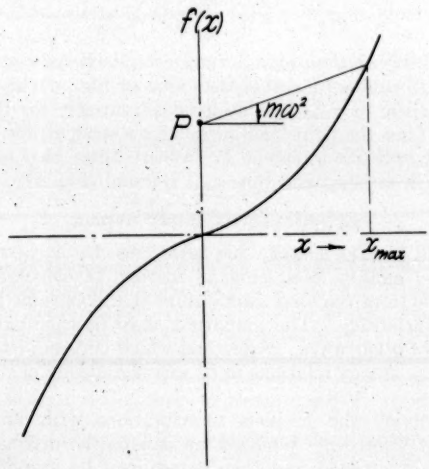

be the solution, which rather will be a curve of considerable complication.

Martienssen, however, assumed the solution to be a sine-wave $x_{max} \sin \omega t$ nevertheless, and then proceeded to calculate the amplitude x_{max} by satisfying a certain requirement. He could only satisfy *one* requirement, having only one parameter x_{max} to work with, whereas the exact solution really has an infinite number of requirements to be satisfied. He chose to put the three forces of eq. (1). in equilibrium at the *end of a stroke*. In other words he chose x_{max} such that at the point $x = x_{max}$ there is equilibrium between the inertia force, the spring force and the external force. The equation (1),

which requires that at any instant t, and consequently for any position x, the three forces are in equilibrium, is replaced by

$$-m\omega^2 x_{max} + f(x_{max}) = P, \qquad (2)$$

which coincides with (1) only for the instant $\omega t = \pi/2$ when $x = x_{max}$.

By writing (2) in the form

$$f(x_{max}) = P + (m\omega^2) \cdot x_{max}, \qquad (2a)$$

a graphical solution of x_{max} suggests itself at once. The left hand member of (2a) is the curve of Fig. (1): the spring characteristic, if x_{max} is considered as variable for the time being. Then the right hand member is a straight line of slope $m\omega^2$ and ordinate intercept P. Where these two meet the equation is satisfied and thus x_{max} is found (Fig. 1).

THE QUARTER-CYCLE ENERGY METHOD.

It will be appreciated, that after once having assumed a sinusoidal motion, Martienssen's method of calculating the amplitude from the force equilibrium at the extreme position is quite arbitrary. The amplitude may be calculated in a number of other ways. A method which suggests itself is to require the energy relations to be satisfied during one quarter cycle.

In solving the problem of vibrations with non-linear damping, Jacobsen [6] replaced an inherently non-harmonic curve by a sinusoid and then determined its amplitude by setting the energy dissipation per cycle equal in two cases. The method was very successful and gave an approximation differing surprisingly little from the exact solution for a special case.

In the present problem no damping has been assumed and consequently no energy dissipation per full cycle can take place. But during a quarter cycle some energy transformation occurs. At $x = x_{max}$ the energy is stored elastically in the spring, while at $x = 0$ it is all kinetic. For the classical case of a linear spring the kinetic energy is the smaller of

[6] L. S. Jacobsen, "Steady Forced Vibration as Influenced by Damping," *Trans. A. S. M. E.*, 1930, Paper APM52, 15.

the two below resonance and the greater of the two above it. The difference between the maximum potential and kinetic energies is made up as positive or negative work done by the external force during the intervening quarter cycle. In the non-linear case the potential energy is

$$\int_0^{x_{max}} f(x)dx$$

and, assuming sinusoidal motion, the maximum kinetic energy becomes $\frac{1}{2}m\omega^2x^2_{max}$.

The work done by the force $P \sin \omega t$ on the displacement $x_{max} \sin \omega t$ over one quarter cycle is easily found to be $\frac{1}{2}Px_{max}$. Thus

$$\int_0^{x_{max}} f(x)dx - \tfrac{1}{2}m\omega^2x^2_{max} = \tfrac{1}{2}Px_{max},$$

or

$$\frac{2}{x_{max}}\int_0^{x_{max}} f(x)dx = P + m\omega^2x_{max}. \qquad (3)$$

The essential difference between (2a) and (3) is that the former depends on one point (x_{max}) of the characteristic only, while the latter takes account of the integrated effect of the entire curve. The graphical construction of (3) is the same as that of (2a), except that instead of the characteristic curve $f(x)$ itself we use the curve representing $\frac{2}{x}\int_0^x f(x)dx$, which can be found from $f(x)$ by a simple graphical integration and division.

It can be immediately verified that (3) as well as (2a) give the same well known result if $f(x)$ is made equal to kx, i.e. for the case of a linear spring.

THE TWO-TERM APPROXIMATION.

It was seen that the solution to the problem is a curve of greater complication than a sine wave. We have prescribed it to be a periodic curve of frequency ω. For a symmetrical spring characteristic the motion must be symmetrical for each 90 degree section of Fig. 2. Moreover the force must be in phase with the fundamental harmonic of the motion, since there cannot be any work dissipation during a *whole* cycle

due to the absence of damping. This condition is also shown in Fig. 2.

The most general expression for the motion as limited by this figure is a Fourier series containing no cosine terms and no sine terms with even arguments:

$$x = a_1 \sin \omega t + a_3 \sin 3\omega t + a_5 \sin 5\omega t + \cdots. \quad (4)$$

FIG. 2.

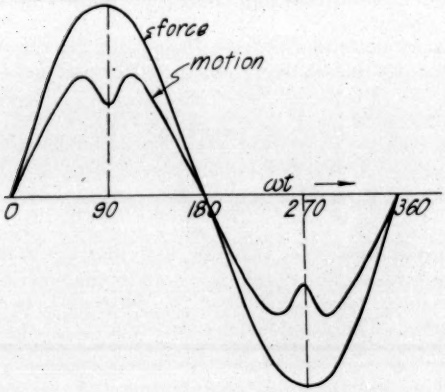

The spring *force* as a function of time due to this motion can be found from the spring characteristic, if a_1, a_3, etc., are known. At any rate it must be a curve subject to the same limitations as the motion:

$$f(x) = A_1 \sin \omega t + A_3 \sin 3\omega t + A_5 \sin 5\omega t + \cdots. \quad (5)$$

The various A's can be found from the a's by the spring characteristic only; but the a's are determined by the differential equation. Now let us substitute (4) and (5) into (1):

$$-m\omega^2 \sum_{1,3,\ldots} n^2 a_n \sin n\omega t + \sum_{1,3,\ldots} A_n \sin n\omega t = P \sin \omega t.$$

This can be written in the form

$$\sum_{1,3,\ldots} (A_n - m\omega^2 n^2 a_n) \sin n\omega t = P \sin \omega t. \quad (6)$$

Since this relation has to be satisfied at any instant of time it is necessary that the coefficients of sin ωt on both sides of the equality sign are equal, and the same holds for the coefficients of sin $3\omega t$, sin $5\omega t$, etc. Thus (6) is replaced by

$$\begin{aligned} A_1 &= m\omega^2 a_1 + P, \\ A_3 &= 9m\omega^2 a_3, \\ &\cdots \\ A_n &= n^2 m\omega^2 a_n. \end{aligned} \tag{7}$$

This satisfies the requirements of the differential equation. The problem consists of finding the values of a_1, a_3, a_5, $\cdots$, such that, when A_1, A_3, $\cdots$ are calculated from (7) the motion and the spring force will bear the relation to each other as is prescribed by the spring characteristic. In its general form the problem cannot be solved exactly. It is necessary to break off the series (4) and (5) somewhere.

If only one term each, a_1 and A_1, is retained we get

$$x = a_1 \sin \omega t, \qquad f(x) = (m\omega^2 a_1 + P) \sin \omega t.$$

The plot of $f(x)$ against x for this case will be the straight line shown in Fig. 1, and thus we are led back to Martienssen's approximation.

Now we advance a step and retain two terms each in the series (4) and (5). Then

$$\begin{aligned} x &= a_1 \sin \omega t + a_3 \sin 3\omega t, \\ f(x) &= (m\omega^2 a_1 + P) \sin \omega t + 9m\omega^2 a_3 \sin 3\omega t. \end{aligned} \tag{8}$$

Here we have two parameters a_1 and a_3 at our disposal, so that we can satisfy two requirements. The simplest solution is obtained by requiring that (8) shall give the correct relation between x and $f(x)$ at $\omega t = \pi/2$ or $x = x_{max}$ (Martienssen's requirement) and moreover that x and $f(x)$ shall be right at $\omega t = \pi/3 = 60$ deg.

Then

$$\omega t = \pi/2, \quad x = a_1 - a_3, \quad f(x) = m\omega^2 a_1 + P - 9m\omega^2 a_3, \tag{9}$$

$$\omega t = \pi/3, \quad x = a_1 \frac{\sqrt{3}}{2}, \quad f(x) = (m\omega^2 a_1 + P) \frac{\sqrt{3}}{2}. \tag{10}$$

For a graphical interpretation these are written somewhat differently, as follows:

$$f\left(a_1\frac{\sqrt{3}}{2}\right) = \left(P\frac{\sqrt{3}}{2}\right) + m\omega^2\left(a_1\frac{\sqrt{3}}{2}\right), \qquad (10a)$$

$$f(a_1 - a_3) = (P - 8m\omega^2 a_1) + 9m\omega^2(a_1 - a_3). \qquad (9a)$$

The graphical construction of the two amplitudes a_1 and a_3 can be performed as indicated in Fig. 3. Take the points P and $P\frac{\sqrt{3}}{2}$ on the vertical axis and as before in Fig. 1 draw from these points two parallel lines under an inclination $\tan^{-1}(m\omega^2)$. The lowest line intersects the characteristic at A, which point has the horizontal projection A'. An inspection of equation (10a) will show that the distance OA' equals $a_1\frac{\sqrt{3}}{2}$. In fact the construction of eq. (10a) is the same as that of equation (2a) where x_{max} is $a_1\frac{\sqrt{3}}{2}$ and P is substituted by $P\frac{\sqrt{3}}{2}$. Then by drawing a line through P parallel to the one connecting $P\frac{\sqrt{3}}{2}$ and A', the point a_1 is found whose abscissa is a_1. Now we proceed to equation (9a) which again is of the same structure as (2a) or (10a). In words equation (9a) reads: The value $(a_1 - a_3)$ is the abscissa of the intersection of the characteristic with a straight line of slope $9m\omega^2$ and ordinate intercept $(P - 8m\omega^2 a_1)$.

In the figure the distance BC has the length $m\omega^2 a_1$. Thus we take BC in the dividers and measure off eight times that length along the vertical axis down from the point P, arriving at D. It is clear that thus the ordinate of D is $(P - 8m\omega^2 a_1)$. The vertical distance between D and B is $DP + CB = 9m\omega^2 a_1$. The horizontal distance between D and $B = PC = a_1$. Thus if D and B are joined by a straight line its slope is $9m\omega^2$. This line represents the right hand side of (9a) if $(a_1 - a_3)$ is considered as the variable and a_1 is constant. The intersection E with the characteristic consequently gives the solution of (9a). The abscissa of E, being the distance OF represents $(a_1 - a_3)$. Consequently the distance a_1F has

FIG. 3.

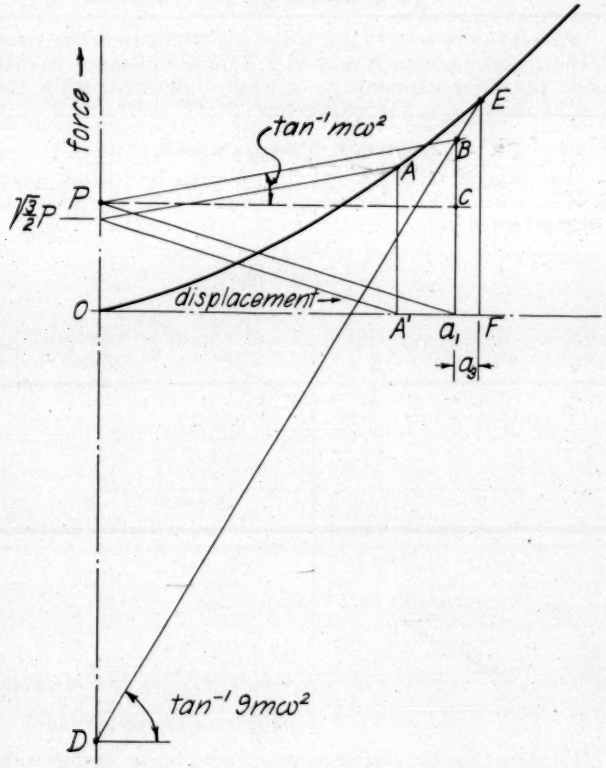

the length a_3, which is negative in the case under consideration.

It can be seen from Fig. 3 that a_3 is rather small with respect to a_1. On the other hand it takes but a very small change in the shape of the characteristic (leaving it pass through O and A) in order to shift the intersection point E

clear out of the drawing, which correspondingly means a very great value of a_3.

Also it can be seen that a rather slight change in the value of the disturbing force P may shift E quite a distance, so that again the third harmonic a_3 is vitally influenced while the first harmonic a_1 is hardly affected.

APPLICATION TO SPECIAL CASES.

The general results found thus far can be written down more specifically if certain simple shapes of the characteristic are assumed.

FIG. 4.

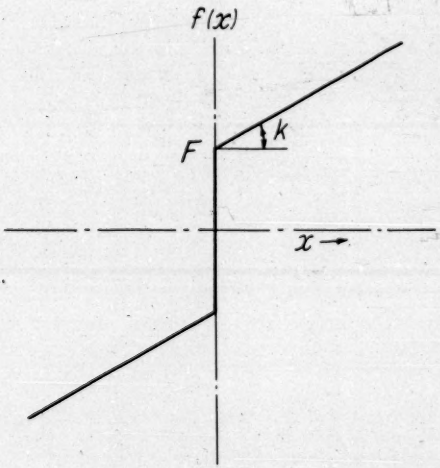

First we take the case of a system with linear springs with an initial set-up, of which the characteristic is shown in Fig. 4 and can be expressed by

$$f(x) = F + kx \qquad \text{for} \qquad x > 0.$$

The Martienssen solution for this is

$$x_{max} = P\frac{1 - F/P}{k - m\omega^2}. \tag{11}$$

The quarter wave energy method gives

$$x_{max} = P\frac{1 - 2F/P}{k - m\omega^2}. \tag{12}$$

The two-term approximation leads to

$$\begin{aligned} a_1 &= P\frac{1 - \frac{2}{\sqrt{3}}\frac{F}{P}}{k - m\omega^2}, \\ a_3 &= P\frac{\left(1 - \frac{2}{\sqrt{3}}\right)\cdot\frac{F}{P}}{k - 9m\omega^2}. \end{aligned} \tag{13}$$

The exact solution [5] has been found before in the form of an infinite Fourier series. The first two terms of this series are:

$$\begin{aligned} a_{1\ exact} &= P\frac{1 - \frac{4}{\pi}\frac{F}{P}}{k - m\omega^2}, \\ a_{3\ exact} &= P\frac{-\left(\frac{4}{3\pi}\right)\frac{F}{P}}{k - 9m\omega^2}. \end{aligned} \tag{14}$$

Next consider a set of springs with clearance

$$f(x) = k(x - a) \qquad \text{for} \qquad x > 0,$$

shown in Fig. 5.

The Martienssen result is

$$x = \frac{P + ka}{k - m\omega^2}. \tag{15}$$

The quarter wave energy method gives

$$x = \frac{P + 2ka}{k - m\omega^2}, \tag{16}$$

and the two-term approximation for this case becomes

$$a_1 = \frac{P + \frac{2}{\sqrt{3}}ka}{k - m\omega^2},$$
$$a_3 = a_1 + \frac{8m\omega^2 a_1 - P - ka}{k - 9m\omega^2}. \tag{17}$$

FIG. 5.

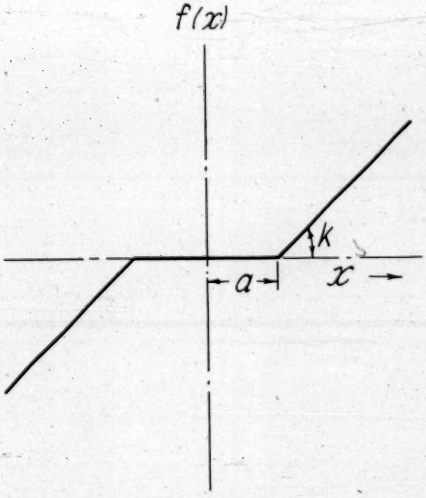

Finally let us take a parabolic characteristic $f(x) = px^2$ as shown in Fig. 6.

The usual Martienssen approximation gives:

$$x = \frac{m\omega^2}{2p} + \sqrt{\left(\frac{m\omega^2}{2p}\right)^2 + \frac{P}{p}}. \tag{18}$$

The quarter wave energy theory gives practically the same result: it is only necessary to replace p by $\frac{2}{3}p$ in (18). In the

two term approximation a_1 also has the same form (18); only p has to be replaced by $\frac{\sqrt{3}}{2}p$, while the third harmonic a_3 is

$$a_3 = a_1 - \frac{9m\omega^2}{2p} - \sqrt{\left(\frac{9m\omega^2}{2p}\right)^2 + \frac{P - 8m\omega^2 a_1}{p}}. \quad (19)$$

FIG. 6.

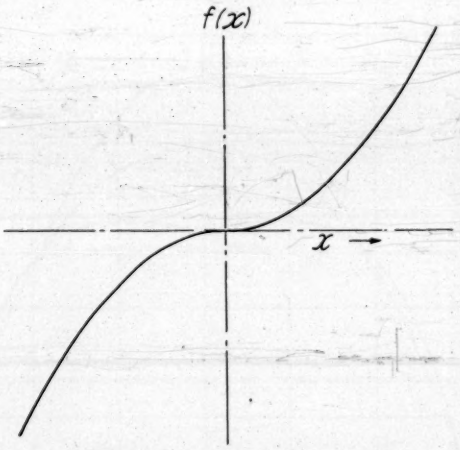

COMPARISON OF THE VARIOUS METHODS.

For the case illustrated in Fig. 4, an exact solution is available, so that a numerical comparison of the results of the various approximations is possible. It is noted that the structure of the various formulæ (11) to (14) is similar; their differences consisting only in the value of some numerical coefficients. The table below gives a picture of these coefficients:

Harmonic No.	Martienssen.	Energy.	Two Term.	Exact.
1	1	2	$1.16 = \frac{2}{\sqrt{3}}$	$1.27 = \frac{4}{\pi}$
3	0	0	$.16 = -\left(1 - \frac{2}{\sqrt{3}}\right)$	$.42 = \frac{4}{3\pi}$

It is seen that the quarter wave energy method gives a result which is quite inaccurate, much more so than the original Martienssen solution. This is rather surprising, since one would expect a calculation from an integrated curve to be more accurate than that considering one point only (though that point is an important one).

No simple physical explanation of this fact can be given by the author.

FIG. 7.

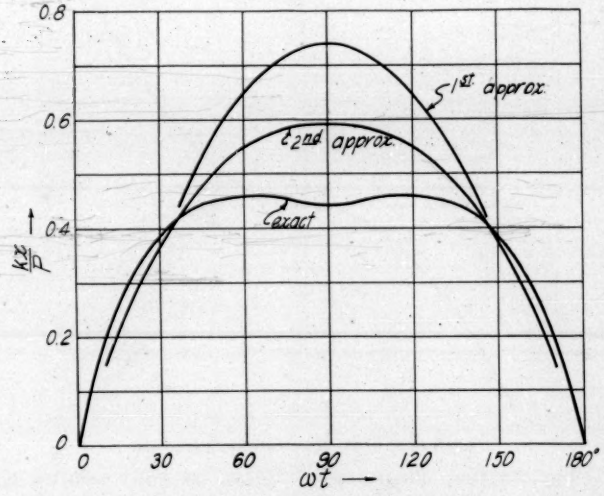

The two-term approximation on the other hand acts quite as expected. For the first harmonic it gives a much better result than Martienssen's solution, whereas the third harmonic is rather far off. Figure 7 gives a typical case: $\omega/\sqrt{k/m} = 4/7$ and $F/P = .5$. Three curves are drawn for the shape of the motion corresponding to (1) Martienssen's solution, (2) the two term approximation and (3) the exact solution.

SUMMARY AND CONCLUSIONS.

1. For the problem of forced vibration of an undamped single degree of freedom system with a non-linear spring of any kind of characteristic two new approximate solutions are given.

2. The first of these, based on an energy consideration over a quarter wave period, unexpectedly proves to give completely unreliable results for the case of the characteristic shown in Fig. 4.

3. The second solution expresses the motion as a sine wave and its third harmonic and gives much better results than the solution of Martienssen, known thus far.

4. Besides discussing the methods in general for any kind of spring characteristic, the solutions are worked out in detail for a number of special cases illustrated in the Figs. 4, 5 and 6.

Iron Plantations of Early Pennsylvania. ARTHUR CECIL BINING (*Penna. Mag. History and Biog.*, 1933, LVII, 117–137) has written an account of these plantations which were located chiefly in the valleys of the Schuylkill, Susquehanna, and Juniata Rivers. They had their origin in the eighteenth century, and many of them remained until the period of the Civil War. Frequently a plantation contained several thousand acres of land, thus that of Elizabeth consisted of 10,124 acres. "The mansion house, the homes of the workers, the furnace and forge or forges, the iron mines, the charcoal house, the dense woods which furnished the material for making charcoal, the office, the store, the grist mill, the saw mill, the blacksmith shop, the common bake oven, the barns, the grain fields, and orchards were part of a very interesting and almost self-sufficing community. In some respects, the iron plantations resembled small feudal manors of medieval Europe." Charcoal was used as the fuel for smelting the ore for the production of pig iron and castings, and for the forges where the pig iron was converted into wrought iron. Water power was used to operate the forge hammers, saw mill, grist mill, etc. Slitting mills, plating mills, and steel furnaces were rarely found on these plantations, but were located in towns and boroughs. The products of the plantation were transported to market on pack horses, in Conestoga wagons, or by water. When the Continental Army crossed the Delaware prior to the battle of Trenton, it used boats which served to transport iron from the Durham furnace to Philadelphia. The Pennsylvania furnaces supplied cannon and cannon balls to Washington's forces.

J. S. H.

Poisoning of Fish by Cyanides in Coke-Oven Effluents. C. H. S. TUPHOLME (*Ind. and Eng. Chem.*, News Ed., 1933, XI, 211) reports the fatal poisoning of young salmon and sea trout by cyanides present in coke-oven effluents which are discharged into the estuary of the river Tees. The toxicity of the water was directly related to its cyanide content as determined by quantitative chemical analysis. The blood of fatally poisoned fish was in the highly oxygenated condition which is characteristic of cyanide poisoning. Trout were rendered helpless in less than 1 hour in water having a temperature of 5° C. and containing potassium cyanide equivalent to a concentration of 0.014 gram of cyanide anion in 100 liters. Since tar acids also occur in the effluents, the experiment with trout was repeated with the substitution of paracresol (0.5 gram in 100 liters) for potassium cyanide; the fish did not exhibit symptoms of poisoning under these conditions.

J. S. H.

A METHOD FOR THE PRECISE MEASUREMENT OF OPTICAL PATH-DIFFERENCE, ESPECIALLY IN STRESSED GLASS.

BY

R. W. GORANSON and L. H. ADAMS.

INTRODUCTION.

It is necessary in connection with many kinds of investigation to measure the path-difference in transparent materials. Well-known devices such as the Babinet compensator or a graduated quartz wedge allow the determination of optical path-difference (and thence birefringence) with ample accuracy for many purposes, but among the methods that have been commonly used there appears to be none with which it is possible to measure large as well as small path-differences to better than about 5 mμ.

In some work to be carried out by the writers, involving the measurement of birefringence, the highest accuracy obtainable consistent with facility of operation and reproducibility by other observers was desired. It was hoped that a method might be found which would enable birefringence of any magnitude to be measured with an accuracy 100 times greater than previously. Among the methods investigated was one that, although proposed many years ago, seems little known, possibly because in the more familiar kinds of investigation involving the measurement of path-difference an extremely high precision is neither necessary nor useful. This method seemed to be the most suitable one for the present purpose. First, by a simple mechanical arrangement the method was made applicable to a Leitz type SM petrographic microscope (and equally applicable to any petrographic microscope with a graduated circle attached to a separately rotatable analyzer); and finally a polarimeter was constructed which incorporated the principles worked out on the microscope. These instruments gave all that was desired in the way of accuracy, speed in taking the readings, and ease of duplication by different

observers. It was therefore thought that a description of the polarimeter might be of interest to other investigators.

Methods That Have Been Proposed or Used.—When a beam of polarized light passes through a birefracting material the transmitted light is in general elliptically polarized. The measurement of path-difference therefore usually becomes a problem in elliptical polarization, although the problem is a comparatively simple one because, for the present purpose, we are primarily interested not in the constants of the elliptical vibration but rather in the condition which produced the ellipticity.

The various methods for the determination of birefringence may be grouped into four main classes, as follows:

1. Methods involving the direct measurement (with linearly polarized light) of the optical path by means of an interferometer, or of the refractive index by the usual technique for refractive index measurements (method of minimum deviation or method of total reflection). The methods of this class are useful but are not capable of very high accuracy. An optical path-difference of 10 mμ, or about 1/50 of an interference fringe is the limit of precision of the usual interferometer methods [1] and, with a 10 cm. path, corresponds to a refractive index difference of 10^{-7}, which is about 10 times the accuracy obtainable by direct refractive index determinations. It may be noted that in the application of the simple methods of this group the vibration direction of the plane polarized light is parallel to one of the principal directions of the birefracting material, so that in this instance elliptical polarization does not occur except in so far as the straight line is a special case of the ellipse (corresponding to $i = 0$ of Table I).

2. Methods utilizing interference phenomena with the material between crossed nicols. These are probably the best-known methods. The simplest one consists in observing the interference color with white light [2] and comparing with a

[1] It may be remarked, however, that by the use of a halfshade it is possible to obtain much higher accuracy than that stated here. See C. A. Skinner and L. B. Tuckerman, *Physik. Zeitschr.*, **12**, 620–626 (1911); and A. Cotton, *C. R.*, **152**, 131–133 (1911).

[2] Apart from its inherent lack of sensitivity the color comparison method is subject to the disadvantage of dependence on the characteristics of the light source. The so-called center of gravity of white light depends on the time of

Newton color scale. For greater accuracy the graduated quartz wedge may be used. The Babinet compensator, when of low range, has a higher sensitivity than the graduated quartz wedge but both are subject to the same type of uncertainty. With either one the observer must estimate the position of a relatively wide black band, which becomes fuzzy at its outer edges. In the case of the graduated wedge there is usually an uncertainty of 10 $m\mu$ in the path difference, and it is difficult to make measurements within better than 5 $m\mu$. The Babinet type of compensator under favorable conditions allows somewhat greater accuracy but only at the expense of a diminished range. In the application of the methods of this group no cognizance need be taken of elliptic polarization provided the specimen and wedge are properly oriented, although it is elliptically polarized light that emerges from the specimen (corresponding to $i = \pm 45°$ of Table I).

3. Methods by which the ellipticity and azimuth of the elliptically polarized light produced by passing plane polarized light through the material are measured and these measurements, together with other data, used to determine the phase lag (see below) and thence the path-difference in the material. The underlying principle is due to de Sénarmont,[3] who discovered that any elliptical vibration may be restored to plane polarized light by insertion of a properly oriented quarter-wave plate, which is called the compensator. The orientation of the compensator and the azimuth of the resultant plane polarized light determine the constants of the elliptical vibration. These methods are capable of high precision since the basic quantities are angular displacements on a graduated circle and can be accurately made by means of a halfshade device. Especially noteworthy is the polarimeter devised by Tool[4] and by Skinner[5] for measuring the constants of an elliptically polarized beam of light. But such instruments are

day and kind of sky or upon the type of artificial light used. For example, the retardation corresponding to sensitive violet of the 1st order, and ordinarily given as 575 $m\mu$, will vary from 535 to 590 $m\mu$, depending on the illumination used. A graduated quartz wedge could be used as an interference color calibrator for a specified illumination.

[3] de Sénarmont, H., *Ann. chim. phys.*, (2) **73**, 337 (1840).

[4] Tool, A. Q., *Phys. Rev.*, **31**, 1 (1910).

[5] Skinner, C. A., *J. Opt. Soc. Amer.* and *Rev. Sci. Instr.*, **10**, 490–520 (1925).

intended primarily for determining the ellipticity and azimuth of the vibration ellipse and become unnecessarily complicated when used for the measurement of the path-difference of a birefracting plate, because for this purpose adjustments and measurements on three graduated circles would be required.

A very simple method for determining ellipticity and azimuth of a beam of elliptically polarized light has recently been described by Szivessy and Dierkesmann.[6] The compensator covers only half of the field and its position is adjusted so that the two halves of the field are equally illuminated. For high precision this method is obviously limited to very small ellipticities since the effective half shadow angle of this two-part field is proportional to the ellipticity of the original elliptically polarized light.

4. Methods by which the birefracting material is combined with other birefracting plates in such a way that a beam of light, initially plane polarized, after passing through the fixed combination is *still plane polarized*, but has its plane of polarization rotated by an amount that is proportional to the path difference of the material under investigation. The measurement of this rotation can be carried out with ease and accuracy. The methods of this class, like those of the preceding class, are limited in accuracy mainly by the precision with which angles can be measured. By any of the methods of groups (3) and (4) the error in path-difference (expressed in $m\mu$) need be no greater than three or four times the angular error (expressed in degrees), which may be as small as 0.01° or even less, but the methods of group (4) are much simpler. They require only one graduated circle (or at most, two) and are especially advantageous for measurements on materials the birefringence of which changes with time, the changing birefringence showing merely as a rotation of the graduated circle.

The methods of group (4) apparently were first clearly enunciated by Friedel,[7] who described three different arrangements. In the most general arrangement (I), the crystal plate under investigation is placed in the diagonal position between two crossed or parallel quarter-wave plates and this

[6] Szivessy, G. and Dierkesmann, A., *Z. Instrumentenk.*, **52**, 337–345 (1932).
[7] Friedel, G., *Bull. soc. min. France*, **16**, 19–33 (1893).

fixed combination is placed between the polarizer and analyzer. The polarizer may have any azimuth, and the rotation of the analyzer for extinction is proportional to the path-difference of the plate. On the other hand, the analyzer may be fixed in any azimuth and the birefringence determined from the extinction position of the polarizer. The other two arrangements may be considered as special cases of this first arrangement. If the *second* quarter-wave plate (the one between specimen and analyzer) be removed and the analyzer set parallel to one of the principal directions of the remaining quarter-wave plate, we have Friedel's arrangement (II), according to which the rotation of the polarizer for extinction determines the path-difference of the specimen.

Still another Friedel arrangement (III), is the one here adopted and is obtained from (I) by removing the *first* quarter-wave plate. In this case the beam of light passes successively through (*a*) the polarizer, (*b*) the specimen with one of its principal directions at 45° to the vibration direction of the polarizer, (*c*) the quarter-wave plate with one of its principal directions parallel to the vibration direction of the polarizer, and (*d*) the analyzer. Here, as before, the angle through which the plane of polarization has been (effectively) rotated by the fixed combination of specimen and quarter-wave plate is proportional to the path-difference of the specimen. More exactly, it equals one-half the phase angle (see below).

As a matter of historical interest it may be worth while to trace the development of these "methods of fixed combinations." Fundamentally they are special cases of the methods which depend on the restoration of elliptically polarized light to plane polarized light by means of a rotatable quarter-wave plate, or compensator. The discovery of the elliptic compensator is properly credited to de Sénarmont,[8] who laid the foundations in about the year 1840 for the quantitative analysis of elliptically polarized light, but it should be noted that the early investigators were primarily interested in the elliptical polarization produced by reflection, and apparently paid little attention to the ellipticity due to transmitted light. Perhaps for this reason a considerable

[8] de Sénarmont, H., *op. cit.* See also *Ann. chim. phys.*, **20**, 397–446 (1847).

period of time elapsed before the important simplification noted above was introduced by Friedel, although Fresnel [9] as early as 1818 had come very close to discovering the principle involved, by observing that when a combination of a birefracting plate in the diagonal position between [the equivalent of] two quarter-wave plates was placed between a polarizer and an analyzer and illuminated with white light the colors observed did not change with the rotation of the combination but varied with the orientation of the analyzer, the combination thus behaving as an optically rotatory substance. Friedel's contribution, especially with reference to arrangements (II) and (III), consisted in taking advantage of the circumstance that in the use of an elliptic compensator there is a position of the birefracting plate with reference to the vibration direction of the polarizer such that the compensator in a certain fixed position, independent of the path-difference of the plate, will restore the light emergent from the specimen to plane polarized light. Thus it is required to rotate only the analyzer, and not the compensator and analyzer separately as in the more general methods of group (3).

Not many references to the subject are to be found in text-books or periodicals. A description of Friedel's arrangements (I) and (II) is given by Bouasse [10] and by Wright [11] and of arrangement (III) by Pockels.[12] The principle of arrangement (III) was used for small ellipticities by Cotton and Mouton,[13] who erroneously attributed it to Chauvin.[14] An interesting variation of arrangement (I) was employed by Tardy,[15] who noted that since in this particular method the polarizer may have any azimuth it may be placed at 45° to the first quarter-wave plate, in which event circularly

[9] Fresnel, A., Ouvres Complètes, Vol. 1, Paris, 1866, pp. 460, 505, 661. Fizeau, H., and Foucault, L., *Ann. chim. phys.*, 30, 147–159 (1850) call attention to the remarkable character of Fresnel's observation.

[10] Bouasse, H., Optique Cristalline Double Réfraction Polarization Rectiligne et Elliptique. Paris, 1925, pp. 49, 125.

[11] Wright, F. E., *Jour. Opt. Soc. Amer.*, 20, 553, 560 (1930). On page 553, line 7 from bottom, the word "half" should read "twice."

[12] Pockels, F., Lehrbuch der Kristalloptik. Leipzig, 1906, pp. 227–228.

[13] Cotton, A. and Mouton, H., *Ann. chim. phys.*, 11, 145–203 (1907).

[14] Chauvin, M., *Ann. fac. sci. Toulouse*, 2, J1–J49 (1889).

[15] Tardy, H. L., *Rev. d'optique*, 8, 59–69 (1929).

polarized light is produced, and consequently the combination of polarizer and first quarter-wave plate may be given any position, since its orientation with respect to the remaining combination of specimen and second quarter-wave plate has no effect on the extinction position of the analyzer. Incidentally, mention may be made of another arrangement involving the use of two quarter-wave plates commonly used for examining birefracting materials in circularly polarized light.[16] In this case one quarter-wave plate is fixed at 45° to the polarizer and the other at 45° to the analyzer. But this arrangement, although often very useful because with white light the color and intensity (and with monochromatic light the intensity) of the emitted light is independent of the orientation of the specimen, does not possess the property of rendering the emergent beam plane polarized.

It is method (III) when used with a halfshade device which seems particularly well suited for the measurement of path-difference, or of birefringence, where high accuracy and simplicity is desired, and which has been applied to the instrument herein described.

THEORY OF THE METHOD.

Definitions.—The plane polarized light incident upon the birefracting material is converted by it to elliptically polarized light, which upon passage through the compensator (*i.e.*, quarter-wave plate) is transformed back to plane polarized light at a certain azimuth depending upon the path-difference of the material. For an understanding of the operation and adjustment of the instrument it is necessary to note briefly the general relations pertaining to elliptically polarized light. These general relations have been given in detail by Wright [17] and others, but it seems desirable to include here a number of definitions and developments, more especially because insufficient attention has been paid to the mutual relationships between the angular parameters when these are not limited to the first quadrant but may have any value, positive or negative, and because, as shown below, apparently minor

[16] See Maxwell, J. C., Scientific Papers, Vol. 1, p. 67. Cambridge, 1890; *Trans. Roy. Soc. Edin.*, 20, 87–120 (1853).

[17] Wright, F. E., *op. cit.*

errors, such as ambiguities in sign, may destroy the utility of the method in certain ranges of birefringence. Furthermore, the errors caused by a failure to have exactly the proper adjustment of the instrument can most readily be evaluated by reference to the fundamental relations in a convenient form.

In the study of polarized light we treat the light as an elliptical vibration, and consider the quantities defining such a vibration and the relations between them.

ϵ is defined as the angle whose tangent is $\pm (b/a)$ where a and b denote the principal major and minor axes respectively, that is, $\pm (b/a)$ is the ellipticity. By convention, with the light coming toward one, $\tan \epsilon$ is positive when the light vector along the emergent elliptical vibration moves counterclockwise and negative when clockwise. It may be noted that $\tan \epsilon$ can vary only from $+ 1$ to $- 1$, or ϵ from $+ 45°$ to $- 45°$.

θ denotes the azimuth of the principal major axis of the elliptical vibration with reference to some fixed X-axis of a chosen (X, Y)-coördinate system. Usually, but not always, the smaller angle is read as θ, which can then vary from $+ 90°$ to $- 90°$ (sometimes from $+ 180°$ to $- 180°$); it becomes indeterminate for circularly polarized light. The elliptical vibration is thus determined by ϵ and θ. Such an elliptical orbit can be readily constructed by assuming a harmonic vibration along the X-axis and another along the Y-axis and that the vibrator along the Y-axis lags behind by a certain angle φ.

φ is defined as the *phase lag* or *phase angle*. The two harmonic vibrations can be expressed as

$$\begin{aligned} x &= A \cos \psi, \\ y &= B \cos (\psi - \varphi), \end{aligned} \tag{1}$$

where A and B denote the amplitudes along X and Y respectively; $\psi° = \dfrac{360\, t}{T}$, where T is the period of one complete vibration and t the elapsed time; φ is the phase lag of the y-component behind the x-component.[18] φ can be *positive*

[18] The ellipse may be constructed as follows: the x-component of a point on the ellipse is the projection, on the X-axis, of a vector which cuts a circle of radius A (and center at the origin) at angle ψ to the X-axis. The corresponding y-

or *negative* depending on which vibration is the faster, and is expressed here in degrees.

Birefracting Plates.—So far the source of this elliptical vibration has not been considered. If a beam of plane polarized light enters a birefracting plate it is in general resolved into two rectangular plane polarized components. These two corresponding directions we shall call the *principal directions* of the plate. The two components traverse the plate with different velocities and consequently emerge from the plate with a difference of phase depending on the thickness of the plate; the faster wave is denoted by α', the slower by γ'. According to general usage the vibration direction is perpendicular to the plane of polarization of the wave and we shall call the principal direction on the plate corresponding to the vibration with the greater retardation the γ'-vibration direction (or simply γ'-direction), the direction at right angles to this, the α'-vibration direction (or simply α'-direction). The phase lag of γ' behind α' is denoted by Φ, which is always positive. Φ is defined as the *phase lag of the plate.* If now the (X, Y)-coördinate system chosen above coincides with the principal directions of the plate then $\varphi = \pm \Phi$. If the X-axis coincides with the α'-vibration direction $\varphi = \Phi$ and if with the γ'-vibration direction $\varphi = -\Phi$ (see equation 12).

i denotes the angle whose tangent is the amplitude ratio which, from equations (1), is B/A. Let a plane polarized beam of light of amplitude P enter a birefracting plate with perpendicular incidence and let its vibration direction make the angle $\mathbf{i}$ with the X-axis which here is one of the principal directions of the plate. Then the amplitude along this direction is $P \cos \mathbf{i}$, that along the other direction is $P \sin \mathbf{i}$; the amplitude ratio is $\tan i = \dfrac{P \sin \mathbf{i}}{P \cos \mathbf{i}}$, or $i = \mathbf{i}$. Therefore in this case i is also the vibration azimuth of the entering plane polarized light with respect to the fixed direction. If the X-axis does not coincide with one of the principal directions of the plate, *i.e.* the (X, Y)-axes have been rotated through a

component of the point is the projection, on the Y-axis, of a second vector which cuts a circle of radius B (and concentric with A), at angle $(\psi - \varphi)$ to the Y-axis. Thus if $\varphi = 0$ this second vector is at 90° to the first vector, if $\varphi = 30°$ this vector is at 60° to the first vector. The point for $\varphi = 0°$, $\psi = 0°$ is $(x = A, y = B)$, for $\varphi = 90°$, $\psi = 0$ is $(x = A, y = 0)$.

certain angle from the principal axes of the plate, then i becomes a function of this angle and the ellipticity of the vibration, and, *in general*, i is not equal to i, which is the angle between the vibration direction of the incident polarized light and the X-axis.

If we start with a known i and Φ of a plate we can calculate the ϵ and θ of the emergent elliptical vibration. If we start with a known ϵ and θ of an elliptical vibration (the latter referred to an arbitrary X-axis), we can calculate an i and φ for this axis. The Φ of the plate can then be evaluated if we know the relation of the (X, Y)-coördinate axes to the α'- and γ'-vibration directions of the plate.

General Relations.—The four quantities ϵ, θ, φ, and i are connected by certain general relations. Those used herein are:

$$\sin 2\epsilon = \sin 2i \sin \varphi, \tag{2}$$

$$\cos 2i = \cos 2\epsilon \cos 2\theta, \tag{3}$$

$$\cot \varphi = \cot 2\epsilon \sin 2\theta, \tag{4}$$

$$\tan 2\theta = \tan 2i \cos \varphi. \tag{5}$$

The following table:[19] which gives the ϵ and θ for different i

[19] In interpreting and visualizing these operations and other such problems representation on a sphere, such as the Poincaré Sphere (see H. Poincaré, "Théorie Mathématique de la Lumière," Vol. 2, Paris, 1892, pp. 275–285; and L. B. Tuckerman, *Studies of Univ. of Nebr.*, 9, 157–219, 1909), or suitable projection such as that described by Wright was found very useful. If the projection is used the front and back hemispheres must be considered as collapsed one on the other. Let the longitude from the extreme right hand point of the equator ("East pole") be 2θ, the front hemisphere denoting plus and the rear hemisphere minus values of 2θ, $+ 180° \leqq 2\theta \leqq - 180°$ or $0 \leqq 2\theta \leqq 360°$; the latitude from the equator be 2ϵ, the northern hemisphere denoting plus and the southern hemisphere minus values of 2ϵ, $+ 90° \leqq 2\epsilon \leqq - 90°$; the hypotenuse of this right-angled spherical triangle is then $2i$ and the angle subtended at the "East pole" is φ. φ can take on all values from 0° to 360° or $+ 180° \leqq \varphi \leqq - 180°$. With the definitions and conventions noted above the projection (including the back side) covers all the necessary values of θ, ϵ, and φ but can be used primarily only for i between 0 and 90, *i.e.*, $0 \leqq 2i \leqq 180°$. In order to take care of negative values of i it is convenient to use the following transformations where they occur:

$$i \rightarrow - i,$$
$$\varphi \rightarrow \varphi \pm 180°,$$

that is, i and φ give the same θ and ϵ as $- i$ and $\varphi \pm 180°$. For example, if

and φ has been found useful in interpreting results and also shows the symmetry with duplication of values found in such periodic functional relations. The table is given only for values of φ from 0° to 180° because the table for values of φ from 180° to 360° is a repetition of the part given, under condition that the signs of θ and ϵ are changed when, for the same i, 180° is added to any value of φ. The table repeats itself for any 360° multiple added to φ. It illustrates strikingly the fact that elliptically polarized light can be considered as having all gradations from plane polarized light (denoted by zero values of ϵ), as one extreme, to circularly polarized light (denoted by 45° values of ϵ, θ becoming indeterminate), as the other extreme.

Two Superimposed Plates.—Let plane polarized monochromatic light vibrating in a known azimuth (by means of a polarizer) enter the unknown birefracting plate I which has one of its principal directions along the axis OX_1. This axis makes a certain angle i with the vibration direction of the polarizer which we can readily identify with i. Let the light then pass through the compensating plate II which has one of its principal directions along axis OX_2.

Let superscripts prime and double prime refer to the ellipses emergent from plates I and II respectively, Arabic subscripts 1 and 2 refer to axes OX_1 and OX_2 respectively, and Roman subscripts I and II refer to plates I and II respectively.

ϵ in general is fixed by the nature of the light entering the crystal plate, the azimuth of the principal directions of this plate with respect to the entering light, and the phase lag, Φ, of the plate. It is therefore independent of the axes chosen for the resultant elliptical vibration, *i.e.*, it remains unaltered by a change in coördinate axes.

Thus

ϵ', ϵ''—refer to the ellipticities of the resultant light emergent from plates I and II respectively.

$i = -30°$ and $\varphi = 210°$, transform to $i = 30°$, $\varphi = 30°$ and determine θ and ϵ graphically by the usual procedure. If φ is to be solved for, and i is minus, change to plus i, solve for φ and add or subtract 180° to this value to obtain the correct φ. Plane polarized light is represented by the sum total of points on the equator; positive and negative circularly polarized light by the North and South poles respectively.

TABLE I.

The upper figure in each square is θ; the lower italicized figure is ϵ. The figures are given in degrees. To extend the table for values of φ from 180° to 360°, add 180° to each value of φ and change the signs of θ and ϵ. The table repeats itself for 360° multiples of φ.

φ \ i	0 −180	15 −165	30 −150	45 −135	60 −120	75 −105	90 −90	105 −75	120 −60	135 −45	150 −30	165 −15	180 0
0	0 *0*	15 *0*	30 *0*	45 *0*	60 *0*	75 *0*	±90 *0*	−75 *0*	−60 *0*	−45 *0*	−30 *0*	−15 *0*	0 *0*
15	0 *0*	14.5 *3.8*	29.5 *6.5*	45.0 *7.5*	60.5 *6.5*	75.5 *3.8*	±90 *0*	−75.5 *− 3.8*	−60.5 *− 6.5*	−45.0 *− 7.5*	−29.5 *− 6.5*	−14.5 *− 3.8*	0 *0*
30	0 *0*	13.2 *7.2*	28.1 *12.8*	45.0 *15.0*	61.9 *12.8*	76.8 *7.2*	±90 *0*	−76.8 *− 7.2*	−61.9 *−12.8*	−45.0 *−15.0*	−28.1 *−12.8*	−13.2 *− 7.2*	0 *0*
45	0 *0*	11.0 *10.3*	25.5 *18.8*	45.0 *22.5*	64.5 *18.8*	79.0 *10.3*	±90 *0*	−79.0 *−10.3*	−64.5 *−18.8*	−45.0 *−22.5*	−25.5 *−18.8*	−11.0 *−10.3*	0 *0*
60	0 *0*	8.0 *12.8*	20.5 *24.2*	45.0 *30.0*	69.5 *24.2*	82.0 *12.8*	±90 *0*	−82.0 *−12.8*	−69.5 *−24.2*	−45.0 *−30.0*	−20.5 *−24.2*	− 8.0 *−12.8*	0 *0*
75	0 *0*	4.3 *14.4*	12.1 *28.2*	45.0 *37.5*	77.9 *28.2*	85.7 *14.4*	±90 *0*	−85.7 *−14.4*	−77.9 *−28.2*	−45.0 *−37.5*	−12.1 *−28.2*	− 4.3 *−14.4*	0 *0*
90	0 *0*	0 *15*	0 *30*	ind. *45*	±90 *30*	±90 *15*	±90 *0*	±90 *−15*	±90 *−30*	ind. *−45*	0 *−30*	0 *−15*	0 *0*

Table I—*Continued.*

φ \ i	0 −180	15 −165	30 −150	45 −135	60 −120	75 −105	90 −90	105 −75	120 −60	135 −45	150 −30	165 −15	180 0
105	0 *0*	− 4.3 *14.4*	−12.1 *28.2*	−45.0 *37.5*	−77.9 *28.2*	−85.7 *14.4*	±90 *0*	85.7 *−14.4*	77.9 *−28.2*	45.0 *−37.5*	12.1 *−28.2*	4.3 *−14.4*	0 *0*
120	0 *0*	− 8.0 *12.8*	−20.5 *24.2*	−45.0 *30.0*	−69.5 *24.2*	−82.0 *12.8*	±90 *0*	82.0 *−12.8*	69.5 *−24.2*	45.0 *−30.0*	20.5 *−24.2*	8.0 *−12.8*	0 *0*
135	0 *0*	−11.0 *10.3*	−25.5 *18.8*	−45.0 *22.5*	−64.5 *18.8*	−79.0 *10.3*	±90 *0*	79.0 *−10.3*	64.5 *−18.8*	45.0 *−22.5*	25.5 *−18.8*	11.0 *−10.3*	0 *0*
150	0 *0*	−13.2 *7.2*	−28.1 *12.8*	−45.0 *15.0*	−61.9 *12.8*	−76.8 *7.2*	±90 *0*	76.8 *− 7.2*	61.9 *−12.8*	45.0 *−15.0*	28.1 *−12.8*	13.2 *− 7.2*	0 *0*
165	0 *0*	−14.5 *3.8*	−29.5 *6.5*	−45.0 *7.5*	−60.5 *6.5*	−75.5 *3.8*	±90 *0*	75.5 *− 3.8*	60.5 *− 6.5*	45.0 *− 7.5*	29.5 *− 6.5*	14.5 *− 3.8*	0 *0*
180	0 *0*	−15 *0*	−30 *0*	−45 *0*	−60 *0*	−75 *0*	±90 *0*	75 *0*	60 *0*	45 *0*	30 *0*	15 *0*	0 *0*

θ_1', θ_2'—denote the azimuths of the ellipse emergent from plate I with respect to axes OX_1 and OX_2 respectively.

θ_2''—denotes the azimuth of the ellipse emergent from plate II with respect to axis OX_2.

i_1', i_2'—denote the antitangents of the amplitude ratios, of light emergent from plate I, along axis OY_1 with respect to OX_1 and along OY_2 with respect to OX_2 respectively.

i_2''—denotes the antitangent of the amplitude ratio, of light emergent from plate II, along axis OY_2 with respect to axis OX_2.

$\mathbf{i}_1$, $\mathbf{i}_2$—denote the angles between the entering plane polarized light (vibration direction of the polarizer), and axes OX_1, OX_2 respectively. Here $\mathbf{i}_1 = i_1'$ but $\mathbf{i}_2 \neq i_2'$.

φ_1', φ_2'—denote the phase lags of the elliptical vibration emergent from plate I referred to axes OX_1 and OX_2 respectively.

φ_2''—denotes the phase lag of the elliptical vibration emergent from plate II referred to axis OX_2.

Φ_I, Φ_{II}—denote the phase lags of plates I and II respectively.

The elliptically polarized light emerging from plate I referred to axis OX_1 (which is here one of the principal directions of the plate), has a certain ϵ' and θ_1' because of a certain $i_1' = \mathbf{i}_1$ and phase lag φ_1'. The relations between these four quantities are

$$\sin 2\epsilon' = \sin 2i_1' \sin \varphi_1', \tag{6}$$

$$\cos 2i_1' = \cos 2\epsilon' \cos 2\theta_1', \tag{7}$$

$$\cot \varphi_1' = \cot 2\epsilon' \sin 2\theta_1'. \tag{8}$$

Now let the reference axis of the elliptical vibration be transformed from OX_1 to OX_2 where $\measuredangle X_1OX_2 = \mathbf{i}_2 - \mathbf{i}_1 = \mathbf{i}_2 - i_1'$. ϵ' remains constant in this transformation but θ_1' is changed to $\theta_2' = \theta_1' + \mathbf{i}_2 - i_1'$, i_1' to i_2', and φ_1' to φ_2'. Relations (6), (7), and (8) in terms of the new axis OX_2 are thus

$$\sin 2\epsilon' = \sin 2i_2' \sin \varphi_2', \tag{9}$$

$$\cos 2i_2' = \cos 2\epsilon' \cos 2(\theta_1' + i_2 - i_1'), \tag{10}$$

$$\cot \varphi_2' = \cot 2\epsilon' \sin 2(\theta_1' + i_2 - i_1'). \tag{11}$$

From equation (11) we find that if the reference axis is rotated 90°, *i.e.* $\measuredangle X_1OX_2 = i_2 - i_1' = 90°$, then

$$\begin{aligned}\cot \varphi_2' &= \cot 2\epsilon' \sin 2(\theta_1' + 90) \\ &= -\cot \varphi_1'.\end{aligned}$$

Thus a 90° rotation of the reference axis is equivalent to changing the sign of the phase lag φ. For example, a phase lag of 30° referred to the α'-direction as the reference axis becomes $-30°$ when referred to the γ'-direction as the reference axis.

We have then for the case in which the reference axis is coincident with one of the principal directions of the plate

$$\varphi_1' = \pm \Phi_I, \tag{12}$$

the plus sign being used when the α'-direction is the OX_1 axis (φ_1' positive), and the minus sign when the γ'-direction is the OX_1 axis (φ_1' negative).

On passing through the compensating plate II the light will vibrate along the principal directions of this plate. If the resultant elliptical vibration which emerges from this plate be referred to the principal directions of the plate as axes then the phase lag φ_2'' of this elliptical vibration will differ from φ_2' by the amount $\pm \Phi_{II}$. The sign used in front of Φ_{II} will depend on which of the principal directions is along the OX_2 axis of the ellipse; it is plus if the α'-direction of plate II be along OX_2 and minus if the γ'-direction of the plate be along OX_2.

Equations (9), (10), and (11) must now be modified to include the effect introduced by plate II. Since the axes remain the same the amplitude ratio does not change. The phase lag of this second ellipse is, however, changed to $\varphi_2'' = \varphi_2' \pm \Phi_{II}$, the antitangent of the ellipticity to ϵ'', and the azimuth of the principal major axis to θ_2''. Therefore

$$\sin 2\epsilon'' = \sin 2i_2' \sin (\varphi_2' \pm \Phi_{II}), \tag{13}$$

$$\tan 2\theta_2'' = \tan 2i_2' \cos (\varphi_2' \pm \Phi_{II}). \tag{14}$$

Expansion of sin $(\varphi_2' \pm \Phi_{II})$ and introduction of values from equations (9) and (11) gives

$$\sin 2\epsilon'' = \sin 2\epsilon' \cos \Phi_{II} \pm \cos 2\epsilon' \sin 2\theta_2' \sin \Phi_{II}. \quad (15)$$

Expansion of cos $(\varphi_2' \pm \Phi_{II})$ and introduction of values from equations (9), (10), and (5) gives

$$\tan 2\theta_2'' = \tan 2\theta_2' \cos \Phi_{II} \mp \frac{\tan 2\epsilon' \sin \Phi_{II}}{\cos 2\theta_2'}. \quad (16)$$

These are the well known relations, in simple and unambiguous form, for obtaining ϵ'' and θ_2''. Where an alternative in sign occurs in expressions (15) and (16) the sign chosen depends on which of the two principal directions of plate II is chosen as the OX_2 axis; if the α'-direction is coincident with OX_2 the upper sign is used, if the γ'-direction is coincident with OX_2 the lower sign is used. Equations (15) and (16) are then the desired general relations we seek; they enable us to calculate directly the ellipticity and azimuth of the elliptically polarized light emerging from the second plate, provided the phase lag and orientation of each plate is known.

Special Case Applicable to the Present Instrument.—Our problem is to determine the phase lag, Φ, of a given plate. This is done by first transforming the elliptically polarized light emerging from the specimen into plane polarized light by means of a second plate (compensator), second measuring the azimuth, θ_2'', of the plane polarized light, and third obtaining a relation between this azimuth and the phase lag, Φ, of the unknown plate.[20]

In order that the elliptically polarized light emerging from the specimen be *plane polarized* on emerging from the compensator, ϵ'' must be zero. Since, from equation (9), ϵ' is not ordinarily zero then Φ_{II} must be 90° or some odd multiple of 90°, and θ_2' either zero or 90°. Now let $i_1 = i_1'$ be 45°, *i.e.* let the angle between the vibration direction of the polarizer and the OX_1 axis (which is one of the principal directions of

[20] To evaluate Φ in terms of path-difference of the plate (birefringence is the optical path-difference divided by the path length), multiply Φ in degrees by the wave-length of the light divided by 360. If wave-length is expressed in millimicrons, in $m\mu$, the path-difference will also be in $m\mu$; for the mercury green line the factor is 546.07/360 or 1.51686.

plate I) be 45°, then it necessarily follows from equation (3) that $\theta_1' = \pm 45°$. From the relation

$$\theta_2' = 0° \qquad \text{or} \qquad 90° = \theta_1' + \mathbf{i}_2 - i_1'$$

we then have $\mathbf{i}_2 - i_1' = \pm 45°$. This would also be true if we made $\mathbf{i}_1 = i_1' = -45°$. There is a duplication of values here and we can therefore arbitrarily fix one of these quantities with no loss of generality; let $\mathbf{i}_2 - i_1' = 45°$, the azimuth of OX_2 is then fixed.

Equation (16) then reduces to

$$\tan 2\theta_2'' = \pm \frac{\tan 2\epsilon'}{\sin 2\theta_1'} = \pm \tan \varphi_1'$$

or

$$\pm \varphi_1' = \begin{cases} 2\theta_2'' \pm n\,360°, \\ 2(\theta_2'' + 90) \pm n\,360°, \\ 2(\theta_2'' - 90) \pm n\,360°, \end{cases} \tag{17}$$

where $n = 0, 1, 2, \cdots$.

We know, however, from physical considerations that φ_1' is a continuous function of θ_2''. Therefore, if we have some known boundary condition we can ascertain which of the above expressions for $\pm \varphi_1'$ is the correct solution. This is given by the condition that for $\varphi_1' = 0$ we have $(\theta_2'')_0 = 90°$, or, in other words, if the phase lag of the specimen is zero the resultant vibration direction is parallel to the vibration direction of the polarizer. Expression (17) then becomes

$$\pm \varphi_1' = 2(\theta_2'' - 90°) \pm n\,360°. \tag{18}$$

In practice we do not read θ_2'' directly, but rather the extinction position by means of an analyzer. If we denote by θ_a the extinction position of the analyzer with reference to the original extinction position (nicols crossed), we have $\theta_a = \theta_2'' - 90°$. Equation (18) then becomes

$$\pm \varphi_1' = 2\theta_a \pm n\,360°. \tag{18a}$$

A possible uncertainty of 180° in φ_1' (and hence in Φ_1) has thus been removed.

An additional and more troublesome uncertainty can be removed by consideration of the orientations of specimen and

compensator. The two solutions of equation (18) or (18*a*) are distinguished as follows:

If the OX_2 axis is coincident with the α'-direction of plate II then

$$\varphi_1' = 2\theta_a \pm n\,360°. \tag{19a}$$

If the OX_2 axis is coincident with the γ'-direction of plate II then

$$-\varphi_1' = 2\theta_a \pm n\,360°. \tag{19b}$$

Now the problem is to evaluate the phase lag, Φ_I, of plate I which is always positive and is here equal to $\pm\varphi_1'$. φ_1' itself may be positive or negative depending on the orientation of plate I. If the α'-direction of plate I is at $+45°$ to the OX_2 axis, φ_1' is positive and $\Phi_I = \varphi_1'$, and if the γ'-direction is at $+45°$ to the OX_2 axis, φ_1' is negative and $\Phi_I = -\varphi_1'$.

From equation (18) then there are four solutions for Φ_I which depend on the orientations of the two plates. It can readily be seen, however, that only two of these solutions will be distinct.

If now the vibration azimuth of the polarizer is North, the OX_2 axis East, the OX_1 axis NE, and the zero position of the analyzer is taken when its vibration azimuth is East (the two nicols are originally set at extinction and the reading of the analyzer in this position is taken as the zero reading of θ_a), the four solutions become:

A. (1) α'-direction of plate I NE, of plate II East,

(2) γ'-direction of plate I NE, of plate II East,

then

$$\Phi_I = 2\theta_a + n\,360°. \tag{20a}$$

The analyzer is rotated to extinction and the *counterclockwise* angle less than 180° turned off is read as θ_a.

B. (1) γ'-direction of plate I NE, α'-direction of plate II East,

(2) α'-direction of plate I NE, γ'-direction of plate II East,

then

$$-\Phi_I = 2\theta_a - n\,360°. \tag{20b}$$

The analyzer is rotated to extinction and the *clockwise* angle less than 180° turned off is read as $-\theta_a$.

Another procedure which may be employed is the following: the orientations of specimen and compensator must be distinguished as A or B but no cognizance need be taken of which extinction angle is read provided that: (1) If the graduations of the analyzer circle increase numerically as the analyzer is rotated counterclockwise the final minus the initial reading is called θ_a, or if the graduations decrease numerically for a counterclockwise rotation this same difference is called $-\theta_a$; and (2) all the values of $2\theta_a \pm n\ 360$ are set down, then for arrangement A all the negative values (for arrangement B all the positive values) are discarded. The correct value of Φ_I (or $-\Phi_I$) is then determined by other means from the remaining values. For example, suppose the analyzer graduations increase for a counterclockwise rotation and suppose θ_a, the final minus the initial reading, is 120°. Set down the various values of $2\theta_a \pm n\ 360$, *i.e.* $\cdots, -840, -480, -120, 240, 800, 1160, \cdots$. For arrangement A the correct Φ_I will be one of the positive values; for arrangement B the correct $-\Phi_I$ will be one of the negative values. The four settings A and B of compensator and specimen are illustrated graphically in Fig. 1.

This is an important step because an uncertainty in Φ_I equal to $4\theta_2''$, that is $4(\theta_a - 90)$, has here been eliminated. This would be of especial importance for values of θ_a close to 90°. For example if θ_a were 90.10° then, according to (18*a*), Φ_I or $\pm \varphi_1'$ could be either 180.2° or 179.8°, whereas if the arrangement of compensator and specimen were that of $A1$ or $A2$ in Fig. 1 the true value of Φ_I must be 180.2° (plus a possible n 360). On the other hand if the arrangement were that of $B1$ or $B2$ the true value of Φ_I would be $179.8° + n\ 360°$.

In using the method with the microscope complementary readings were made from positions $A1$ and $B1$; with the polarimeter readings were made from positions $A1$ and $B2$. The two complementary readings should be symmetrical about the zero position of the analyzer if the settings are correctly made.

There still remains an uncertainty of n 360° in Φ_I which may be considered as due to the inevitable uncertainty in the azimuth θ_a. The particular multiple, n, of 360° can readily be determined by inspection of the interference colors in white

light or by determining the order of the interference color with a quartz wedge. For example, if the mercury line 546.07 mμ is used as the source of monochromatic light, if the reading, θ_a, for setting $A1$ is 90.10°, and if the interference color in white light is green of the second order, which is

FIG. 1.

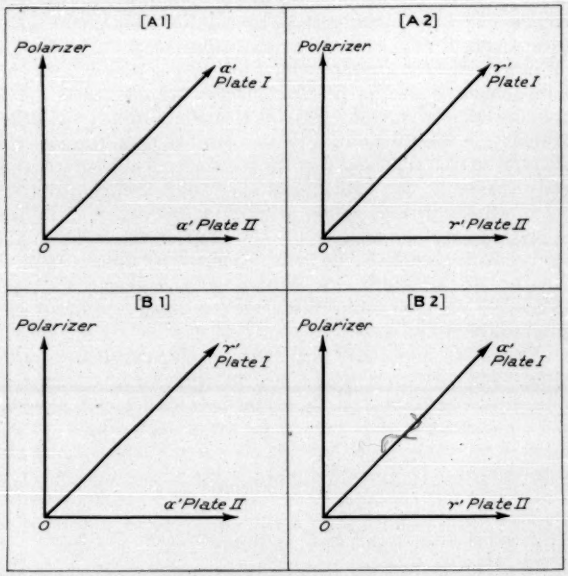

A representation of the four possible orientations of specimen and compensator applicable to this method. The solutions of A and B are distinct but 1 and 2 are identical.

approximately 800 mμ, or 530° for the monochromatic light used, then

$$\Phi_1 = 2(90.10°) + 360° = 540.20° \quad \text{or} \quad 819.41 \text{ m}\mu.$$

DISCUSSION OF ERRORS.

Since absolute mechanical accuracy is an unattainable goal and high precision of measurement is here sought, a discussion

of the possible sources and magnitudes of errors which may be encountered is vital. The four major sources of error that can exist are: (1) The compensator may not be exactly a quarter-wave plate for the light used; (2) the compensator and/or (3) the specimen settings may not have been correctly made; and (4) the analyzer may not be accurately set at the position of minimum illumination in taking readings. The first three will be considered here, the fourth under "Details of the Polarimeter."

(1) If Φ_{II} of the compensator is not exactly 90° for the wave-length of light used, the value obtained as above from the analyzer readings will not correspond exactly to the Φ_I of the specimen. If we let $\Phi_{II} = 90 \pm \delta$ then, as a consequence of equation (16), the error introduced can be computed from the equation

$$\frac{\tan 2\theta_a}{\tan \varphi_1'} = \cos \delta \qquad (21)$$

$$\doteqdot 1 - \tfrac{1}{2}\delta^2. \qquad (21a)$$

In the approximations given here and below δ is expressed in radians. The symbol $\doteqdot$ denotes "approximately equal to."

Because it is difficult to make a compensator which is exactly a quarter-wave plate, it will be of interest to note that even though the compensator be 5° off, *i.e.* 90 ± 5°, the error introduced by such a compensator will be very small and in ordinary practice nearly negligible, averaging about 0.1° or 0.15 mμ for mercury green light. The following table illustrates this.

TABLE II.

Errors Resulting from the Use of a Compensator of Incorrect Phase Lag.

They are given as $2\theta_a - \Phi_I$, the observed minus the true value of the phase lag.

True Phase Lag of Specimen Φ_I. $n = 0, 1, 2, \ldots$	Error in the Value of Φ_I Obtained from $2\theta_a$ with a Compensator Which Deviates from 90° by 1°.	5°.
n 180	0.000°	0.000°
n 180 ± 15	∓ 0.002	∓ 0.055
n 180 ± 30	∓ 0.004	∓ 0.094
n 180 ± 45	∓ 0.004	∓ 0.109
n 180 ± 60	∓ 0.004	∓ 0.094
n 180 ± 75	∓ 0.002	∓ 0.055
n 180 ± 90	0.000	0.000

In this and the following two tables the rows have been compressed as follows: for a Φ_1 of $n\ 180 + x (x = 15, 30, \cdots)$ the upper sign is used and for a Φ_1 of $n\ 180 - x$ the lower sign is used in the table of errors.

It is advisable, however, for the compensator to be as near 90° as can be obtained conveniently because otherwise $\tan \epsilon''$ which is the resultant ellipticity, and $\sin^2 \epsilon''$ which may be taken as a measure of the resultant minimum intensity, will not be zero. These quantities can be computed from equations (22) or (22a) which are derived from equation (15):

$$\sin 2\epsilon'' = \mp \sin \varphi_1' \sin \delta \qquad (22)$$

$$\doteq \mp \delta \sin \varphi_1'. \qquad (22a)$$

from which it can be seen that they become numerically maxima for $\varphi_1' = 90°$ or multiples of 90°. Therefore if the compensator be 90 ± 5 the resultant ellipticity and minimum intensity will be equal to or less than $\mp$ 0.048 and 0.0023 respectively; if the compensator be 90 ± 1 these quantities will be equal to or less than $\mp$ 0.009 and 0.000 076 respectively. These intensities represent the fractional part of the original intensity emergent from the polarizer. Except with a weak source they will therefore lie above the "threshold" level of vision of the human eye. Consequently the analyzer settings will be not on extinction but on some minimum brightness level which, for the same instrumental conditions, is a function of the compensator deviation from 90° and the phase lag of the specimen. The sensitivity with which these settings can be made will therefore be correspondingly lowered. The compensators made and used by the writers do not deviate more than 0.1 or 0.2 from 90°.

(2) Suppose now that the phase lag of the compensator is 90° but let its α'-direction make an angle $90 \pm \delta$ with the vibration direction of the polarizer, *i.e.* the angle $i_2 - i_1' = 45 \pm \delta$, then from equation (16) we have

$$\frac{\tan 2\theta_2''}{\tan \varphi_1'} = \frac{1}{\cos 2\delta} \qquad (23)$$

$$\doteq 1 + 2\delta^2 \quad [\delta \text{ in radians}]. \qquad (23a)$$

Errors which may be expected from the analyzer readings with a compensator deviating 0.5°, 1°, and 2° from its correct

azimuthal position are given in the following table. If, as is ordinarily the case, the zero position of the analyzer is fixed, an additional error in Φ equal to 2δ will occur because θ_2'' is reckoned from the position of the compensator.

TABLE III.

Errors Resulting from the Use of an Incorrectly Oriented Compensator.

They are given as $2\theta_a - \Phi_1$, the observed minus the true value of the phase lag, on the assumption that *the zero position of the analyzer is maintained coexistent with one of the principal directions of the compensator.*

True Phase Lag of Specimen Φ_1, $n = 0, 1, 2, \ldots$	Error in the Value of Φ_1 Obtained from $2\theta_a$ with a Compensator Which Deviates from Its Correct Position by		
	0.5°.	1°.	2°.
$n\,180$	0.000	0.000	0.000
$n\,180 \pm 15$	± 0.002	± 0.009	± 0.035
$n\,180 \pm 30$	± 0.004	± 0.015	± 0.060
$n\,180 \pm 45$	± 0.004	± 0.017	± 0.070
$n\,180 \pm 60$	± 0.004	± 0.015	± 0.060
$n\,180 \pm 75$	± 0.002	± 0.009	± 0.035
$n\,180 \pm 90$	0.000	0.000	0.000

An error of 0.5° in setting the position of the compensator will therefore permit readings to be taken which will give values of Φ_1 correct to better than ± 0.01°.

The resultant ellipticity, tan ϵ'', caused by an improperly placed compensator, can be computed from expressions (24) or (24*a*) which follow directly from (16).

$$\sin 2\epsilon'' = \mp \cos \varphi_1' \sin 2\delta \qquad (24)$$

$$\doteq \mp 2\delta \cos \varphi_1'. \qquad (24a)$$

Here ϵ'' becomes numerically a maximum for $\varphi_1' = 0°$ or multiples of 180°.

(3) Assume (1) and (2) to be correct but let the α'-direction of the specimen make an angle of $45 \pm \delta$ with the vibration direction of the polarizer, that is, $i_1' = 45 \pm \delta$ and $i_2 - i_1' = 45 \mp \delta$, then from (16) we have

$$\frac{\tan 2\theta_a}{\tan \varphi_1'} = \frac{\cos \varphi_1'}{\sin 2\delta \tan 2\delta + \cos 2\delta \cos \varphi_1'} \qquad (25)$$

$$\doteq \frac{\cos \varphi_1'}{4\delta^2 + (1 - 2\delta^2) \cos \varphi_1'}, \qquad (25a)$$

$$\tan 2\theta_a \doteqdot \frac{1}{4\delta^2} \quad \text{if} \quad \varphi_1' = 90°. \quad [\delta \text{ in radians}] \qquad (25b)$$

Errors which may be expected when the specimen deviates 0.5°, 1°, and 2° from its correct azimuthal position are given in the following table.

TABLE IV.

Errors Resulting from the Use of an Incorrectly Oriented Specimen.

They are given as $2\theta_a - \Phi_1$, the observed minus the true value of the phase lag.

True Phase Lag of Specimen Φ_1. $n = 0, 1, 2, \ldots$	Error in the Value of Φ_1 Obtained from $2\theta_a$ When the Specimen Deviates from Its Correct Azimuth by		
	0.5°.	1°.	2°.
$n\,360$	0.000	0.000	0.000
$n\,360 \pm 15$	$\mp$ 0.003	$\mp$ 0.009	$\mp$ 0.037
$n\,360 \pm 30$	$\mp$ 0.005	$\mp$ 0.020	$\mp$ 0.079
$n\,360 \pm 45$	$\mp$ 0.008	$\mp$ 0.032	$\mp$ 0.128
$n\,360 \pm 60$	$\mp$ 0.011	$\mp$ 0.046	$\mp$ 0.184
$n\,360 \pm 75$	$\mp$ 0.016	$\mp$ 0.059	$\mp$ 0.237
$n\,360 \pm 90$	$\mp$ 0.018	$\mp$ 0.070	$\mp$ 0.279
$n\,360 \mp 105$	$\mp$ 0.019	$\mp$ 0.076	$\mp$ 0.305
$n\,360 \mp 120$	$\mp$ 0.019	$\mp$ 0.076	$\mp$ 0.303
$n\,360 \mp 135$	$\mp$ 0.017	$\mp$ 0.067	$\mp$ 0.268
$n\,360 \mp 150$	$\mp$ 0.013	$\mp$ 0.050	$\mp$ 0.201
$n\,360 \mp 165$	$\mp$ 0.007	$\mp$ 0.027	$\mp$ 0.108

In order then to obtain results correct to $\pm$ 0.01° the orientation of the specimen must be accurate to $\pm$ 0.3° (which leads to a maximum error of $\mp$ 0.006°), or better.

The resultant ellipticity, tan ϵ'', caused by an incorrectly oriented specimen can be computed from expressions (26) or (26*b*) which follow directly from (15)

$$\sin 2\epsilon'' = \mp \tfrac{1}{2} \sin 4\delta(1 - \cos \varphi_1') \qquad (26)$$

$$\doteqdot \mp 2\delta(1 - \cos \varphi_1'). \quad [\delta \text{ in radians}] \qquad (26b)$$

Here ϵ'' becomes numerically a maximum for $\varphi_1' = 90°$ or multiples of 90°.

The errors discussed under cases (1), (2), and (3) have been treated by Friedel,[21] who derived equations for intensity in connection with (1) and (2) and derived also equation (21). His interpretation of the intensity equation for case (2) does not seem to be correct.

[21] Friedel, G., *op. cit.*

DETAILS OF THE POLARIMETER.

This method is therefore capable of attaining the precision desired; there remain only the mechanical details of the instrument itself.

From the foregoing it is seen that if the principal directions of the specimen and quarter-wave plate bear certain relations to the vibration direction of the incident plane polarized light the net result is emergent plane polarized light, the plane of which has been rotated a certain angle from that of the incident light; twice the angle between the polarization directions of the incident and emergent light is a measure of the phase lag of the specimen.

The essentials are a source of plane parallel monochromatic light, a polarizer, a compensator which is a quarter-wave plate for the light used, and an analyzer mounted on a graduated circle. If it is assumed that these items have been correctly placed and adjusted the accuracy of the results will depend on the accuracy with which the extinction positions are determined by the analyzer settings. It is a well-known fact in optics that the most accurate visual determinations are obtained by a photometric match. Some device [22] for obtaining a divided field is therefore necessary.

The schematic arrangement of the polarimeter can be seen from Figs. 2 and 3. Figure 4 illustrates the polarimeter with a furnace inserted.

FIG. 2.

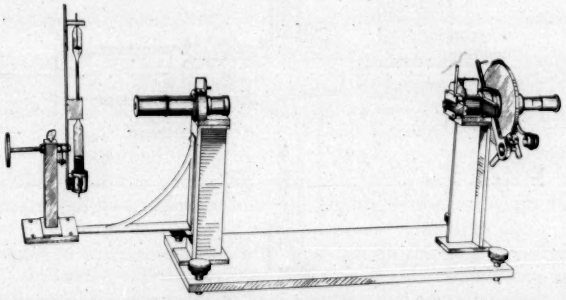

Polarimeter assemblage.

[22] Tuckerman, L. B., *op. cit.*

The illumination is obtained from a mercury arc lamp specially constructed to give a high intensity. The light is made plane parallel by means of suitable lenses. In *ILL* to L_1 of Fig. 3 is shown the simplest type of arrangement; here the optical path *ILL* to L_1 is made equal to the focal length of lens L_1. Strains in glass are, however, not uniform but vary

FIG. 3.

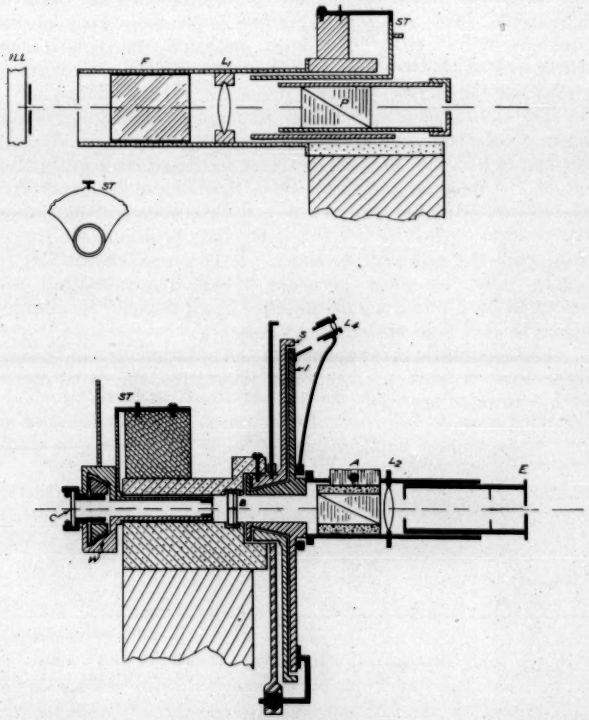

Diagrammatic cross-section of the polarimeter. *ILL*, mercury arc lamp; *F*, color filter; L_1, lens; *P*, polarizing prism; *ST*, stop arrangement for setting polarizer positions; *C*, compensator; *W*, slider for removing compensator; *B*, biquartz wedge; *St*, stop arrangement for setting compensator positions; *S*, graduated circle; *I*, indicator circle; L_4, reading lens; L_2, lens.

from point to point, and since the reading obtained from the polarimeter will be an integration over the whole area in the field of view, it may be necessary to diaphragm down the field to a considerable extent for certain experiments. Such diaphragming will usually result in a diminished field intensity at the exit slit; consequently if, for such cases, a higher intensity is desired than can be supplied by this simple system there can be supplied for it a shorter focus achromatic lens. This light is filtered to eliminate all but the mercury green line, 546.07 mμ. The plane parallel monochromatic light then passes in turn through a Glan-Thompson prism (polarizer), a

FIG. 4.

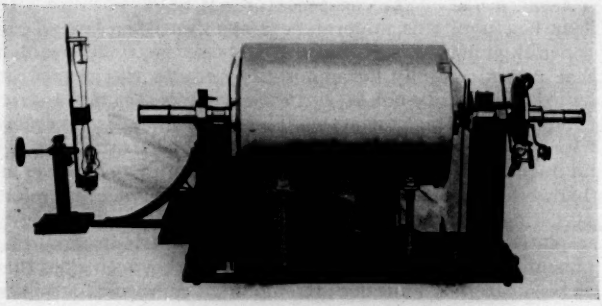

Polarimeter with a furnace inserted for the measurement of birefringence at high temperatures.

diaphragm, the specimen investigated (suitably diaphragmed), the compensator, a Wright bi-quartz wedge, a diaphragm, a Glan-Thompson prism (analyzer), and a lens which focuses on the dividing line of the Wright bi-quartz wedge.

Since this method is unable to distinguish between 360° multiples of the phase lag (n of equations 20a and 20b) a graduated quartz wedge interchangeable with the Wright bi-quartz wedge is used for this purpose. The light filter is removed when readings are to be taken on the quartz wedge.

Polarizer.—The polarizer is set in a tube which can be adjusted for azimuth in a mounting. This mounting is rotatable about the axis of the instrument and has three

positions spaced 45° apart which are obtained by stops set on the circumference of a circular arc. The radius of the circular arc can be varied to suit the accuracy of setting desired; in this instrument it is 4 cm.

In Fig. 3 the polarizer sketched is a Glan-Thompson prism. It is considered [23] that for best practice in polarimetric work ordinary nicol prisms with inclined end faces and long axis inclined to the optic axis should not be used; if a sufficiently intense source of light is used, the field, when viewed through two such crossed nicols, will not be uniform, furthermore the non-uniform pattern of this field will change in position if either nicol be rotated slightly; hence appreciable systematic errors can occur.

Compensator.—The compensator was made of muscovite. Clear blocks of this mineral were split until a plate of the proper thickness was obtained. It is necessary to examine these plates carefully for uniformity because the surfaces so formed will usually not be single cleavage planes but a series of step-wise cleavage surfaces. This mineral was used because of its low birefringence when viewed normal to the cleavage and its perfect cleavage. It has the disadvantage, however, of a high birefringence viewed parallel to the cleavage; therefore any tilting of the plate will alter materially the phase lag of the plate. Unless special precautions are made in mounting to insure that the plate be mounted flat and between glass that has been carefully annealed, the mounted compensator will be found to have a different phase lag from the unmounted specimen. Furthermore, any deviation of the light from plane parallelism will cause the plate to read higher.

The compensator can be adjusted about the axis of the instrument in a mounting. This mounting is rotatable about the axis and three stops mark three positions at 45° to each other in a manner similar to that of the polarizer.

Halfshade.—A Wright bi-quartz wedge is used to give a two-part field for a photometric match and therefore an increased accuracy in measuring extinctions. This wedge has a variable half shade angle which can be changed at will to suit the observer. A lens L_2, whose magnification is made low

[23] "Handbuch der Physik," edited by H. Geiger and K. Scheel, Vol. XIX, Berlin, 1928, pp. 727–729.

to insure a field of not too low intensity, is set in the tube to focus on the dividing line of the half-shadow wedge. The aperture E is placed so that the eye pupil will be at or near the focal point of L_2. A Galilean type telescope was found very useful for collimating the instrument and specimens but was discarded when making readings because of its sensitivity to the eye position.

Analyzer.—The analyzer is a Glan-Thompson prism which is attached to the reading circle. The circle on this instrument is graduated so that the vernier reads to 0.02° and may be interpolated to 0.01°. The vernier is read by means of a lens provided with a telecentric stop. Fine adjustments of the circle are made with a slow motion screw.

Accuracy.—The accuracy is such that readings can be repeated to 0.02°, and by averaging several readings to 0.01°. This accuracy can be duplicated by independent observers. To insure this precision the instrument was set up in a darkened room, the eye permitted to acquire its maximum sensitivity before making the readings, and eye fatigue avoided.

In order to realize that accuracy, it is necessary to insure that any glass used between the polarizer and analyzer be well annealed—easily measurable effects were obtained from microscope cover glasses 0.1 mm. thick.

The sensitivity of this instrument is then about $\pm$ 0.05 mμ, a sensitivity about one hundred times greater than that obtainable with a graduated quartz wedge.

The authors wish to acknowledge their indebtedness to Dr. F. E. Wright for many valuable suggestions received in the course of numerous discussions on the subject of polarized light, which led them to a consideration of the determination of path-difference as a general problem in elliptical polarization.

SUMMARY.

In connection with an investigation that involved the measurement of optical path-difference and thence birefringence it became necessary to have much higher accuracy than is ordinarily attained. After a careful study of the various methods available it appeared that the one which best meets the requirements of precision and simplicity is a method

first elaborated by Friedel (1893), and based on an interesting property possessed by a fixed combination of (1) a polarizer, (2) the birefracting material, and (3) a quarter-wave plate, each placed in a definite orientation to the others. When plane parallel monochromatic light passes through the elements of this fixed combination in the order shown above, the emergent light is plane polarized and the azimuth is related in a simple manner to the path-difference of the specimen. Since this azimuth can be measured by means of an analyzer and graduated circle, the determination of path-difference thus reduces itself to the measurement of an angular displacement, which can be done easily and with high precision.

The method was first made applicable to a petrographic microscope for the purpose of determining the path-difference at a given spot in small specimens. Later, there was constructed a separate polarimeter in which large specimens could be conveniently measured. This instrument has given all that was expected of it in facility and rapidity of taking readings, and for any path-difference has a sensitivity about one hundred times greater than that of the devices in common use.

A resumé of the general relations for elliptically polarized light as applied to the present method is given, and the magnitude of the errors that may arise is discussed in detail.

GEOPHYSICAL LABORATORY,
CARNEGIE INSTITUTION OF WASHINGTON,
March, 1933.

TURBINE GENERATOR VENTILATION.

BY

CARL J. FECHHEIMER,

Consulting Engineer, Milwaukee, Wis.

The ventilation of turbine generators has undergone many changes since the early days of this type of machine. Undoubtedly, the improvements that have been effected, and the changes from the rule-of-thumb methods to means whereby the ventilation is calculated, have contributed largely to the reduction in size for a given rating and to our present abilities to manufacture machines of much greater power for the high angular velocities at which they now operate. The subject may be conveniently divided into three principal headings: (1) Stator ventilation, (2) Fan design, (3) Rotor ventilation. These three will be discussed in that order.

I. STATOR VENTILATION.

The turbine generator is distinct from other types of machines, such as salient pole alternators or D.C. machines, as in the longer machines of those types the major part of the cooling air is caused to flow through the rotor before it passes into and through the stator. The rotor is too crowded in the turbine-generator to admit of more than limited volumes of air, generally entirely inadequate for cooling the stator. On the other hand (for electromagnetic reasons), the air gap in the turbine generator is large, and consequently for the shorter machines the cooling air can be caused to flow from both ends through the air gap, to be discharged through radial vent ducts in the stator core, such as shown in Fig. 1.

As machines for larger ratings were demanded, the lengths were increased, with proportionate increase in radial vent duct area, but without any change in gap area. Consequently, the gap area was too small for long machines, and the distribution of air for the radial vents was far from uniform, about like that shown in Fig. 2. Consequently,

FIG. 1.

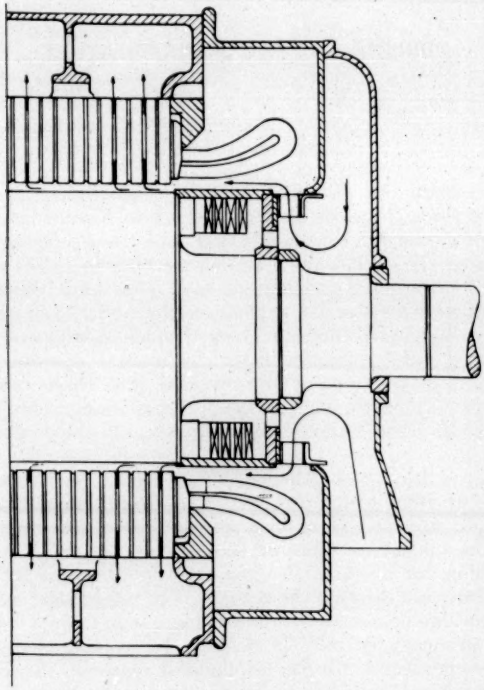

Simple radial ventilation.

with such long machines the middle of the machine would be considerably cooler than the ends.

It then became necessary to introduce more paths for the air. There are then two possible general solutions or modifications, or combinations thereof, as follows:

(*a*) Axial ventilation, for which the air flows in axial vent ducts in the stator core, in parallel with the air gap, the air being discharged radially. See Fig. 3.

FIG. 2.

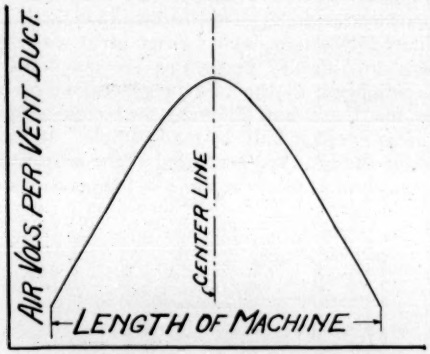

Air volume distribution in long machine with simple radial ventilation.

(*b*) Multiple path radial systems, for which, in parallel with the paths shown in Fig. 1, air introduced at suitable places at the back of the core is caused to flow radially inward, and then is discharged radially outward at other suitable places. In passing from radially inward to radially outward, the air may be caused to flow either normal, or parallel, to the axis, and there are considerable differences in results according to which of these two ways is selected. When, in this intermediate path, the air flows normal to the axis, the scheme is sometimes called the "Circumferential Radial," or "Aichele System," after its inventor, and is shown schematically in Fig. 4. For the air flowing parallel to the axis, which we shall call the "multiple path radial system," the scheme is indicated in Fig. 5. These schemes will be discussed more fully in the following:

(*a*) *The axial system* (Fig. 3) was used for a number of years by one large manufacturer in the U. S. As the machines were made for greater lengths, and as the slots were deepened, it was found that the temperatures near the middle were prohibitively high. This was due to the following reasons: (1) The vent duct section near the slots and teeth was too small to permit the flow of sufficient volumes of air to cool those regions; (2) The surfaces of the same vent ducts were

too small to admit of low temperature drop from the steel laminations to the air; (3) The distance that the heat had to flow radially to the vent ducts was too great with deep slots. There was no difficulty in keeping the core cool near its external periphery, as the rate of generation of heat was relatively low there, and the vent duct cross-sectional and surface areas could readily be made ample. It was at the region where the heat was generated at the greatest rate and where it was important to secure low temperatures that the

FIG. 3.

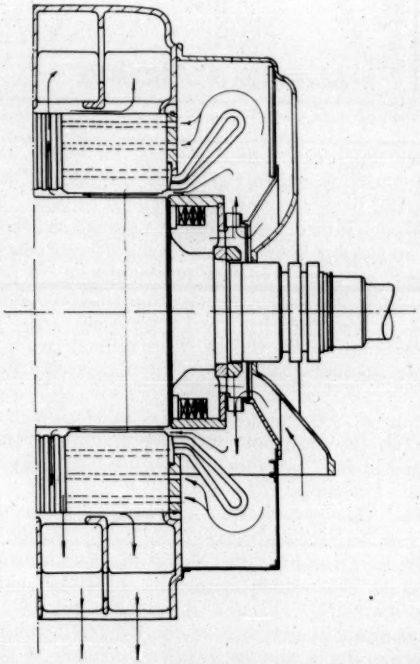

Axial ventilation.

FIG. 4.

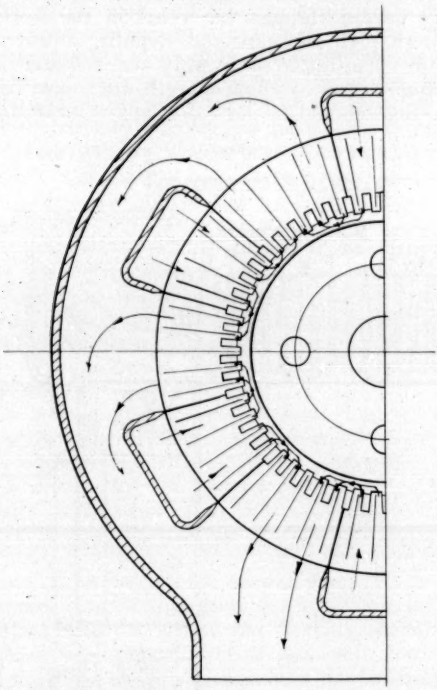

Circumferential system.

needed conditions could not be obtained. For long machines, an improvement can be effected by introducing some of the air at more positions axially, by feeding some air back of the core into radial ducts, whence it flows axially to other radial ducts and is eventually discharged therefrom. As applied to the large modern machines, the gains effected thereby are, however, usually not sufficient.

(*b*) In the *circumferential radial system*, the air may partly

flow in vents behind the slots and teeth, and the remainder then flows inward through the vents in the teeth circumferentially through the gap, and radially outward through other teeth. The latter paths only are indicated in Fig. 4. In order that adequate cooling of teeth and copper be effected, the proportions should be such that appreciable air volumes

FIG. 5.

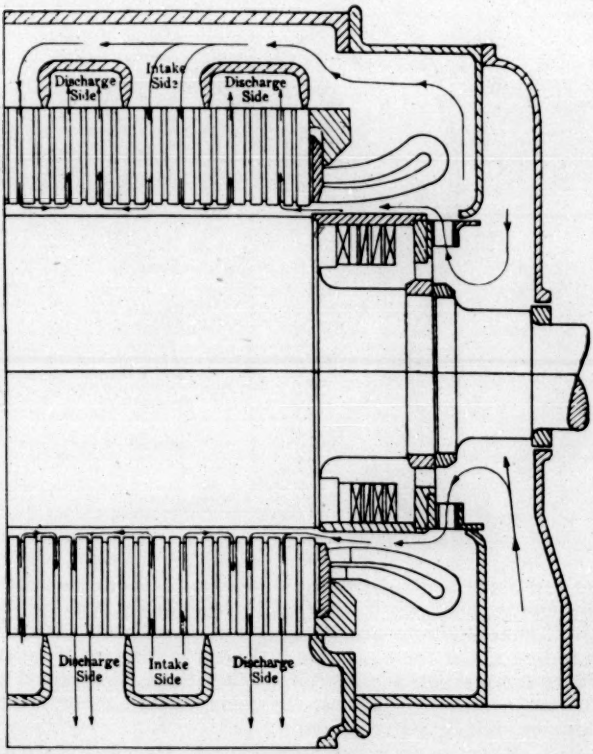

Multiple radial system.

be made to flow along such paths. In order to study the distribution of air with this scheme, a full scale model was built simulating one-half of a machine. It was found that with a large number of teeth in a belt circumferentially the influence of the high peripheral velocity of the rotor is to make for non-uniform distribution of air circumferentially; some radial vents had scarcely any air flowing through them, whereas others had an abundance. Consequently, with a large number of teeth in a belt, there is likelihood that there would be large variations in the teeth and copper temperatures, depending upon the location. If some of the air is shunted through paths back of the teeth, the distribution of that air is not influenced by rotation, but with deep teeth, a large percentage of the air should flow through vents in the tooth zone. The importance of using a small number of teeth in a belt has been recognized by engineers of the Allis-Chalmers Manufacturing Company that uses the circumferential system.

(*c*) *The multiple path radial system* (Fig. 5) has been adopted at the General Electric and Westinghouse Companies in U. S., and by the Brown Boveri and other European companies, except for the shorter machines, for which the simple radial system can safely be used. Unlike the circumferential radial system, with the air flowing axially in the air gap, the vent duct volume distribution circumferentially for a given position axially must be uniform. While it is true that there are departures from uniformity in an axial direction, the axial length of the intake and discharge belts can be so chosen that the departures from uniformity can be made small, or in any case, the differences in the tooth and copper temperatures for various axial positions in a belt are of low magnitude. As will be seen from a comparison of Figs. 1 and 5, the multiple system is an extension of the simple radial system. In both, air enters directly from the inner end bells, all flowing that way in the simple system, and only a portion in the multiple system. For the latter, holes are provided in the stator end plates through which the air passes, they being of such size that the pressure drop (which is proportional to the square of the velocity) is relatively small. There are several practical ways of constructing the

stator, but from the ventilation standpoint the results are the same, and the general scheme only will be described. If made as shown in Fig. 5, the regions with the holes are in only a portion of the end plates, say in the upper half, and the air passes axially to a circular duct which affords the means for the air to distribute circumferentially, and it then enters the intake radial vent ducts. After passing radially inward, some air flows to the left, and some to the right in the air gap. The planes between left and right flows in the air gap have been called "balance planes." At such positions, the axial velocity in the air gap is zero. After passing axially through the air gap, the air flows radially outward through the discharge vents, it being gathered in encircling ducts, and is finally discharged through a hole in the frame, usually at the bottom.

The flow in the stator and air gap will be better understood from an inspection of Fig. 6. This shows, in the upper half, the model on which the investigations were conducted. The air gap is closed off at the right end, the only end bell being at the left end; thus, the model was the equivalent of one-half of a machine. There are two intake belts, and $2\frac{1}{2}$ discharge belts, the center line being at the middle of the last discharge belt. The arrows will make clear the paths of air flow. In the lower part of Fig. 6 is a picture of the velocity curves in the various parts. The division planes in the lower picture correspond in position to the divisions in the upper picture. The gap velocities at the divisions are always maxima, and at some intermediate positions, i.e. at the balance planes, shown by dotted lines, the axial velocity becomes zero. It should be noted that, on the intake side, the axially moving air streams in the gap are away from each other, whereas on the discharge side they are directed toward each other. Furthermore, the gap velocities do not generally reach the same maximum for different division planes, and are lower than at the entrance from the end bells.

The velocity curves in the vent ducts are of the same forms as the volume distribution curves; this is so because the sections for all vent ducts are alike, the vents are equally spaced, and the volume per duct is equal to the velocity multiplied by the cross-sectional area. The vent duct curves

FIG. 6.

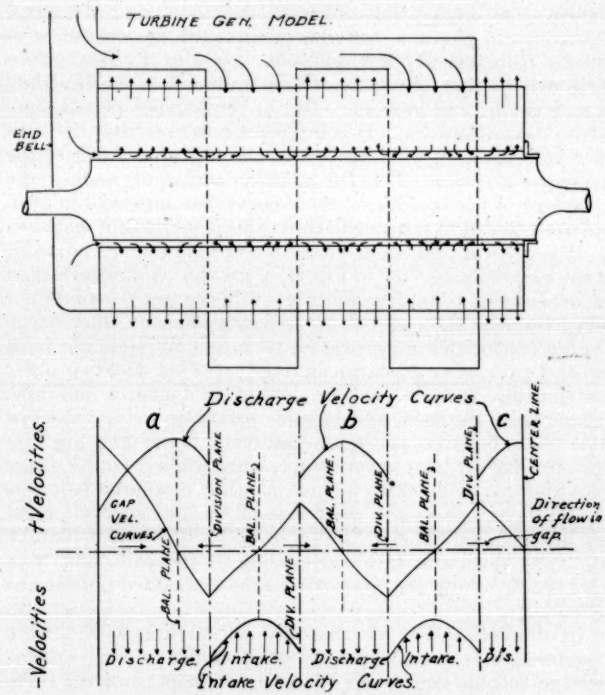

Schematic diagram to show directions of air flow and distribution of velocities.
Multiple radial system of turbine gen. vent.

are drawn smooth in Fig. 6, not with breaks corresponding to individual vents. The general forms in Fig. 6 are like those in a machine. They are plotted plus and minus, according to direction of flow; in the air gap from left to right is arbitrarily taken as positive, and in the vents the discharge is positive. In the intake belts, the vent duct velocities are maxima at the division planes, whereas in the discharge belts

the vent velocities are minima there. Also, at the balance planes, the intake velocities are minima, and discharge velocities are maxima, but the minima (or the maxima) for several belts usually are different. At the division planes there are distinct discontinuities in radial flow, in direction, in magnitude, and in slope. But at the balance planes there are no discontinuities. It is interesting to note that the vent duct velocities are proportional to the negative slopes of the air gap velocities. For the simpler forms of wedges the equations of the various forms of curves are now well known, and are utilized in the calculation of ventilation of a machine.

It is general practice to make the discharge belts adjacent to the end bells, as "a" in Fig. 6, of greater axial length than the other belts. As shown in Fig. 6, this causes the vent duct velocities near the end bell to be lower than in other parts. The end velocities may readily be raised by stepping back the end packages, as shown in Fig. 7. This and two other contributing factors prevent high temperatures in these regions being reached, and in some machines reduce it below other embedded copper temperatures. Those two are: (1) The entering air is at lower temperature when it comes direct from the end bells than for air in other discharge belts, as "b" and "c," or in the right side of "a," as such air must first have passed through, and absorbed heat from, the intake side. (2) With the excellent cooling of the coil ends, heat flows readily along the copper from the embedded portions to the ends.

In discussing Fig. 6, the only air streams which were considered in the air gap were those which moved axially. In large turbine generators the peripheral speed of the rotor is of the order of 5 miles per min., and the rotor surface carries some of the air with it circumferentially. Thus, if no air were caused to flow in an axial direction for cooling, the air would move circumferentially in the gap. Or, if the rotor were stationary, the cooling air would flow axially. Actually, the direction of flow is at an angle with the axis, the angle changing from one axial position to the next. The problem becomes very complicated. Rather exhaustive researches were made with apparatus simulating the simple wedge construction, for which rotation had very little influence. The

results enabled the determination of coefficients, with the aid of which the volumes and their distribution and the pressure drops could be predicted.

By changing the forms of wedges and fingers, advantage may be taken of the effect of the circumferential component

FIG. 7.

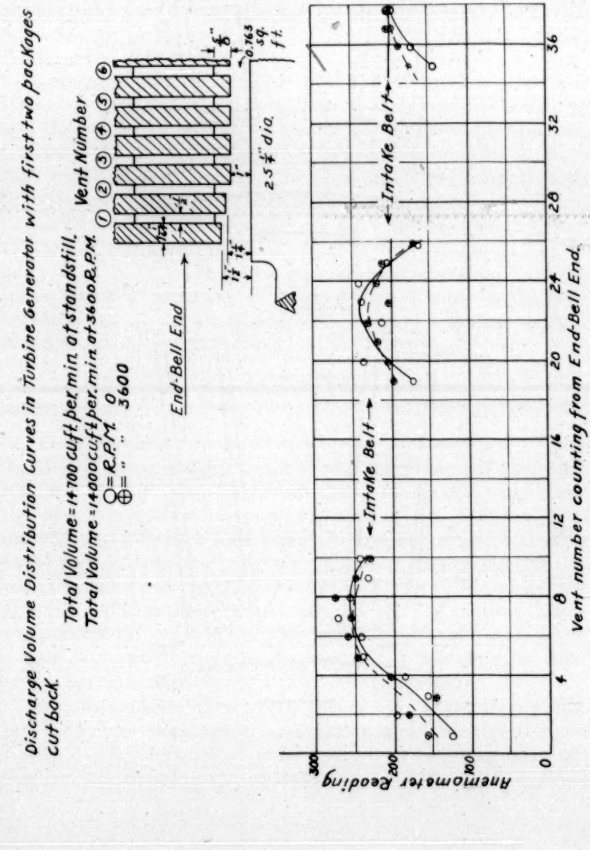
Discharge Volume Distribution Curves in Turbine Generator with first two packages cut back.
Total Volume = 14700 cu ft per min at standstill.
Total Volume = 14000 cu ft per min at 3600 R.P.M.
R.P.M. 0
3600
Vent Number
1 2 3 4 5 6
End-Bell End
25½" dia.
0.163 sq. ft.
Intake Belt
Intake Belt
Intake Belt
Anemometer Reading
300
200
100
0
4 8 12 16 20 24 28 32 36
Vent number counting from End-Bell End.

FIG. 8.

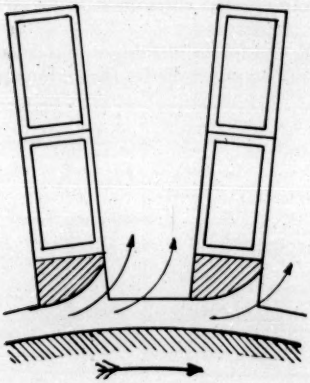

FIG. 9.

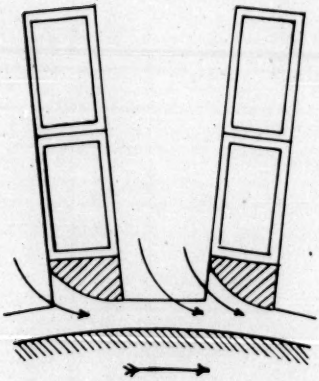

Improved form of stator wedges to assist air flow.

of the air gap velocity to assist the air to turn a right angle corner when issuing from a vent duct on the intake side, or when entering a vent on the discharge side. The General Electric Company were the first to improve the forms of wedges to assist ventilation. Their wedges are turned opposite for discharge than for intake, as indicated in Figs. 8 and 9. In consequence of considerable experimental work, the performances with wedges of various forms were compared. A discussion of the merits of different wedge forms is beyond the scope of this article.

Combined with the whole problem of turbine generator stator ventilation is the determination of the end bell pressures and the requisite amount of cooling air. When internal fans are used, the pressure generated by the fans must be equal to that required to overcome the summation of pressure drops in the various passages. The air volume needed for cooling is proportional to the losses absorbed by the air and inversely to the air temperature rise. If Q is the volume in cu. ft. per min., "K.W." the power in kilowatts represented by the losses (usually exclusive of bearing losses), and t is the temperature rise of the air in degrees C., then for normal density of 0.074 pound per cubic foot,

$$Q = \frac{1765 \text{ K.W.}}{t}. \qquad (1)$$

Thus, having calculated the losses, and assumed a value for the air temperature rise, the volume of air per unit time follows. A fair value for the air rise is 24 deg. C., which from the above equation corresponds to 73.5 cu. ft. of air per minute per kilowatt loss absorbed by the air. Thus, in a 1250 K.V.A. machine, the air volume is about 3800 cu. ft. per min., which corresponds to a loss of 53.5 K.W. for 24 deg. air rise. For a machine of 100,000 K.V.A. rating, about 120,000 cu. ft. per min. are needed, which, on the same basis, is equivalent to 1630 kilowatts loss. It is believed that these and other figures in Table I may be of interest.

A comparatively few years ago, about 3.5 cu. ft. per min. per K.W. loss were allowed for machines rated about 20,000 K.V.A. The very great reduction in air volumes has been due in part to allowable increase in air temp. rise of about

TABLE I.

K.V.A. Rating.	R.P.M.	Air Temp. Rise.	Air Vol. cu. ft./min.	Corresponding K.W. Loss.	Cu. ft./min. / K.V.A. Rating	K.W. Losses / K.V.A. Rating
1250....	3600	24°	3800	53.5	3.05	0.043
100,000.	1800	24°	120,000	1630	1.20	0.0163

20 per cent., and especially to the large reduction in losses, made possible by improved designs. The relatively low losses will be evident from an inspection of Table I.

An interesting point in this connection is that in many machines, even with the low losses and the light weight of air of only 0.074 lb. per cu. ft., the weight of air circulated in 3/4 hour is about equal to the weight of the entire generator.

In the design of the air circuit in a turbine generator, the first thing that is calculated is the air volume by equation (1). The pressure drop due to the summation of resistances to air flow is largely a function of velocities. The maximum velocities generally increase with the peripheral velocity. For a machine in which the rotor peripheral speed is 25,000 feet per min., the maximum velocities are given in Table II.

TABLE II.

Maximum Velocities, Feet Per Minute.

Air gap—at extremities	10,500
Air gap—at division planes	5,500
Radial vent ducts intake	7,500
Radial vent ducts discharge	10,000

The maximum velocities give air pressure drops of about 5 inches of water for a 1250 K.V.A., up to about 9 inches of water for a 100,000 K.V.A. generator.

The second step in the design of the air circuit is to determine approximately the number of radial vent ducts. In his electrical calculations, the designer had decided upon the total axial length of the iron, and from past experience he knows the approximate axial spacing of the vents. (The vents are usually 3/8 or 1/2 inch wide.) The total number of vents can then be calculated.

The third step in the design of the air circuit is the determi-

nation of the number and axial lengths of the intake and discharge belts. With the maximum velocities given in Table II as a basis, with a little cut and try, these can readily be laid out.

The final check on the air circuit is the calculation of the balance planes, the velocity distribution in the various belts, and the total pressure drop. As in most design work, that may mean several trials with changes in proportions until the engineer is satisfied with the proportions. Having determined the pressure drop and the volume of air, he next designs the fans to deliver that volume and pressure. This will now be discussed in Part II.

II. DESIGN OF FANS.

In this discussion internal fans only will be considered. External fans are used on some very large machines for which the space or other limitations prevent internal fans from performing well, or of giving reasonably high efficiency. The gains achieved by internal fans are reduction in auxiliary apparatus and the greater safeguard that would accompany the insurance of adequate ventilating air for all loads on the generator.

The internal fans are of two general types: centrifugal and propeller. The *centrifugal* fan derives its name from the fact that most of its pressure is generated by centrifugal force. The ordinary fan used for ventilating buildings or mines is usually of the centrifugal type. The air passes in a general radial direction through the runner of the centrifugal fan. In the *propeller* type fan, the air moves parallel to the shaft, the pressure generated being largely due to the velocity created by the fan blades moving through the stream. A typical example of propeller type fan is the ordinary desk ventilating fan.

Some of the earliest fans on turbine generators were of the propeller type. There were no data on which to base the air volumes or the pressures generated, and they were found entirely inadequate. Such fans were designed by appearance only. As they performed poorly, those fans were abandoned a great many years ago, and various other types have followed them.

On most of the turbine generator rotors centrifugal fans have been provided. Those fans were also designed by rule-of-thumb methods for many years, until it was appreciated that the losses in the fans were relatively high so that the temperature rise of the air due to the fan loss was of appreciable magnitude. Furthermore, there was no means

FIG. 10.

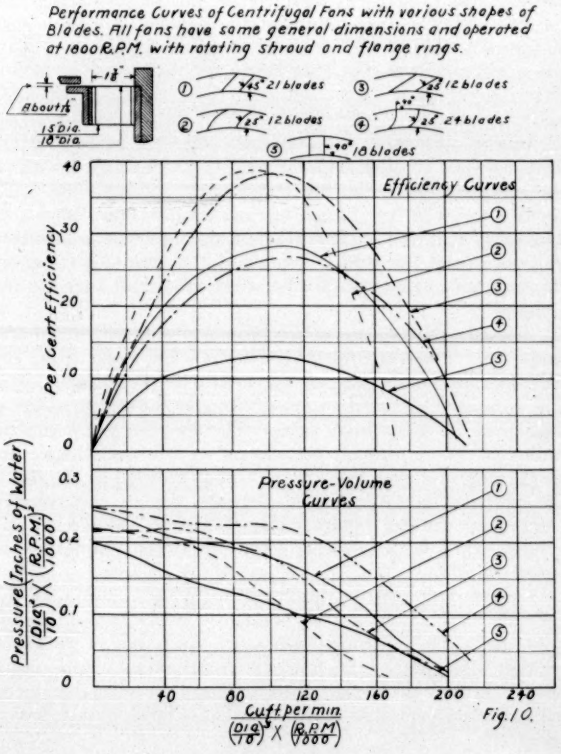

Fig. 10.

available for predicting the volume and pressure which the fan delivered. Researches were conducted, beginning in 1917, on performance of centrifugal fans, from which investigations the blade shape for improved efficiency could be determined, and also methods were developed by means of which the proportions could be predicted. Insofar as the influence of blade shape upon performance is concerned, an idea may be obtained from Fig. 10, which shows the marked influence of the blade shape upon the efficiency of, and

FIG. 11.

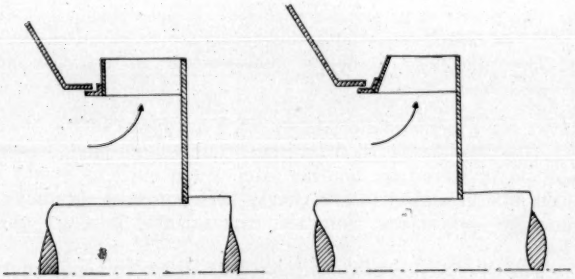

Centrifugal fans with flat and conical outer walls.

pressure developed by, the fan. It will be noted that the maximum efficiency is about the same for straight blades that are inclined backward, making an angle of 25 degrees with the periphery, as for those that are curved backward for the same angle at entrance. The straight blade fan is simple to manufacture, and gives slightly more volume at the lower pressures. However, the curved back blade has the advantage of delivering a somewhat lower pressure while giving fairly high efficiency, and in many machines the lower pressure is desired. Consequently, the curved back blade fan is also used in many machines. In the investigations which were conducted, the influence of the width of the fan, the number of blades, and the depth of blades were also studied. It was found, for instance, that the volume delivered by a fan does not necessarily increase in direct proportion to the width. Another improvement is to make the outer wall of the fan conical instead of a simple flat disc, such as indicated in Fig. 11.

For most practical applications, the relations which obtain between the fans of one size and those of another are of importance and may be of use. Generally, the performance of a large fan is slightly better than for a small one. Disregarding that small gain, for a given point on the curve, they may be put in simple form, as follows: For fans that are similar (i.e., the small fan is the large fan scaled down):

1. The volume is proportional to dia. × peripheral velocity × width.
2. The pressure is proportional to (peripheral velocity)^2.
3. The power is proportional to (peripheral velocity)^3 × dia. × width.
4. The efficiency is nearly independent of the size and speed.

If we have performance curves such as shown in Fig. 10, it is extremely simple to determine what volume and pressure will be delivered by another similar fan such as would be used in a generator. The checks between data obtained on machines and those from the experimental fans are quite close.

The application of centrifugal fans to a turbine alternator is as shown in Fig. 12. The fan is at the position shown in "A." In this particular case, a partition is used half way across the fan to add strength to the blades against the high centrifugal forces. As generators become larger, it is found that the area between the inner periphery of the fan and the outer periphery of the shaft is too small to admit the volume of air required unless prohibitively high velocities are reached, which in turn affects the performance adversely. To overcome this difficulty, a double entrance fan was developed as shown in Fig. 13.[1] This fan has been used on some of the more difficult ratings of large 3600 R.P.M. and 1800 R.P.M. turbine generators. After passing through the outer end bell, approximately half of the air passes directly into the fan; the other half passes through the axial triangular stationary

[1] For more detailed description, see article by M. D. Ross—"A Recent Improvement in Generator Ventilating Fans," *Elec. Journal*, March, 1929, p. 134.

ducts shown in Section B–B at the right. That air passes through the right side of the fan, and the air from both the left and right sides of the fan is discharged between the triangular stationary ducts, which now act as stationary guide vanes for the air.

FIG. 12.

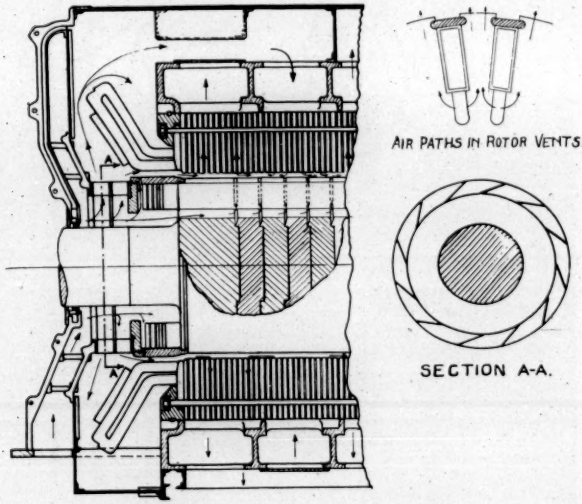

Single entrance fan. Early scheme of rotor ventilation.

The double entrance fan was found somewhat difficult to manufacture and assemble. Furthermore, with all centrifugal fans as used in the large machines, it was found that more pressure was developed by the fans when worked at their point of maximum efficiency than was needed to drive the air through the machine. With the great demand for high efficiencies this led to a return to the propeller type, and a study of the performance has been made. With this type of fan it is possible to use large fan diameters entailing high peripheral speeds, secure large volumes and lower pressures, and still work at, or near, the maximum efficiency of the per-

FIG. 13.

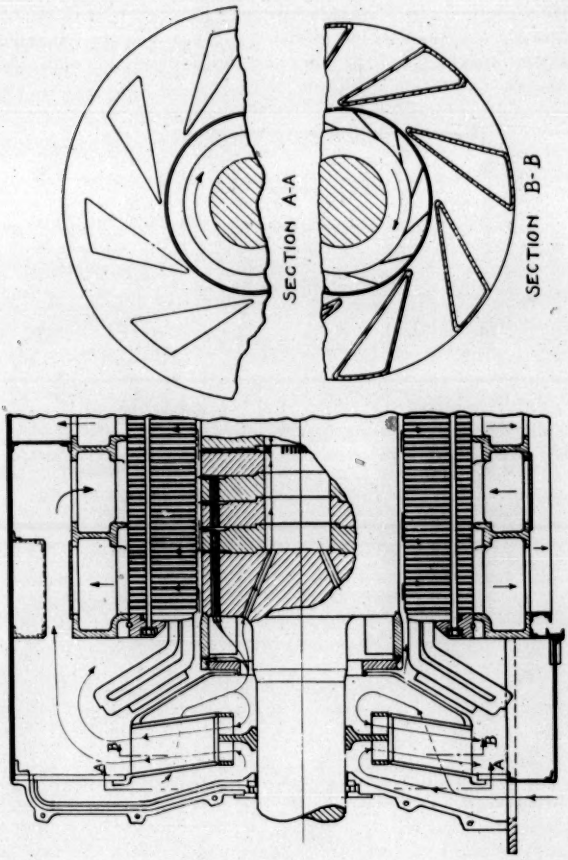

Double entrance fan. Improved scheme of rotor ventilation.

formance curve. The application of a propeller type fan to a large 3600 R.P.M. rotor is shown in Fig. 14. The blades are curved—there are usually four or six per fan. They are comparatively easily built and assembled. A cross section of a machine showing the propeller type fan is given in Fig. 15. Frequently, one or more stationary guide vanes are provided ahead of the fan, so as to help the air around the corner before entering.

FIG. 14.

With the improved efficiencies of fans and the reduction of pressure, as well as the reduction of losses in other parts of the machine, it has been possible to decrease the volume of air needed for cooling and windage loss due to power required to drive the fans. This, however, is today perhaps one-third of what it was ten years ago for the same size machine. It is of the order 0.25 to 0.50 per cent. of the K.V.A. rating of the machines to which they have been applied.

Considerable confusion exists as to the meaning of efficiency as applied to fans. The fan is similar in every way

FIG. 15.

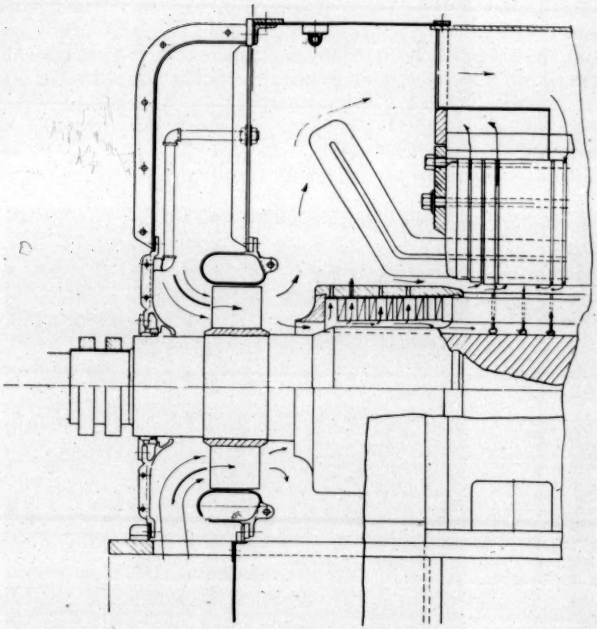

Propeller fan.

to a centrifugal pump; using hydraulic terms, the power output is proportional to the head pumped against multiplied by the volume per minute. The efficiency then is:

$$\frac{\text{cu. ft./min.} \times \text{pressure in inches of water}}{\text{k.w. input} \times 8500}. \qquad (2)$$

III. ROTOR VENTILATION.

Some of the earlier turbine generator rotors were not ventilated internally at all, as the mechanical difficulties were considered to be too great. Heat can be transferred from

the outer rotor cylindrical surface to the air in the air gap at a high rate, but the surface is limited, and the radial distance that the heat must flow introduces a considerable thermal drop. For a given copper temperature rise the rating can be appreciably increased by good internal ventilation. One of the early types of ventilation is shown in Fig. 12. The ventilating air for the rotor did not pass through the centrifugal fans, but passed underneath them, radially below, or through holes in, the rotor end plate, below the end windings of the rotor, and then into ducts below the rotor slots. The air was discharged through a multiplicity of radial ducts from the axial slots below the main rotor slots. For rotors built up of steel plates, the part of the plate which included the slots was machined back to permit the air to pass from the axial ducts out through the teeth into the air gap, as indicated in the sketch at the right in Fig. 12. The centrifugal force due to the difference in peripheral velocities at the external diameter and at the axial duct was sufficient to propel the air through the tortuous paths. This scheme serves for the shorter rotors. For long rotors, the limitation imposed by the comparatively small section of the axial duct prevented sufficient air getting in to supply all the radial vents, and the volume of air issuing from the middle vents was very much greater than at the end vents. The distribution was comparable to that shown for the stator in Fig. 2. This scheme, modified in some structural details, is still used, particularly for 2-pole rotors. It is often best, in order to improve the distribution, to use fewer vents and space them closer near the ends than near the middle.

More recently, this difficulty has been overcome in the large four-pole plate rotors, by means of a large central hole in the plates, as shown in Fig. 13. All but the vents adjacent to the ends are then fed from this large central hole. The axial velocities in this central hole are comparatively small, so that the distribution between vent ducts axially is scarcely affected thereby. The large central hole is fed by diagonal holes drilled through the end forging to a position just below the coil ends. The air issues from the central hole through radial rectangular slots machined into the teeth. The centrifugal forces arising from the large difference in peripheral

speeds between the external and internal diameters of these slots create a considerable pressure, so that the air moves through the slots at high velocities. Even though the air flows through the diagonal holes from a larger to a smaller diameter, this is compensated for by the great relative depths of the rectangular slots in the teeth. The first one to four ducts in the rotor are not fed from the central hole, but are fed through axial round holes drilled through the end forging and through the rotor plates, and that air is discharged through the radial slots in the plates. In some recent machines the end plate is entirely free from the shaft, such as is indicated in Fig. 12, providing for easy access for the air. The area of the annular space between the end plate and the shaft is such that the velocities there are considerably lower than they are in other places. At the present time, the principal limitation to this scheme of ventilation is in the diagonal holes where the velocities are high. It is of interest that the foregoing schemes of rotor ventilation now admit of calculation.

As stated previously, the scheme shown in Fig. 12 is used largely with 2-pole rotors. The large central hole (Fig. 13), suitable for 4-pole rotors, cannot be adopted for 2-pole machines, as all of the steel below the slots is needed for the return of the magnetic flux. The above described schemes have been used by the Westinghouse Company, and the first scheme, modified in details, by other companies.

An ingenious scheme, due to the late R. B. Williamson of the Allis-Chalmers Manufacturing Company, is shown schematically in Fig. 16. Radial ventilating ducts in the teeth are fed from the air in the air gap, and the air is discharged through diagonal ducts back into the air gap. The air is impelled through the ducts by so shaping the entrance as to simulate a propeller type fan. One advantage of this scheme is that the length of the machine does not impose a limitation. With this scheme the developed pressure is that which can be generated with the scooping effect at entrance, and while that is not so great as with other schemes in which a very high centrifugal head is generated, the entrance restrictions which impose limitations with the other schemes do not apply.

FIG. 16.

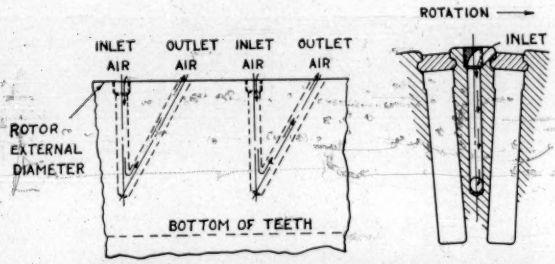

SCHEME 4. VENT DUCTS FED FROM AIR GAP AND DISCHARGING FROM DIAGONAL HOLES INTO AIR GAP

ROTOR COIL END VENTILATION.

The cooling of the rotor coil ends is equally important with that of the rotor body. For a number of years the coil ends were not ventilated. The heat generated by I^2R loss in the ends was then conducted along four paths—(1) radially outward to the surface of the retaining ring; (2) radially inward, to be absorbed by the axially moving air before that air entered the main axial vents in the rotor body; (3) axially away from the center to the rotor end plate; and (4) along the copper to the embedded copper in the slots. All four paths offered large resistance to the flow of heat, with the result that when the coil ends were long (particularly in 2-pole, 25-cy. rotors) there were very high temperatures in parts.

Following this, radial holes were drilled in the retaining rings at positions to correspond to the coil corners, as indicated in Fig. 17. The improvement was only slight. The reasons therefor were: (1) While the velocities through the retaining ring holes were high, the velocities at the coil surfaces were low; (2) The coil surfaces adjacent to which the air flowed were a small percentage of the total coil surfaces.

Both of these objections have been met in the recent rotors by the scheme shown in Figs. 18 and 19. Blocking is put between adjacent coil ends with slots machined in the sides of the block. The openings in these slots are made narrow in

FIG. 17.

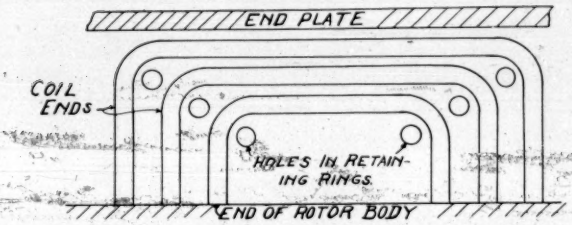

Simple rotor end winding ventilation.

FIG. 18.

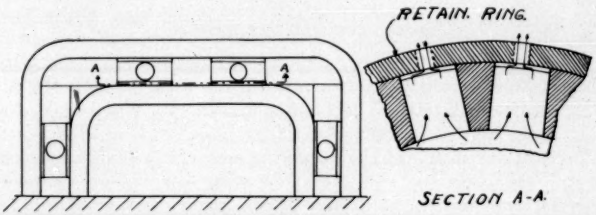

Improved rotor end winding ventilation.

order that the velocity of the air adjacent to the coil sides is high, affording excellent cooling. The air is discharged through radial holes drilled in the retaining ring. The pressure generated by centrifugal forces, due to the difference between the peripheral velocities at the outside of the retaining ring and the inside of the coil surfaces, is large, and insures that ample cooling air volumes are supplied at high velocities. The coil surfaces exposed to the radially moving air are about one-half the total. The temperatures of the coil surfaces not exposed to the air streams are but little greater than the exposed surfaces, as the generated heat is readily conducted for short distances. Tests on a laboratory model showed that the temperature rise with the improved ventilation was only 23 per cent. of what it would have been without ventilation, there being the same electric current in both

FIG. 19.

Improved rotor end winding ventilation.

cases. This improvement was developed at the Westinghouse Company.

CLOSED CIRCUIT SYSTEM OF VENTILATION.

For many years the cooling air was taken from, and discharged into, the power house room. The generator

became filled with dirt in a comparatively short time, filling the vent ducts (thereby impeding ventilation), covering the insulation, and generally being harmful. Then air washers were introduced to clean the air. These entailed expensive and large air ducts, which occupied valuable space, in addition to the expense of the washer. Further, these washers were not able to remove all the dirt, and in the course of time, considerable dirt would still be deposited in the machine. Practically every recent large turbine generator installation is of the closed circuit type. The same air is used continuously; as the amount of dirt in the air within the system is small, very little dirt is deposited. In this system, the air is cooled, usually by surface coolers, finned on the air side, the heat being abstracted by means of water flowing in tubes in the cooling coils. In nearly all cases the internal fans on the generator are so designed that they generate sufficient pressure to force the air through the generator ventilating passages plus the external ducts and cooler. In the closed circuit system of cooling, it is important to close all surface joints or cracks, as at high pressure points air is discharged through the openings, and at low pressure points it is drawn in, and with it some dirt enters. The gathering of dirt with this system may be attributed to not having surface joints sealed.

NOTES FROM THE U. S. BUREAU OF STANDARDS.*

COMPARATIVE FUEL ECONOMY WITH GASOLINE AND WITH ALCOHOL–GASOLINE BLENDS.

One of the outstanding points of interest in connection with the use of alcohol-gasoline blends in automobile engines is the comparative fuel economy with gasoline and with the blend. Recently, the Bureau of Standards has undertaken two series of tests along this line.

In the first series of tests, runs were made with 15 cars, mainly of 1932 and 1933 models. All of them were in typical operating condition and were not reconditioned for the tests except that in some cases changes were made in the carburetor equipment to make possible adjustment of the mixture ratios in the course of the tests. The cars and the fuels were both selected with a view to being typically representative of products now in use on the highway. Tests were run over a course of about 89 miles, with the usual precautions to assure accurate measurements of distance, car speed, fuel consumption, and such other quantities as were necessary to secure accurate results. The cars were driven, in all cases, by experienced drivers who were not informed as to the fuel in use on any particular test, thus avoiding any possible prejudice in this regard.

Since cars are operated on the road using a variety of carburetor adjustments or corresponding mixture ratios, these conditions were reproduced as follows: The fuels were classed in pairs, one of each pair being a straight gasoline and the other the same gasoline with 10 per cent of absolute alcohol. Several carburetor adjustments were made on each of the cars and either one or both pairs of fuels were run in each car with each of the carburetor adjustments. Thus there was obtained a total of 43 direct comparisons between gasoline and the corresponding alcohol-gasoline blend, each run at the same setting of the carburetor in a given car. In making these

* Communicated by the Director.

tests, the cars were run as close to the legal speed limits throughout the course as traffic and traffic lights permitted. The driving time to cover the course of 89.2 miles was in most cases very close to 2 hours and 50 minutes.

Four of the 15 cars showed on the average more than 1 per cent poorer fuel economy with the gasoline than with the alcohol-gasoline blends and six cars showed at least 1 per cent poorer fuel economy with the alcohol-gasoline blends. From the results on all cars, it was found that the average fuel economy with the two gasolines was 15.91 miles per gallon and with the two blends containing 10 per cent of absolute alcohol it was 15.85 miles per gallon.

On the average, it was observed that somewhat poorer acceleration was obtained with the alcohol blend than with the gasoline. In order to obtain further information on this point, runs were made with two cars using carburetor adjustments for equal acceleration. Under these conditions, the average fuel economy in these two cars was 18.65 miles per gallon with the gasoline and 18.00 miles per gallon with the alcohol blend.

A second series of tests was conducted in cooperation with the American Automobile Association using 4 cars run at constant speed over a 10 mile course. Several different carburetor settings were employed with each car and runs with each carburetor setting were made using gasoline and a blend of this gasoline with 10 per cent of absolute alcohol. The atmospheric temperature was much higher than during the first series of tests, so that the runs were conducted under conditions approaching vapor lock such as are encountered frequently during hot weather operation. The average fuel economy with the gasoline was 16.54 miles per gallon while with the alcohol blend, it was 16.02 miles per gallon. Greater differences in fuel economy were obtained with individual cars during the first series but the higher atmospheric temperature during these runs may have influenced the results, owing to the fact that an alcohol-gasoline blend boils more readily in the fuel lines than does the gasoline with which the alcohol is blended.

The foregoing results lead to the following conclusions:

1. When a 10 per cent. blend of absolute alcohol with

gasoline is substituted for the same gasoline without alcohol, without any change in carburetor adjustment, there is, on the average, no significant change in the miles per gallon under normal operating conditions and in the absence of vaporization in the fuel lines. If vaporization is occurring, as often is the case in hot weather, the fuel consumption will tend to increase more rapidly with the alcohol blend than with the gasoline.

2. The substitution of the 10 per cent. alcohol blend, under the above conditions, on the average, results in a small loss in acceleration or get-away.

3. In order to restore the acceleration to that obtained with gasoline, a different carburetor adjustment must be made for the alcohol blend, and when this adjustment is made the alcohol blend gives, on the average, 4 per cent. less miles per gallon than the gasoline. It is found by experience that carburetors on the average are adjusted to give maximum acceleration.

Many models of automobiles are furnished with a fixed or unchangeable carburetor adjustment which is designed for maximum acceleration. If the character of fuel changes it is to be expected that a new fixed adjustment will be chosen such as still to secure the maximum acceleration, with an accompanying loss in fuel mileage for the blended fuel.

EFFECT OF OZONE ON ENGINE KNOCK.

Ozone has been found to be more potent in causing detonation, or "fuel knock," than tetraethyl lead is in suppressing it. As little as two thousandths of a per cent. will cause an increase in detonation equal to that occassioned by substituting regular gasoline for premium gasoline. By using somewhat higher concentrations—up to one hundredth of a per cent.—regular and premium gasolines were made to knock as badly as does kerosene. These concentrations of ozone, however, had no effect on power or efficiency when the compression of the engine was such that no detonation occurred.

While the average motorist is more interested in suppressing detonation than in obtaining it, and while stratosphere flights are still too far in the future to cause concern over the

possible effect of ozone in that region on the engines used, this discovery gives automotive and petroleum technologists a new tool with which to study detonation and to test theories thereof. As ozone and tetraethyl lead have opposite effects of the same order of magnitude, a study of the action of ozone may throw light on the mechanism whereby tetraethyl lead suppresses detonation.

EXTREME PRESSURE LUBRICANTS.

About two years ago, the Society of Automotive Engineers requested the Bureau to undertake an investigation of extreme-pressure lubricants, in cooperation with the automotive and petroleum industries, gear and bearing manufacturers, and various operator's organizations, with the object of developing satisfactory test methods which would be significant as regards service performance. A progress report on this work was presented at the meeting of the Society of Automotive Engineers, August 28—September 4, and a description was given of a new lubricant tester developed at the Bureau.

The problems connected with extreme-pressure lubricants are of comparatively recent origin. In order to make possible further lowering of automobile bodies, many companies introduced a new type of gear in the differential housing. This new type of gearing, called hypoid gears, could not be satisfactorily lubricated with mineral oils, and it became necessary to develop special lubricants capable of standing up under the higher pressures involved. Since the development of extreme-pressure lubricants opened up a new field in lubrication, test methods for these lubricants were almost entirely lacking. Many test methods are required but the most important one is for the load-carrying capacity since if the lubricant will not stand a high pressure, it does not make any difference how many other desirable properties it has. The Bureau's work to date has been confined to an investigation of load-carrying capacity, but will be extended to include other properties of extreme-pressure lubricants as soon as possible.

After considerable experimentation on methods for meas-

uring load-carrying capacity, a machine was developed at the Bureau which appears to be satisfactory. Its basic principle is the use of two rotating steel rolls, essentially toothless gears, which rub against each other and which are lubricated by the extreme-pressure lubricant. The pressure between the two rolls is gradually increased until scoring of the metal surfaces occurs. The weight required to produce this pressure through suitable levers is called the load-carrying capacity of the lubricant. New rolls must be used for each lubricant and for each of the speeds, lubricant temperatures, and rates of loading at which it is tested. Lubricants were tested which had a load-carrying capacity 20 times as great as mineral oils.

Tests were made on a number of lubricants which had been run in cars on the road by various companies, and the new tester was found to rate the lubricants in the same order as their service performance. These results appear so promising that a recommendation has been made that a number of these machines be constructed and that coöperative tests be conducted with them by several laboratories, as a basis for standardization of the machine.

FIRE HAZARD OF DOMESTIC HEATING INSTALLATIONS.

An annual fire loss for the country as a whole of about $20,000,000 is reported as caused by stoves, furnaces, boilers, and their pipes; or between 9 and 10 per cent. of the loss from all known causes. If domestic heating installations are responsible for the same proportion of fires, the causes of which could not be ascertained, the total fire loss per year from such installations would be about $45,000,000, equivalent to the destruction of the homes of some 50,000 people.

Fires may result from placing stoves, furnaces, and other heating equipment too near combustible walls, partitions, and ceilings, or from absence of adequate protection for floors. Definite information on the required spacings of heating equipment from unprotected combustible construction and on the protections needed for closer spacings has been lacking, the requirements in building codes being based on fragmentary information obtained from actual fires.

In tests recently completed at the Bureau, the results of which will appear as Research Paper No. 596 in the September number of the *Bureau of Standards Journal of Research*, stoves, furnaces, and their pipes were spaced at different distances from unprotected partitions, ceilings and floors, and hot fires maintained for periods ranging from one to seven hours. Protections of sheet metal, asbestos, or brick were then applied and the least resistance determined that would be safe from the standpoint of hazardous temperatures that might cause ignition of the wood. It was found that stoves for house heating should be spaced not less than 24 inches from walls faced with wood, and the smokepipes not less than 12 inches below wood joists or ceilings. If bright sheet metal is applied to the walls, the spacing can be decreased to 12 inches. Similarly, plastered wood stud partitions, while requiring a spacing of not less than 18 inches when unprotected, will be safe if only 9 inches from stoves where the area exposed is covered with bright metal. Bright metal, such as galvanized iron, was found considerably more effective than black iron, since it reflects more of the radiant heat.

Tests with smokepipe thimbles indicated that a ventilated air space of not less than 4 inches all around the pipe, or of 2 inches if filled with insulation, is necessary where smokepipes pass through combustible partitions.

If stoves are without ashpits, or if ashpits are heated to near redness, an air space of 5 inches or more should be provided between the stove and a wood floor and the latter covered with incombustible insulation 1/4-inch thick under sheet metal. If the fire box rests directly on the floor, the latter should be of incombustible materials throughout for the area surrounding the stove. For this condition, temperatures high enough to cause ignition of wood were transmitted through a 4-inch brick base. This explains the frequent occurrence of fires caused by ignition of wood forms left in place under brick or concrete arches supporting fireplaces.

Furnaces for hot-water installations and their pipes were found to present little hazard to adjacent construction as fired with either coal, oil, or gas. The hazard from warm-air heating ducts was found to be moderate, protections being required only where they enter floors or partitions relatively

close to the furnace. In the case of the "pipeless" furnace, the down-draft of cold air around the warm-air duct protects the adjacent construction, the hazard with this equipment resulting mainly from placing combustible materials on the warm-air register or locating the latter beneath or too close to partitions.

Tests with a gas range having an oven without insulation indicated that 6-inch separation between the side of the oven and a wood partition gives reasonably safe conditions.

DAMPNESS IN MASONRY WALLS ABOVE GRADE.

Many inquiries regarding causes and methods of preventing dampness on the interior surface of exterior walls of brick, structural clay tile, concrete block, stone, and stucco are received by this Bureau. These inquiries come with greatest frequency during periods immediately following unusually severe rains. Those received recently indicate that the storm during the latter part of August, which was most intense along the Atlantic Coast, caused many damp walls. In order to answer such inquiries more fully than would be feasible by individual letters, a letter circular is being prepared, single copies of which will be obtainable upon request addressed to the Bureau of Standards.

Although nearly all building walls are permeable in the sense that they would leak if subjected to water under pressure, most walls of any type are satisfactory in service. Descriptions and observations of structures where dampness has occurred indicate that faulty design and construction usually is the cause. Apparently the possibility of damp walls is not always considered during construction. These masonry materials sometimes are used as if they were impermeable and non-absorbent, whereas most of each type are readily permeable and all will absorb water.

It is evident, therefore, that in order to avoid dampness in masonry, provisions should be made to prevent the relatively large volumes of water which are collected on roofs or other horizontal surfaces from flowing onto the masonry. Horizontal surfaces of masonry, unless continuous and nearly impervious, either should be water-proofed or separated from

the masonry below by flashing of durable materials. Also, constructions which project beyond exposed faces of walls should be provided with undercut drips, in order to shed the water away from the walls. As wind-blown rain may enter in relatively large quantities through cracks or other openings in the exposed vertical faces, exposed joints between the masonry and other materials and in the masonry, unless well sealed, offer an easy path for water.

Moisture from the ground or from rain splash may rise in the masonry by capillarity. This may be prevented by placing a layer of impervious materials, such as slate or sheet copper, in a horizontal joint 5 to 10 inches above the surface of the ground. This provision costs but little during construction.

Most builders agree that adequate flashing, the sealing of exposed joints and the insertion of dampproofing are essential for maintaining freedom from dampness. Also furring generally is conceded to be desirable but this is often omitted on account of its cost in spite of the fact that in regions subject to storms of considerable duration dampness is apt to occur occasionally on masonry walls 8 or 9 inches in thickness if the plaster is applied directly to the masonry. The amount of water which may strike an exposed vertical surface during severe rain storms greatly exceeds the water-holding capacity of ordinary masonry walls 8 inches thick. Moreover, in storms lasting one to four days, there is ample time for the water to pass through such walls in sufficient quantities to cause dampness in the plaster. Examples of unfurred 8-inch walls which have given satisfactory service are numerous but it is believed that many of these are protected by surrounding objects such as buildings and trees.

The application of a so-called colorless waterproofing to the exposed faces of walls is often resorted to in attempts to check dampness. This is not always successful. In some cases lack of success may be attributed to failure to make needed repairs to flashings, inadequately waterproofed horizontal surfaces and unfilled cracks. As none of the liquid waterproofings will seal openings that are large enough to be visible, these should be sealed before applying the solution. Moreover, the partial sealing of vertical surfaces by means of coat-

ings when water may enter behind those surfaces may increase dampness on interiors, accelerate disintegration and increase efflorescence.

Firms which specialize in the waterproofing of masonry walls generally prefer to follow the methods and to use the materials which they have found to be satisfactory. For home owners who desire to make their own repairs, probably the most satisfactory liquid waterproofing is a solution of paraffin wax, about 12 ounces of the wax to a gallon of gasoline. The melting point of the wax should be above that of summer wall temperatures (135° F. or higher). For satisfactory results the solution should be applied only when the masonry is dry and warm.

THERMAL EXPANSION OF COLUMBIUM.

An error occurs in this item on page 85 of Technical News Bulletin No. 196, August 1933. The equation and the sentence immediately following it in paragraph three of this article should read:

$$L_t = L_0[1 + (7.06\,t + 0.00144\,t^2)10^{-6}].$$

In this equation L_0 represents the length of a specimen of columbium at 0° C. and L_t the length at any temperature t between −135° and +305° C.

THE ANGSTROM.[1]

"In view of the present unanimous agreement and general practice in expressing optical wave-lengths in terms of the so-called 'international angstrom' the Bureau of Standards considers the time opportune to represent the international angstrom by the symbol 'A.'

"Where the Rowland scale of wave-lengths is intended it should be clearly specified as such.

"The 'angstrom' as at present used was defined and adopted in 1907 by the International Union for Cooperation

[1] Extract from October 1933 issue of the *Bureau of Standards Journal of Research*, article by Dr. C. C. Kiess, "Some Wave Lengths in the Spectrum of Silicon," and approved as general Bureau practice by Lyman J. Briggs, Director of the Bureau of Standards, August 23, 1933.

in Solar Research (now the International Astronomical Union) and also adopted in 1928 by the International Conference on Weights and Measures.

"The angstrom is equal to $\frac{1}{6438.4696}$ of the wave length of cadmium red radiation, and within the limits of the most refined measurements of Michelson, and of Fabry, Perot, and Benoit, this value of the angstrom is identical with the definition 1 angstrom = 10^{-10} meter."

August 23, 1933.

Approved, L. J. Briggs, Director.

LACQUER-COATED RESISTORS OF HIGH RESISTANCE.

Reliable resistors of high resistance of the order of 10^8 to 10^{12} ohms have usually been found difficult to prepare. In a paper which has been submitted for publication in the Review of Scientific Instruments a method of preparation is described which has proved very successful. It consists essentially in coating a pyrex rod with graphite and coating the rod thus prepared with glyptal lacquer. This coating does not alter the value of the resistance, so that the resistance may be adjusted to the value desired before applying the lacquer. The lacquer effectively seals the resistance material against moisture. Such resistors appear to maintain a constant resistance indefinitely.

INTERNATIONAL MEETINGS ON WEIGHTS AND MEASURES.

The International Committee on Weights and Measures is to hold its regular biennial meeting in Paris beginning September 26; a General Conference on Weights and Measures, which is held at intervals of 6 years, will be convened October 3. The Conference includes representatives of all the 32 countries which have joined in the Metric Convention, while the International Committee consists of 18 members elected individually. Dr. Arthur E. Kennelly of Harvard University has recently been elected as a member, succeeding the late Dr. S. W. Stratton. Dr. Kennelly and Mr. Theodore Marriner, Counselor of the Embassy at Paris, will represent the United States at the General Conference.

Important subjects scheduled for discussion at these meetings include the use of light waves as standards of length, the confirmation of the international scale of absolute temperatures, the adoption of a revised system of electrical units to supersede the present international units, and the acceptance of a common fundamental standard for intensity of light.

EDUCATIONAL COURSES AT THE BUREAU OF STANDARDS, 1933–1934

Plans are now being formulated for a number of graduate study courses in Physics, Mathematics and Chemistry, to be given at the Bureau during the coming winter. Courses of this character have been given regularly for the past 25 years, and have been recognized by many of the leading universities in allowing credit for advanced degree. Although these courses are planned primarily for members of the Staff of the Bureau of Standards, they are open on the same terms to any person who can furnish the instructor evidence of satisfactory preliminary training.

The educational committee has adopted the following two cycles as constituting the fundamental part of a graduate training in Physics:

Physics cycle:

- Theoretical mechanics.
- Electricity and magnetism (due this year).
- Advanced optics.

Mathematics cycle:

- Theory of functions.
- Differential equations (due this year).
- Fourier series.

One course of each cycle is normally given each year. Following is the list of courses which will be given during the current year.

Course A.—Electrical theory, Dr. C. Snow. Sixty lectures given two hours per week throughout the year. Tentative time: Mondays and Wednesdays at 8:00 A.M. in the East Building Lecture Room. The first meeting of the class will be Monday, October 9. Prerequisites: Ordinary differential

equations, vector analysis and mechanics. The subjects discussed will be in this order, general vector fields, electrostatics, magnetostatics, stationary electric currents, Ampere's theory of magnetism, the Maxwell-Lorentz field equations for the stationary state, electric conduction and Ohm's law, induced electric fields and the summarizing of the theory in the Maxwell-Lorentz field-and-force equations for time-variable fields, with a formulation of the concepts of electromagnetic energy, momentum and energy flow.

Course B.—Differential equations, Dr. W. Edwards Deming. Sixty lectures given two hours per week throughout the year. Tentative time: Tuesdays and Thursdays at 8:00 A.M. The first meeting of the class will be Tuesday, September 26, in Room 300 South Building. Prerequisite: Calculus.

The course will begin with a review of some of the necessary calculus. An attempt will be made to cover the integrable types of differential equations, especially those of the first and second order. Equations with several variables will be treated together with their applications to physics. Symbolic methods will be devised for special types, but emphasis will be laid on general methods having wide utility. A review of series will be given, followed by the method of Frobenius for the solution of the more difficult types of equations by series. Numerical approximations by series and by Picard's and Runge's methods will be discussed. Singular solutions and their interpretations will be treated. The course will conclude with special types of equations encountered in modern physical problems.

Course C.—Atomic and nuclear structure, Dr. C. J. Humphreys. Sixty lectures given two hours per week throughout the year. Tentative time: Mondays and Wednesdays at 4:30 P.M. The first meeting of the class will be Monday, September 25, in Room 214 Chemistry Building. Discussion of the basic phenomena of radiation including spectral series and radioactivity. A brief introduction to quantum mechanics discussing the modifications of the Bohr-Sommerfeld theory required by the concepts of Heisenberg, Schrödinger, Dirac and Fermi. Application of the methods of Pauli and Hund to the determination of the distribution of energy levels in the atom. Discussion of fine structure and multiplet

separations using Goudsmit's vector model. Zeeman effect, Paschen-Back effect, and phenomena appearing in the transition between strong and weak magnetic fields. Relation of hyperfine structure to nuclear theory. Present conceptions of nuclear structure. References to standard treatises and current literature.

Tuition.—The fee for each sixty-lecture course will be twenty-five dollars. Fees for courses continuing through the year are payable in two installments, if desired.

Further information regarding the above courses may be obtained by addressing the educational committee, Bureau of Standards, Washington, D. C.

INDUSTRIAL STANDARDIZATION AND COMMERCIAL STANDARDS MONTHLY.

In Technical News Bulletin no. 195 (July 1933) the announcement was made that because of the limited funds available for printing, the *Commerical Standards Monthly* had been discontinued with the June number. The Bureau of standards now desires to announce that through the courtesy of the American Standards Association the publication is being continued in combination with "Industrial Standardization" under the joint title "Industrial Standardization and Commercial Standards Monthly."

Arrangements have been made with the Superintendent of Documents for the American Standards Association to take over the subscription list of the "Commercial Standards Monthly" and to send the combined magazine to all names on this list during the remaining period covered by their subscriptions. The subscription rate for the combined magazine is $4.00 per year (foreign, $5.00); single copies, 35 cents. Subscriptions should be sent to the American Standards Association, 29 West 39th Street, New York, N. Y.

The Bureau is coöperating with the American Standards Association in the preparation of material for the magazine to the end that it may meet as completely as possible the needs of all those interested in commercial standardization.

Treated Water for Locomotives.—From a bulletin of the Canadian National Railways we learn that the natural waters of the prairie country contain sufficient hardness to make necessary the installation of treating plants wherever it is to be used in locomotive boilers. The treatment consists of removing from the water certain dissolved salts such as sulfate of lime, carbonate of lime and carbonate of magnesia. The combined concentration of these mineral salts may amount to 500 parts per million or more and if they are left in the boiler water, evaporation causes a deposition of these salts upon the tubes and other heating surfaces in the form of a hard, dense and heat-resistant scale. A locomotive, such as the 6100 type, uses about 14,000 gallons of water on an average run of 185 miles and if the water were not previously treated, scale formation would rapidly reach serious proportions.

C.

The Dutch Elm Disease.—The U. S. Department of Agriculture issues a warning that the Dutch elm disease has broken out anew in this country. The recently discovered infected area lies west of the Hudson River and falls within the Essex, Hudson and Passaic counties of New Jersey. Owners of elms and all tree lovers should watch for wilting or yellow or brown leaves accompanied by brown streaks in the wood. Since these symptoms are shown by other diseases, pieces of the infected twigs as big as a lead pencil should be cut and sent to the Dutch Elm Disease Laboratory, care Experiment Station, Wooster, Ohio. If you live within the infected area send the specimens to, or communicate with, the Shade Tree Commission, City Hall, East Orange, N. J.

C.

Tomorrow—Colder?—The nadir of absolute temperature has been brought several steps nearer attainment. *Science Service* describes how eighty-five thousandths of a degree on the Absolute scale has been achieved in the Kammerlingh-Onnes laboratory at the University of Leyden. Prof. W. J. de Haas of Leyden and Prof. H. A. Kramers of Utrecht used the method that is known as the "adiabatic demagnetization of paramagnetic salts." This takes advantage of the fact that when a substance is magnetized, it heats up. The substance is cooled as low as possible by means of liquid helium, then it is magnetized and the temperature rises. The heat is removed through evaporation of the liquid helium. Keeping the substance well insulated, it is now demagnetized and becomes colder as a result. Thus, a lower temperature than ever before attained has been reached.

C.

THE FRANKLIN INSTITUTE.

MEMBERSHIP NOTES.

ELECTIONS TO MEMBERSHIP.

(Stated Meeting, Board of Managers, September 20, 1933.)

FAMILY MEMBERSHIP.

MR. HENRY BUTLER ALLEN, Metallurgical Engineer, Henry Disston and Sons, For mailing: 8112 St. Martins Lane, Chestnut Hill, Pa.

DR. HOWARD MCCLENAHAN, Secretary and Director, The Franklin Institute, Philadelphia, Pa.

MR. W. CHATTIN WETHERILL, Director of Student Welfare, University of Pennsylvania, Philadelphia, Pa. For mailing: 1673 Willow Grove Avenue, Chestnut Hill, Pa.

RESIDENT.

PROF. WILLIAM H. BARTON, JR., Professor of Civil Engineering, Pennsylvania Military College, Chester, Pa.

MR. EDWARD L. FORSTALL, Telephone Engineer, Bell Telephone Company, 1835 Arch Street, Philadelphia, Pa.

MR. NELSON W. GOODWIN, Chemist, Electric Storage Battery Company, Philadelphia, Pa. For mailing: 200 East Clivenden Avenue, Mt. Airy, Philadelphia, Pa.

MR. IRWIN S. HOFFER, Instructor, Temple University, Philadelphia, Pa. For mailing: 146 Fernbrook Avenue, Wyncote, Pa.

MR. JOSEPH F. MCDONNELL, JR., Pharmacist, 409 Old York Road, Jenkintown, Pa.

MR. ROBERT G. RICHARDSON, Draftsman, National Airoil Burner Company. For mailing: 5824 North Thirteenth St., Philadelphia, Pa.

MR. JAN M. VAN NIEUKERKEN, Electrical Engineer, Scientific writer, Philadelphia, Pa. For mailing: 400 Bethlehem Pike, Chestnut Hill, Pa.

NON-RESIDENT.

LT. COM. FRED W. BELTZ, U. S. N., Naval Officer, Navy Department, Washington, D. C. For mailing: Schwenksville, Pa.

STUDENT.

MR. GEORGE GRAFFMAN, Photographer, 47 North Millick Street, Philadelphia, Pa.

CHANGES OF ADDRESS.

MR. BARNETT BACHIN, 5234 Warnock Street, Philadelphia, Pa.

LIEUT. JOHN C. CORNELIUS, JR., Architects Building, Seventeenth and Sansom Streets, Philadelphia, Pa.

MR. DANIEL B. CURLL, JR., Apartment 417, Lincoln Court, Overbrook, Pa.

MR. ELLIOTT CURTISS, 1234 Hamilton Street, Philadelphia, Pa.

MR. F. L. DUBOSQUE, 51 Bayview Avenue, Great Neck, N. Y.
MR. WILLIAM G. ELLIS, 2019 Rittenhouse Street, Philadelphia, Pa.
MR. CHARLES F. FORSTALL, Reading Company, Shamokin, Pa.
MR. WALTON FORSTALL, United Gas Improvement Company, 1800 North Ninth Street, Philadelphia, Pa.
MR. N. E. FUNK, 419 Bolsover Road, Wynnewood, Pa.
MR. E. J. GANGWERE, Reading Company, Reading, Pa.
MR. G. R. HALL, Denville Post Office, Denville, Morris County, N. J.
MR. JOHN M. HAMMOND, 16 D Street, N. W., Washington, D. C.
MR. WALTER G. HENSEL, 43 East Utica Street, Buffalo, N. Y.
MR. M. M. HUBBARD, 8 Cottage Street, Newport, R. I.
MR. D. M. HUBER, 921 Mason Avenue, Drexel Hill, Pa.
MR. LAWRENCE J. MORRIS, 240 South Fourth Street, Philadelphia, Pa.
MR. GEORGE F. OTTO, 2751 Germantown Avenue, Philadelphia, Pa.
MR. F. PALMER, JR., Wellfleet, Mass.
MR. EDWARD W. PARKER, Primos, Delaware County, Pa.
MR. DAVID PEPPER, 345 Roumford Road, Mt. Airy, Philadelphia, Pa.
MR. ERNEST R. RECHEL, 4339 Whitaker Avenue, Philadelphia, Pa.
MR. ALEXANDER E. REOCH, c/o R. C. A. Victor Co. Inc., 30 Rockefeller Plaza, New York, N. Y.
MR. FRANK H. SAUER, 1266 Liberty Street, Camden, N. J.
MR. G. N. SIEGER, Box 405, Slatington, Pa.
REAR ADMIRAL ELLIOT SNOW, c/o Mr. S. C. Snow, 1401 Arch Street, Room 616, U. G. I. Building, Philadelphia, Pa.
MR. LEWIS B. STILLWELL, Elm Road, Princeton, N. J.
MR. E. W. UPHAM, P. O. Box No. 395, Birmingham, Mich.
MR. JAN M. VAN NIEUKERKEN, 301 Ashbourne Road, Elkins Park, Pa.
MR. A. RAYMOND WHITE, 11443 South Union Avenue, Chicago, Ill.
MR. EDWIN M. WOODS, 628 North Thirty-second Street, Philadelphia, Pa.
MR. HOWARD SELLERS WORRELL, 116 Bleddyn Road, Ardmore, Pa.

NECROLOGY.

Dr. H. D. Arnold, New York, N. Y.
Mr. Walter Atlee, Baltimore, Md.
Mr. Cyrus H. K. Curtis, Philadelphia, Pa.
Mr. Paxson Deeter, Philadelphia, Pa.
Mr. Elisha Lee, Philadelphia, Pa.
Mr. Frank W. Peek, Jr., Pittsfield, Mass.
Prof. Wm. Cawthorne Unwin, London, England.

LIBRARY NOTES.

RECENT ADDITIONS.

ADAMS, GEORGE. Micrographia Illustrata, or, The Knowledge of the Microscope Explained: Together with an Account of a New Invented Universal, Single or Double, Microscope, Either of which is capable of being applied to an Improv'd Solar Apparatus. . . . The Second Edition. 1747.

American Institute of Electrical Engineers. Transactions, June, 1933, Volume 52, No. 2. 1933.

Astronomy's Advancement, or, News for the Curious; Being a Treatise of Telescopes: And An Account of the Marvelous Astronomical Discoveries of late years made throughout Europe. . . . Done out of French by Jos. Walker. 1684.

BANCROFT, WILDER D. Applied Colloid Chemistry: General Theory. Third edition. 1932.

BRITTEN, F. J. Watch and Clock Makers' Handbook, Dictionary and Guide: Thirteenth edition: with appendix. 1922.

Forschungsinstitut der Čechoslovakischen Zuckerindustrie in Prag. Bericht für das Jahr 1932–33. Bd. 36. 1933.

HASWELL, J. ERIC. Horology. The Science of Time Measurement and the Construction of Clocks, Watches and Chronometers. 1928.

Jahresbericht über die Leistungen der chemischen Technologie für das Jahr 1932. 78 Jahrgang, 2 Abteilung: organischer Teil. 1933.

MATHEWS, ALBERT P. The Nature of Matter, Gravitation and Light. 1927.

NOAD, HENRY M. The Inductorium, or Induction Coil; Being a Popular Explanation of the Electrical Principles on Which It Is Constructed. With the Description of a Series of Beautiful and Instructive Experiments, Illustrative of the Phenomena of the Induced Current. Third edition. 1868.

PHIPPS, CONSTANTINE JOHN. A Voyage towards the North Pole. Undertaken by his Majesty's Command 1773.

Scientific and Learned Societies of Great Britain and Ireland. The Official Year-Book. With a Record of Publications Issued During Session 1931–1932. Forty-ninth Annual Issue. 1932.

Society of Automotive Engineers. S. A. E. Handbook. 1933 Edition.

University of Pittsburgh—Members of the Physics Staff, An Outline of Atomic Physics. 1933.

Welsh Journal of Agriculture. The Journal of the Welsh Agricultural Education Conference. Vol. IX. 1933.

BOOK REVIEWS.

NATIONAL ADVISORY COMMITTEE FOR AERONAUTICS.

Report No. 458, Relative Loading on Biplane Wings, by Walter S. Diehl, 17 pages, illustrations, 23 × 29 cms. Washington, Government Printing Office, 1933. Price ten cents.

It is shown that the lift coefficients of the individual wings of a biplane are given by

$$C_{L_U} = C_L + \Delta C_{L_U}$$

and

$$C_{L_L} = C_L - \Delta C_{L_L},$$

where C_{L_U}, C_{L_L}, and C_L are the lift coefficients for the uper wing, lower wing, and biplane, respectively.

For the upper wing it is shown that

$$\Delta C_{L_U} = K_1 + K_3 C_L,$$

K_1 and K_2 being functions of gap/chord, stagger, aspect ratio, decalage, overhang and wing thickness. The combination of existing biplane theory and experimental data supply curves from which K_1 and K_2 can easily be determined for any biplane. This enables the designer to calculate with reasonable accuracy the relative loading for any condition of flight.

Report No. 461, Interference on an Airfoil of Finite Span in an Open Rectangular Wind Tunnel, by Theodore Theodorsen, 6 pages, illustrations, 23 × 29 cms. Washington, Government Printing Office, 1933. Price five cents.

The wall interference on an airfoil of finite span in an open-throat rectangular section has been treated theoretically and the result is presented in a convenient formula. Numerical results are given in tables and diagrams.

MESSENTLADUNGSSTRECKEN (IONENSTRECKEN), von Dr.-Ing. Siegfried Franck, 192 pages, illustrations, tables, 16.5 × 24.5 cms. Berlin, Verlag von Julius Springer, 1931.

"Discharge Space Measurements" deals exclusively with independent electrical discharges in gases. These so-called independent discharges are distinguished from the dependent type in that the latter depend upon an external energy source for their actuation. The hot cathode vacuum tube and the photoelectric tube furnish examples of dependent discharges.

In this work the author has arranged the various types of independent "electrical discharges in gases" in regard to their application to measuring processes. Accordingly then, the principles of measurement receive the greatest emphasis, while the theory of gas discharges is considered only to a degree necessary for an understanding of the above principles. The arrangement of subject matter does not follow the usual order of dealing with the various measurable quantities such as potential, current, capacity, radiation, time and pressure but rather considers the phenomena of gas discharges in the light of their physical constitution. This departure from the usual method of treatment is partially compensated by placing at the end of the book a systematically arranged series of tables containing standard data for the simpler forms of discharge apparatus.

The subject matter is divided into two main sections. The first part includes those phenomena that are free of space charges. The simpler bi-electrode arrangement is accorded precedence and a description given of conditions existing in plane, spherical, cylindrical and "point" static fields. Multiple electrode fields also receive due attention. The influences of alternating, high frequency and impulse potentials are described. Attention is directed to internal influences such as radiation, polarity, composition of the electrodes, composition and water vapor content of the gases, magnetic fields and narrow passages. Discharges of the nature described above find practical application when used with nonhomogeneous dielectrics. By means of the Lichtenberg figures thus formed, the magnitude and character of an electric current may be measured.

Under the heading of "electrical discharges accompanied by space charges" will be found an elaborate treatment of the well-known glow discharge so well exemplified in the Geissler tubes. Some of the practical applications to which such discharges can be put include the determination of time amplitudes, tempor-

ary fluctuations in voltage and amperage, measurement of field strength and direction, use of the glow tube as a voltage reducer, amplification of fluctuations in potential, holding the voltage of circuit constant, measurement of high resistances and light intensities, production of alternating and intermittent discharges and the measurement of the circuit's resistance, capacity, frequency and tube characteristics. Regulation of potential may also be accomplished through the addition of a grid electrode to the glow tube. The glow tube can be used as an oscillograph whereupon its range of usefulness is extended still further. Spark discharges find application in the measurement of potentials, wave-periods, as well as the form, duration and polarity of irregular electrical impulses.

T. K. CLEVELAND.

PUBLICATIONS RECEIVED.

Industrial Chemistry, an elementary treatise for the student and general reader, by Emil Raymond Riegel, 784 pages, illustrations, tables, 15.5 × 23.5 cms. New York, The Chemical Catalog Company, Inc., 1933. Price $6.00.

Allen's Commercial Organic Analysis, a treatise on the properties, modes of analysis, and proximate analytical examination of the various organic chemicals and products employed in the arts, manufactures, medicine, etc., with concise methods for the detection and estimation of their impurities, adulterations, and products of decomposition. Vol. X, Hæmoglobin and its Derivatives, Albuminoids of Scleroproteins, Structural Proteins, Examination of Foodstuffs for Vitamins, The Hormones, The Identification of Unknown Woods and Charcoals, The Pectic Substances. Editor, C. Ainsworth Mitchell. Fifth edition, revised and partly rewritten. 817 pages, tables, illustrations, 16 × 24 cms. Philadelphia, P. Blakiston's Son & Co., Inc. Price $7.50.

Liquid Dielectrics, by Dr. Andreas Gemant, English translation by Vladimir Karapetoff, 185 pages, tables, illustrations, 15.5 × 23.5 cms. New York, John Wiley & Sons, Inc., 1933. Price $3.00.

The Electrical Properties of Glass, by J. T. Littleton and G. W. Morey, 184, pages, tables, illustrations, 15.5 × 23.5 cms. New York, John Wiley & Sons, Inc., 1933. Price $3.00.

Experimental Electrical Engineering and Manual for Electrical Testing for Engineers and for Students in Engineering Laboratories, Vol. 1, by V. Karapetoff, revised by Boyd C. Dennison, 781 pages, illustrations, 15 × 23.5 cms. New York, John Wiley & Sons, Inc., 1933. Price $6.00.

The Inventor and His World, by H. Stafford Hatfield, 269 pages, 12.5 × 19 cms. New York, E. P. Dutton and Company, 1933. Price $2.40.

Consciousness: Brain-Child, by Percy A. Campbell, 109 pages, 13.5 × 20.5 cms. Cleveland, The Caxton Company, 1933.

L'Arithmétique a la Portée de Tous Nombres Entiers Fractions Calculs Approches, par J. Poiree, 96 pages, 14.5 × 22.5 cms. Paris, Gauthier-Villars et Cie., 1932.

La Géométrie a la Portée de Tous, par J. Poiree, 17 pages, diagrams, 16 × 24 cms. Auch, Imprimerie Cocharaux, 1931.

L'Algèbre et la Trigonométrie a la Portée de Tous, Tomes I and II, illustrated, 14.5 × 22.5 cms. Paris, Gauthier-Villars et Cie., 1933.

Report of National Conference on the Financing of Education, held under the auspices of the Joint Commission on the Emergency in Education, 78 pages, 15 × 23 cms. Washington, National Education Association, 1933.

National Advisory Committee for Aeronautics, Technical Notes No. 467, Simplified Aerodynamic Analysis of the Cyclogiro Rotating-Wing System, by John B. Wheatley, 13 pages, illustrations, 20 × 26 cms. Washington, Committee, 1933. No. 468, A Study of Factors Affecting the Steady Spin of an Airplane, by Nathan F. Scudder, 20 pages, illustrations, 20 × 26 cms. Washington, Committee, 1933. No. 469, A Summary of Design Formulas for Beams Having Thin Webs in Diagonal Tension, by Paul Kuhn, 23 pages, illustrations, 20 × 26 cms. Washington, Committee, 1933.

Bell Telephone Laboratories, Monographs: No. B–737, Developments in the Application of Articulation Testing, by T. G. Castner and C. W. Carter, 24 pages, illustrations, 15 × 23 cms. No. B–738, Carrier in Cable, by A. B. Clark and B. W. Kendall, 13 pages, illustrations, 15 × 23 cms. No. B–739, Some Contemporary Advances in Physics—XXVI. The Nucleus—I, by Karl K. Darrow, 43 pages, illustrations, tables, 15 × 23 cms. New York, 1933.

THE FRANKLIN INSTITUTE

OFFICERS FOR 1933

President	NATHAN HAYWARD
Vice-presidents	HENRY HOWSON C. C. TUTWILER WALTON FORSTALL W. CHATTIN WETHERILL
Secretary	HOWARD MCCLENAHAN
Assistant Secretary and Librarian	ALFRED RIGLING
Treasurer	BENJAMIN FRANKLIN
Assistant Treasurer	MARSHALL S. MORGAN
Controller	WILLIAM F. JACKSON, JR.

Board of Managers

HENRY BUTLER ALLEN
GEORGE H. BENZON, JR.
EDWARD G. BUDD
FRANCIS T. CHAMBERS
G. H. CLAMER
THEOBALD F. CLARK
WALTON CLARK
CHARLES H. EWING
SAMUEL S. FELS
ARTHUR W. GOODSPEED
CLARENCE A. HALL
GEORGE A. HOADLEY
A. ATWATER KENT
L. H. KINNARD
ROBERT W. LESLEY
HORACE P. LIVERSIDGE
MALCOLM LLOYD, JR.
CHARLES PENROSE
GEORGE WHARTON PEPPER
JAMES S. ROGERS
GEORGE D. ROSENGARTEN
HASELTINE SMITH